THE UNIVERSITY OF ADELAIDE

DEPARTMENT OF MECHANICAL ENGINEERING

A COMPUTATIONAL SCHEME FOR

CALCULATING REFRIGERANT PROPERTIES &

HEAT TRANSFER IN BOILING TUBE FLOW

Supervisor : Dr. Geoff Tansley

Student : Edwin C. F. Au

Course : Masters degree in Engineering Science

Date : 15 [th] October 1998

TABLE OF CONTENTS

LIST OF TABLES

LIST OF FIGURES

CHAPTER SIX

ABSTRACT

A good understanding of transport properties of the refrigerant is important in the design of direct expansion heat exchangers. However, the characteristics of a boiling refrigerant flowing through a tube are too complicated to analyse from first principles, so experimental correlations are necessary. This study aims to develop a computational scheme (AuCFD) for calculating refrigerant properties, two-phase heat transfer coefficients and pressure drop of R12 and R134a in a horizontal tube. The scheme can help to understand the characteristics of refrigerant flow under different conditions and estimate the performance of direct expansion heat exchangers.

The computational scheme (AuCFD), based on the correlations of other researchers, was developed to predict refrigerant properties, two-phase heat transfer coefficients and pressure drops throughout an evaporator. Using a finite difference method, the horizontal pipe is sub-divided into several sections to calculate the refrigerant transport properties at any section. If the pipe is L metres long and is divided into n equal sections, the spacing between the sections with the same distance is defined as L/n, and is called the grid spacing Δl. The heat energy entering any given section in the refrigerant plus the refrigerant's internal energy must be equal to the energy leaving the section in the refrigerant. If a refrigerant property is ascertained at section inlet, the property can be found out at section outlet. The section outlet's property will be the next inlet section's property.

After a series of comparisons of the experimental published data and computational data based on various correlations, it was found that Jung and Radermacher's (1989a) correlation for two-phase heat transfer coefficient and Souza and Pimenta's (1995) correlation for two-phase pressure drops of pure refrigerants were with the mean deviations of 5-10% and 15-20% respectively. In computational scheme presented here first order accurate implementations were deemed to sufficiently minimise numerical errors, round-off and discretization errors.

The major conclusions drawn are:

- For pure refrigerants, the computational results showed that Jung and Radermacher's (1989a) correlation yield a good prediction of heat transfer coefficients, generally.

- Within a range of heat flux from 5 kW/m^2 to 30 kW/m^2, the results indicated that Souza and Pimenta's (1995) correlation gave a reasonable prediction of two-phase pressure drops in pure refrigerants. However, if the constant heat flux is greater than 30 kW/m^2, the prediction will have a higher mean deviation.

- An independent grid spacing (Δl) is determined to reduce the errors and increase the accuracy of the equations under all flow conditions of refrigerants.

- The computational scheme (AuCFD) is used for more practical application as a design tool for Dx-coil heat exchangers - this can provide design engineers with improved preliminary estimations for the size and capacity of an evaporator.

STATEMENT OF ORIGINALITY

This thesis contains no material which has been accepted for the award of any other degree or diploma in any university or other tertiary institution. To the best of my knowledge and belief, it contains no material previously published or written by another person, except where due reference has been made in the text.

I give content to this copy of my thesis, when deposited in the University Library, being available for loan and photocopying.

Signed:

Date: 15 October 1998

ACKNOWLEDGEMENTS

This thesis is dedicated to my Lord and Saviour Jesus Christ, to whom I owe all that I have. He is the "Supervisor" that I lean on; without him I would fall.

I would like to express my sincere thanks to my supervisor, Dr. G.D. Tansley, for his consistent guidance and advice which have been given during this project. It is greatly appreciated that he committed to supervise the project, with frequent meetings with me, for three years after he left the University of Adelaide.

My appreciation and thankfulness to my co-supervisor, Dr. Gerald Schneider, who gave valuable advice, final editing and proof-reading, enabling the project to be finished.

I am greatly indebted to my dearest wife, Carmen, for her patience, encouragement and support without which the completion of this thesis would not have been accomplished. This masters degree will be a late wedding gift for her.

NOMENCLATURE

Symbol	Meaning	Unit
A or AI	internal surface area of tube	m^2
AO	external surface area of tube	m^2
Bo	boiling number, $Bo = q/(G\,i_{fg})$	
C_D	dimensionless constant, Chapter 3.2.3	
Co	convective number, $Co = ((1-x)/x)^{0.8}(\rho_v/\rho_l)^{0.5}$	
Cp	specific heat capacity of fluid	kJ/kgK
C_1-C_2	empirical constants, (Chapter 2.3)	
D	internal diameter of tube $= ID$	m
OD	external diameter of tube	m
Dx	direct heat exchanger	
F	heat transfer enhancement factor (Chapter 2.3)	
F_{fl}	fluid specific term (Chapter 2.3)	
Fr	Froude number, $Fr = G^2/(\rho_l^2 gD)$	
f	friction factor, defined by Eqt. (2.10)	
f^{IV}	fourth order accuracy	
G	mass flux, mass flow rate / area	kg/m^{2}s
g	acceleration of gravity	m/s^2
h	heat transfer coefficient	W/m^2 K
h_SH	superheated heat transfer coefficient $= h_{sh}$	W/m^2 K
h_air	heat transfer coefficient of air $= h_a$	W/m^2 K
h_airt	total heat transfer coefficient of air	W/m^2 K
h_airav	average heat transfer coefficient of air	W/m^2 K
htc_av	average heat transfer coefficient	W/m^2 K
htc_t	total heat transfer coefficient	W/m^2 K
h_l	single phase heat transfer coefficient for liquid only flow	W/m^2 K

h_{cec}	heat transfer coefficient due to convective evaporative contribution	W/m^2 K
h_{nbc}	heat transfer coefficient due to nucleate evaporative contribution	W/m^2 K
h_{sa}	a pool boiling heat transfer coefficient, Chapter 2.3	W/m^2 K
h_{tp}	two-phase heat transfer coefficient = h_tp, Chapter 2.3	W/m^2 K
h_{fg}	heat of evaporation, Equation 2.12	J/kg
i	number of grid point	
i_{fg}	latent heat of vaporisation	J/kg
k	thermal conductivity	W/mK
k	turbulent kinetic energy	J
k_cu	thermal conductivity of copper	W/mK
Kf	Pierre's boiling number, Chapter 2.4	
l	fin height	m
L	tube length	m
Δl	grid spacing	m
M_w	molecular weight	
m	mass flow rate = $mdot$	kg/s
N	heat transfer factor due to nucleate boiling, Chapter 2.3	
Nu	Nusselt number, hx/k	
Nu_air	Nusselt number of air	
n	number of iteration	
P	saturated pressure	Pa
PI or π	circle constant	
Pc	critical pressure	Pa
Pr	Prandlt number, $C_p\mu/k$	
pr	reduced pressure, $pr = Pc/P$	Pa
ΔP	pressure drops, Chapter 2.4	Pa
ΔP_f	two-phase friction pressure drops = dp	Pa
ΔP_{fa}	friction pressure drops with liquid only flowing at its mass velocity	Pa

ΔP_{tp}	two-phase pressure drops, Chapter 2.4	Pa
ΔP_a	two-phase acceleration pressure drops, Chapter 2.4 = dp_a	Pa
dp_t	total two-phase pressure drop	
Q	heat transfer	W
q	constant heat flux	W/m^2
Re	Reynolds number	
S	suppression factor, Chapter 2.3	
s	distance between adjacent fins	m
T_air	air temperature	C
Tc	critical temperature	K
Tr	reduced temperature, $Tr=Tc/Ts$	K
T_{mn}	mean temperature	
Ts	saturated temperature of refrigerant	$^\circ C$
t	fin thickness	m
u	velocity of fluid	m/s
X_{tt}	Martinelli's parameter, Eqt. (2.20)	
x	vapour quality	
x_{av}	average vapour quality	
Δx	quality change between inlet and outlet	
z_c	compressibility factor at critical point, Chapter 2.5	
μ	viscosity of fluid	kg/ms
α	void friction	
β	contact angle	degree
ρ	density of fluid	kg/m^3
Υ	property index, Eqt. (2.29)	
ϕ	Martinelli pressure drop multipliers, Chapter 2.4	
ξ	value between 0 and pipe length, Chapter 4.3	m
ξ	viscosity parameter characteristic to each component, Chapter 2.5	

ε	round-off error, Chapter 3
θ	variable

Subsript

a	acceleration
f	frictional
fo	total flow assumed as liquid
g	vapour phase
i	grid point in x direction
j	grid point in y direction
l	liquid phase
lo	liquid only
n	inlet to a section
o	test section outlet
v	vapour state
vo	vapour only
v	viscous
t	turbulent
tp	two-phase
tt	turbulent-turbulent
x	x - coordinate
y	y - coordinate

Chapter 1

INTRODUCTION

1.1 Background

Boiling heat transfer of refrigerants in horizontal tubes (in evaporators and many other major items of chemical and power plants) has been studied by many researchers and scientists for several decades. Much work has also been carried out by researchers in the development of correlations for heat transfer coefficients and pressure drops for refrigerants, but results of their correlations are inconsistent, based on different mass flux, heat flux, inlet vapour quality, geometry and working fluids. For instance, Jung and Radermacher's (1989a) correlation for heat transfer coefficient predicted their own experimental data well within 7% deviation in a particular length of horizontal tube. However, when Jung and Radermaker's correlation for heat transfer coefficients was used to predict other researchers' experimental data, the results were found to have 10 - 15 % deviation. It seems that some researchers developed their correlations for their own experimental purposes rather than for general application.

In the air conditioning and refrigeration industry, evaporators which are supplied with cold liquid/vapour refrigerant mixtures from the metering device and carry this refrigerant through tubing in which it is evaporated (thus effecting heat transfer) are called direct expansion evaporators. Design of direct expansion (Dx) evaporators draws on a knowledge of the fluid dynamics and heat transfer processes occurring during convective boiling. Convective boiling of refrigerants is the addition of heat to a flowing liquid and vapour refrigerant in tubes (evaporators) such that evaporation of vapour refrigerants occurs. Therefore, a good understanding of heat transfer processes and transport properties of the refrigerant is very important in the design of direct expansion heat exchangers. The following figure is a typical application of a direct

1

expansion evaporator where the hot air will be cooled down as it passes over the outside surface of the tubing.

Mixture of liquid and vapour refrigerant from metering device, 90% liquid, 10% vapour; saturated temperature is 4°C

Fluid in cross-flow

Vaporised refrigerant is flowing through the evaporator with remaining liquid

50% liquid 50% vapour 4°C

100% vapour, 4°C

100% vapour, 10°C superheated to compressor
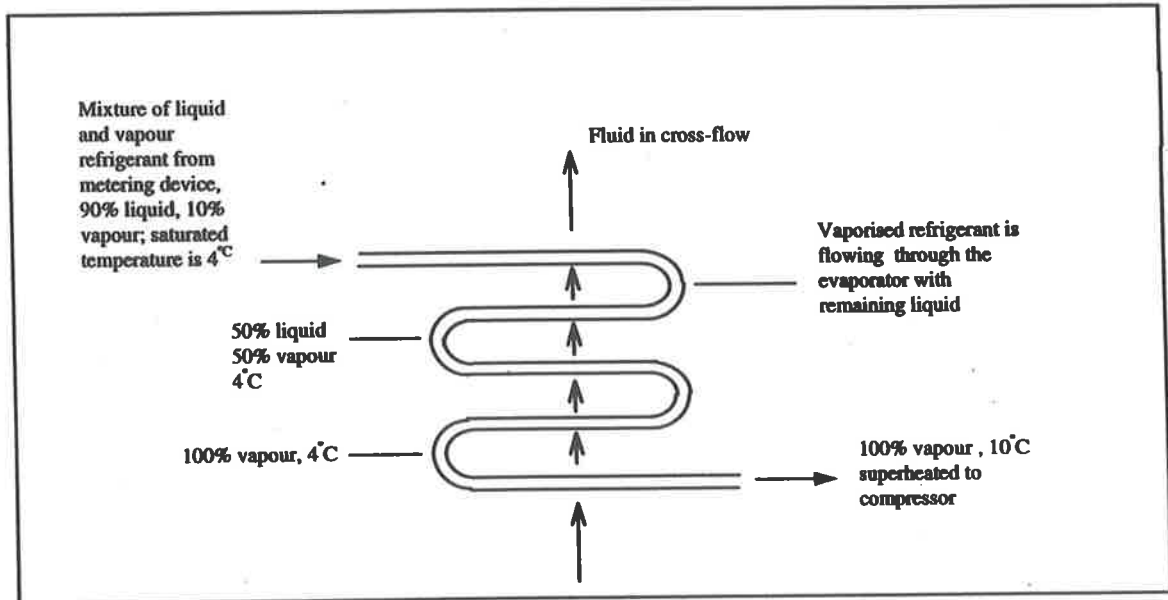
Figure 1.1 - Direct expansion evaporator in cross-flow

In Figure 1.1, as the refrigerant moves through the tubing, it absorbs heat from the tube walls, which themselves are heated by air or water which is cooling in cross-flow. The absorption of heat causes more liquid refrigerant to vaporise, but the temperature of the refrigerant does not rise. As long as there remains some unboiled refrigerant, the temperature at which the boiling takes place remains at the saturation temperature: this might be constant, if there is no pressure gradient in the pipe, or might drop as the saturation pressure drops because of friction and acceleration of the refrigerant. If the evaporator coil has been sized correctly, there will be liquid refrigerant present through 90 percent of the coil. Then in the last 10 percent of the coil, with only cool vapour refrigerant inside the tubing, the continued addition of heat will cause the temperature of the refrigerant to rise. The refrigerant will be superheated as it flows out of the direct expansion heat exchanger into the compressor.

The size of evaporators is typically determined using previous systems' data, and oversizing or undersizing evaporators may significantly affect the performance of air conditioning systems. Oversized evaporators save energy whereas undersized ones cannot provide sufficient cooling capacity to the area being cooled. The mathematical model/design tool proposed here can solve this problem and estimate the size of evaporators depending on the requirement of cooling capacity of the areas, leading to improved design processes, more optimal evaporator performance and increased cost effectiveness.

Due to the phase out of the Ozone Depleting Potential (ODP) R12, a new low ozone-depletion potential (low-ODP) refrigerant, R134a is being used to replace the common refrigerant R12. R134a operates at pressures similar to R12 and is compatible with materials in R12 systems. From the experimental results of researchers such as Jung and Radermacher (1989a), Eckels and Pate (1990) and Souza et al (1993), it can be seen that R134a performs much better than R12 under similar operation conditions.

In the current study, R134a and R12 were selected as the working fluids for a computer program which was developed to estimate the two-phase heat transfer and pressure drop of the refrigerant inside a horizontal pipe with constant and variable heat flux. The technique used in the computational scheme was a finite difference method which checks the refrigerant properties, the two-phase heat transfer coefficients and pressure drops of the refrigerant at any particular position within a horizontal pipe. Using this computational scheme (AuCFD), the transport properties of the refrigerant were found under different flow conditions. The parameters used in the tests were comparable with the experimental data of other researchers.

1.2 Objectives

The major aim of this research program was the development of a computational scheme (AuCFD) for calculating refrigerant properties and heat transfer in horizontal tubes. This work is an essential step in improving the design of direct expansion (Dx) heat exchangers in air conditioning applications. One product of this work is a computational scheme (AuCFD) which can be used to determine transport properties, heat transfer coefficients and pressure drops of refrigerants at various locations in a heat exchanger. It will enable design engineers to estimate the size and the capacity of evaporators in air conditioning and refrigeration applications.

A second major aim of this work was the investigation of the accuracy of other researcher's empirical correlations for heat transfer and pressure drop in general application to heat exchanger design.

The characteristics of two-phase boiling refrigerant flowing through a tube are too complicated to analyse from first principles. Due to these difficulties, a computational study using a finite difference method is introduced to predict refrigerant properties at any location within a given pipe, based on empirical, rather than analytical models.

This thesis describes a comprehensive series of computational tests of different correlations for heat transfer coefficients and pressure drops with R134a and R12 in different sizes of horizontal tubes. It also describes the details of the numerical fluid-property equations of R12 and R134a, the algorithms used in the model of direct expansion evaporators, validation of this model in terms of the order of modelling accuracy and computational error, and recommendations for future work. The order of accuracy represents the degree of truncation error in the finite series expansion of spatially varying flow parameters. More terms in the finite series leads to higher-order

accuracies reducing truncation errors (second and third order accurate implementations are common in commercial computational fluid dynamics suites).

The following outlines the contents of each chapter in the thesis:

Chapter 1 is an introduction of the background and objectives of the project.

Chapter 2 is a literature survey of past work on correlations for two-phase heat transfer coefficients and pressure drop in refrigerants. Transport properties of refrigerants, R12 and R134a are also presented. A summary of different correlations for two-phase heat transfer coefficients and pressure drops is included.

Chapter 3 contains a detailed description of the numerical fluid-property equations, finite differences, algorithms and comparison of conventional CFD and this project's numerical modelling approaches (AuCFD). Using the techniques in this chapter, a main computer program and three sub-programs for air, R12 and R134a transport properties are structured for verifying the correlations for two-phase heat transfer coefficients and pressure drops. Different correlations for two-phase heat transfer coefficients and pressure drops in refrigerants are selected and established in the computational scheme (AuCFD) for further testing.

Chapter 4 describes verification and numerical accuracy considerations of the finite difference methods used. A correlation for two-phase pressure drops is used to check the order of accuracy applied to the scheme. It also shows how to select an appropriate grid spacing for the horizontal tube throughout the computational scheme (AuCFD).

Chapter 5 contains a comparison of the computational results and the experimental data from different researchers. The results of computational data are analysed and discussed. The graphs presented show the effect of varying parameters in the tests.

Chapter 6 is a final model for a Dx tube. The most reliable correlations for two-phase heat transfer coefficients and pressure drops are used in the final model. It also shows how to utilise this model for the prediction of refrigerant transport properties, heat transfer coefficients and pressure drops.

Chapter 7 contains the conclusions drawn from the current research; some specific suggestions are made for future work.

References to the literature are included.

Appendices contains the lists of programs and correlations.

Chapter 2

LITERATURE REVIEW

2.1   Introduction

The aim of this chapter is to examine available correlations for two-phase heat transfer coefficients and pressure drops for refrigerants in horizontal tubes for use in a computational model. Before the final model for a Dx evaporator can be established, the following steps are used to describe the flow qualitatively and review the historical development of correlations for two-phase heat transfer coefficients and pressure drops.

Firstly, a flow pattern model will describe the different types of fluid flow, to illustrate the vapour quality of fluids in a horizontal tube. Secondly, a typical equation for single phase heat transfer coefficient and a development of correlations for two-phase heat transfer coefficients of fluids is presented. A review of two-phase flow for pressure drops, via homogenous and separate models, is necessary because pressure drops affect the heat transfer capability of fluids. This chapter also introduces the development of some numerical equations for testing the fluids to be modelled, namely R12 and R134a. Finally, a summary leading to objectives of this study are presented.

2.2   Flow patterns

The flow patterns observed in two-phase flow in a horizontal tube which are given by Alves (1954) and are divided into several flow regions, see Figure 2.1. This Figure shows a horizontal tubular channel heated by a uniform low heat flux and fed with liquid at saturated temperature. As the enthalpy rises, the fluid will change from liquid to vapour state. The volumetric flow will increase due to decreased density with constant mass flow rate. As the cross-sectional area of tube is constant, the vapour velocity will increase along the tube.

In Figure 2.1, the sequence of flow patterns shown corresponds to a relatively low inlet velocity. It is noted that, from a heat transfer point of view, there is the possibility of intermittent drying and re-wetting of the upper surface of the tube in wavy flow and the progressive drying out over long tube lengths of the upper circumference of the tube wall in annular flow. At higher inlet liquid velocities the influence of gravity is less obvious, the phase distribution becomes more symmetrical; in other words, the tube wall is surrounded by a liquid film in annular flow.
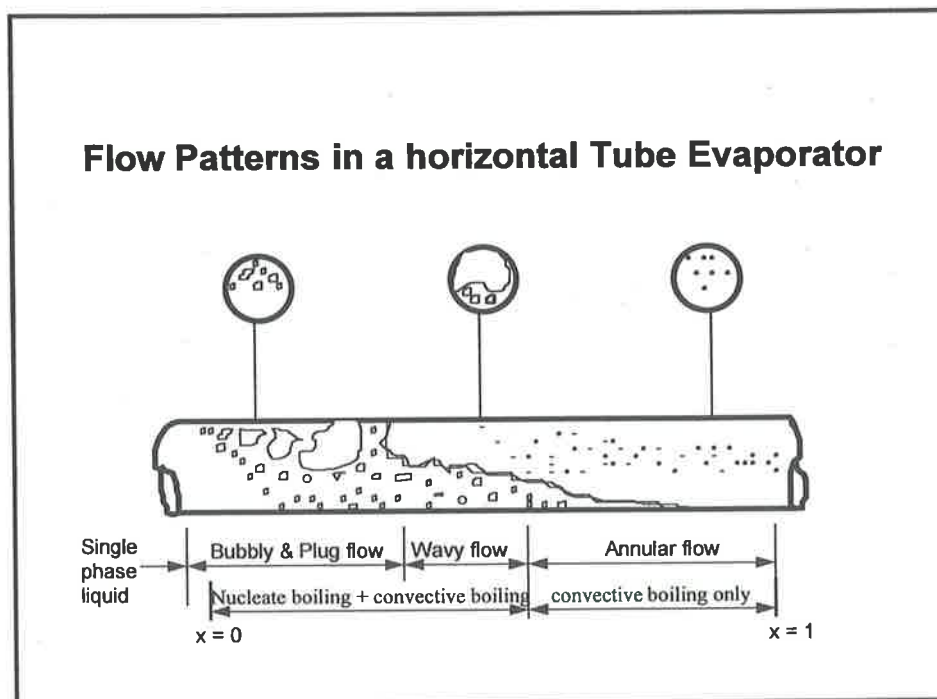
Figure 2.1 - Flow patterns in a horizontal tube evaporator

Regions are classified by Alves (1954) as:

- Bubbly and plug flow - in bubbly flow, the vapour phase is distributed as discrete bubbles in a continuous liquid phase. At one extreme the bubbles may be small and spherical and at the other extreme the bubbles may be large with a spherical cap and a flat tail; the vapour bubbles tend to travel in the upper half of the pipe. At moderate velocities of both vapour and liquid phases the entire pipe cross-section

contains bubbles, while at still higher velocities a flow pattern is equivalent to the whispy-annular pattern.

- Wavy flow - as the vapour velocity is increased the interface becomes disturbed by waves travelling in the direction of the flow. A further increase in vapour velocity causes the waves to be picked up to form a slug which is propagated along the channel at a high velocity. The upper surface of the tube behind the wave is wetted by a residual film which drains into the bulk of the liquid.

- Annular flow - a still higher vapour velocity will result in the formation of a gas core with a liquid film around the periphery of the tube. The film may or may not be continuous around the entire circumference but it will be thicker at the base of the pipe.

Additionally,

- when vapour quality is greater than 1, the fluid is superheated vapour in mist flow. Beyond this point, the wall may become dry and the wall temperature usually rises significantly for a particular heat flux.

2.3 Correlations for two-phase heat transfer coefficient

Over the past 30 years, many researchers have used different types of the theoretical or experimental approaches to establish their correlations. In practical boiling tubes, when very high mass velocities are absent, the two-phase heat transfer coefficient is most likely to be associated with the annular flow pattern. Heat is transferred by conduction and convection through the liquid film and vapour is generated continuously in the interface.

One of the earliest equations used for fully developed turbulent flow heat transfer in a smooth tube is the Dittus-Boelter (1930) equation. Dittus-Boelter's single-phase heat transfer equation is as follows:

$$h_l = 0.023 \frac{k_l}{D} \text{Re}_l^{0.8} \text{Pr}_l^{0.4} \tag{2.1}$$

where:

k_l = Thermal conductivity (W/m)

Re_l = Reynolds number = $\dfrac{uD\rho}{\mu}$

Pr_l = Prandtl number = $\dfrac{C_p \mu}{k}$

C_p = specific heat capacity of fluid (kJ/kg K)

D = diameter of tube (m)

u = velocity of fluid (m/s)

h_l = single phase heat transfer coefficient (W/m^2 K)

μ = viscosity of fluid (kg/m s)

ρ = density of fluid (kg/m^3).

Subscript

l = liquid.

This equation was based on experimental data covering the Prandtl number range 0.7 to 120, Reynolds numbers from 10,000 to 120,000 and L/D >60. In a tube, the Reynolds number is used as a criterion for judging the laminar to turbulent flow transition. If Re is greater than 2,300, the flow is usually observed to be turbulent. The Dittus-Boelter equation is still a very good approximation to the available experimental data for this range of variables. Although it is a single phase flow equation, it is widely used in correlation for two-phase heat transfer coefficients.

Lockhart and Martinelli (1947) presented a correlation of data for isothermal two-phase, two component flow in pipes and defined four types of flow mechanisms, namely: turbulent-turbulent, viscous-turbulent, turbulent-viscous and viscous-viscous. The four flow types were correlated by means of a parameter X which was equal to the square root of the pressure drop of the liquid to the pressure drop of the vapour, assuming each

phase flows separately. Although this correlation is for pressure drops and not for heat transfer, Lockhart and Martinelli's parameter X appears in many of the following heat transfer correlations (and so is mentioned here); these equations are discussed in detail in section 2.4.3.

Chen (1966) developed a correlation for two-phase heat transfer coefficient on the basis of six different data sources. The proposed correlation includes both the 'saturated nucleate boiling region' and the 'two-phase forced convection region' in Figure 2.1. It was assumed that both mechanisms occur to some degree over the entire range of the correlation and that the contributions made by the two mechanisms are additive. Chen's correlation is as follows:

$$h_{tp} = \underset{\substack{\text{saturated} \\ \text{nucleate boiling}}}{h_{nbc}N} + \underset{\substack{\text{two-phase} \\ \text{forced convective}}}{h_l F} \qquad (2.2)$$

where:

h_{tp} = two-phase heat transfer coefficient

h_{nbc} = heat transfer coefficient due to saturated nucleate boiling region

N = nucleate boiling suppression factor

h_l = Dittus-Boelter's equation for single phase heat transfer coefficient

F = two-phase enhancement factor.

In the 1970s, the correlation developed by Chen was the best available for saturated forced convective boiling regions and was recommended for use with all single component non-metallic fluids. For a given heat flux, the proper treatment of the heat flux dependence of N accounts for the decrease in the nucleate boiling contribution with increasing quality. In other words, as the vapour quality increases, the nucleate boiling contribution is suppressed. In the convective region, as the vapour quality increases, the two-phase enhancement factor, F is proportionally increased with quality. The correlation is satisfactory for horizontal conduits provided all surfaces of the channel

11

remain wetted and provided stratification is not severe. Since the correlation predicted coefficients lower than measured with the boiling refrigerants, Gouse and Dickson (1965) suggested that the correlation be re-optimised for horizontal conduits.

Dittus-Boelter (1930), Lockhart and Martinelli (1947) and Chen (1966) contributed the early important correlations for two-phase flow heat transfer coefficient inside boiling tube flow. Although Chen's correlation was only applied to some particular fluids, it was commonly accepted in heat transfer fields. Shah (1982) presented a generalised correlation for two-phase heat transfer coefficients using 780 data points from experimental studies of eight fluids. Recently, Kandlikar (1990) presented an another generalised correlation for two-phase heat transfer coefficient based on 5,246 data points from twenty-four experimental investigations using ten fluids. Jung and Radermacher (1989) also developed their correlation by using Dittus-Boelter's single phase correlation for heat transfer coefficient and modified Chen's correlation for two-phase heat transfer coefficient.

The correlations which were examined in detail, for possible inclusion into the computational model are reviewed below.

2.3.1 Shah

Shah (1982) developed a generalised correlation for two-phase heat transfer coefficient based on 780 data points from 19 independent experimental studies. His results which had a mean deviation of 14% for eight different fluids were correlated based on different regimes of boiling. The regimes include a nucleate boiling, a convective boiling, and a bubble suppression regime in which both bubble nucleation and convective effects are significant. The Shah (1982) correlation is:

$$h_{tp} = \psi h_l \qquad (2.3)$$

where:

h_l = single phase heat transfer coefficient from the Dittus-Boelter correlation

h_{tp} = two phase heat transfer coefficient (W/m^{2}K).

The parameter ψ can be found from equations that are functions of the boiling number, Bo, and convective number, Co. The boiling and convective numbers are used to determine the two-phase enhancement factor, F and boiling suppression factor, N in fluid flows. Finally, the value for ψ can be determined as the largest values of nucleate boiling ψ_{nb}, convective boiling ψ_{cb} or boiling suppression ψ_{bs}.

Where F, the two-phase enhancement factor is determined from the following:

for Bo$\geq 11\times10^{-4}$ *then F = 14.7*

for Bo$< 11\times10^{-4}$ *then F = 15.43*

and N, boiling suppression factor can be determined from the following:

For horizontal tubes:

$N = Co$

For horizontal tubes with $Fr_l \leq 0.04$ then

$N = 0.038 Fr_l^{-0.3} Co.$

For N>1.0

$\psi_{nb} = 230 Bo^{0.5}$ *for* Bo$>0.3\times10^{-4}$

$\psi_{nb} = 1 + 46 Bo^{0.5}$ *for* Bo$<0.3\times10^{-4}$

$\psi_{cb} = 1.8/N^{0.8}$

For 0.1<N≤1.0

$\psi_{bs} = F Bo^{0.5} exp(2.74 N^{-0.1})$

For N≤1.0

$\psi_{bs} = F Bo^{0.5} exp(2.74 N^{-0.15}).$

where:

Bo = boiling number = $\dfrac{q}{G\,i_{fg}}$

Co = convective number $= \left(\dfrac{1-x}{x}\right)^{0.8}\left(\dfrac{\rho_v}{\rho_l}\right)^{0.5}$

q = heat flux (W/m^2)

G = mass flux (kg/m^{2}s)

i_{fg} = latent heat of vaporisation (J/kg)

x = vapour quality

ρ_l = liquid density (kg/m^3)

ρ_v = vapour density (kg/m^3).

Shah did not break up his correlation into nucleate boiling and convective boiling terms. However, he used Chen's two-phase enhancement factor, F for convective boiling and nucleate boiling suppression factor, N to determine which boiling regime dominates the flow. It should be noted that of the 60 experimental points, only 6 are found to be within the bubble suppression regime with the others in the convective regime. This meant that the Shah correlation is appropriate for high vapour quality and low heat flux rather than low vapour quality and high heat flux as in Figure 2.2.

2.3.2   Jung and Radermacher

The Jung and Radermacher (1989a) correlation was developed on both pure and mixed refrigerants using a modified form of the Chen (1966) correlation. Since the results support Chen's (1966) supposition that the two-phase heat transfer coefficient can be predicted by superimposing the two contributions, nucleate boiling contribution, h_{nbc} and convective evaporation contribution, h_{cec}. The original form of Chen's correlation was retained. This final correlation for pure refrigerants became:

$$h_{tp} = h_{nbc} + h_{cec} = Nh_{sa} + Fh_l \tag{2.4}$$

where:

h_{nbc} = heat transfer coefficient due to the nucleate evaporation contribution

h_{cec} = heat transfer coefficient due to the convective evaporation contribution

N = a boiling suppression factor

h_{sa} = a pool boiling heat transfer coefficient

F = two-phase enhancement factor

h_l = a single-phase heat transfer coefficient for liquid-only flow.

The nucleate boiling term, h_{sa} is based on the pool boiling heat transfer coefficient obtained by Stephan and Abdelsalam (1980). They stated that in order to set up correlations with wide application, the method of regression analysis was applied to the nearly 5000 existing experimental data points for natural convection boiling heat transfer. As demonstrated by the analysis, these data can be best represented by sub-dividing into four different fluids and employing a different set of dimensionless numbers for each fluid. The nucleate boiling term, h_{sa} is multiplied by a suppression factor, N which is based on the Lockhart-Martinelli (1947) parameter, X_{tt} and boiling number, Bo. The amount of heat flux is dependent on N which accounts for the decrease in the nucleate boiling contribution with increasing vapour quality for a given heat flux.

The convective evaporation term, h_{lo} is based on the single-phase heat transfer coefficient obtained by the Dittus-Boelter (1930) correlation. This term is multiplied by a two-phase enhancement factor, F which is based on the Lockhart-Martinelli (1947) parameter only. The Lockhart-Martinelli parameter, X_{tt} correlated the ratio between the two-phase flow and single phase liquid heat transfer coefficients by applying the Reynolds analogy. The form of this correlation is as follows:

$$\frac{h_{tp}}{h_l} = f(X_{tt}).$$
(2.5)

On the other hand, it was observed that nucleate boiling could occur simultaneously with evaporation along an extensive liquid-vapour interface. The boiling number, Bo is introduced to account these effects into the form of equation (2.6) as follows:

$$\frac{h_{tp}}{h_l} = f(X_{tt}, Bo) \,. \qquad (2.6)$$

Chen (1966) proposed a correlation based on the superposition of heat transfer coefficients due to nucleate and convective boiling effects as follows:

$$h_{tp} = Sh_{nb} + Fh_l \qquad (2.7)$$

where S is a suppression factor and F is a function of X_{tt}. It can be noted that F may assume similar characteristics as $f(X_{tt})$ in Equation (2.5).
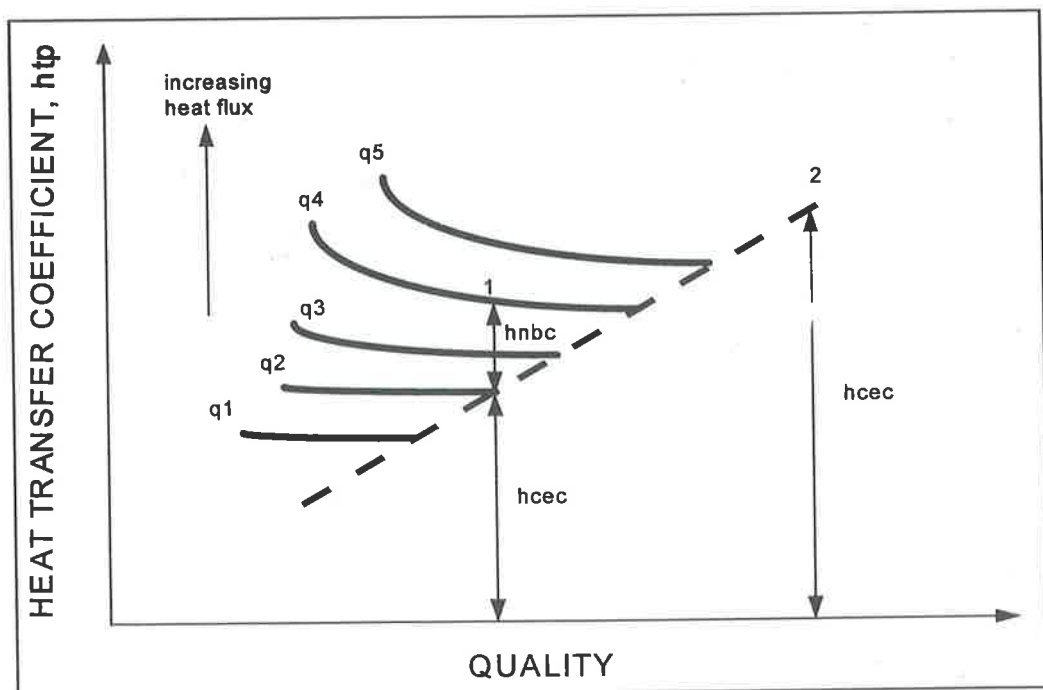
Figure 2.2 - *Nucleate boiling and convective evaporation contributions in two-phase heat transfer coefficient*

Jung and Radermacher's results indicated that nucleate boiling was fully suppressed at qualities greater than 20% for all pure refrigerants studied. In the partial boiling region, the quality of less than 20%, (line 1 in Figure 2.2), the heat transfer coefficients were

strongly influenced by the heat flux. Once the heat flux was increased from q1 to q5, the heat transfer coefficients due to nucleate boiling contribution, h_{nbc} were also increased. However, the heat transfer coefficient due to the convective boiling contribution, h_{cbc} was independent of heat flux in the convective evaporation region, which extends from 20% to 90% (line 2 in Figure 2.2). Hence, in the convective region, heat transfer coefficients at various heat fluxes merged into a single line, depending only upon such flow parameter as quality, as shown in Figure 2.2. Furthermore, heat transfer coefficient in the convective region increases in proportion to quality.

2.3.3 Kandlikar

Kandlikar (1990) presented a generalised correlation based on 5246 data points from 24 experimental investigations using ten fluids. This correlation is presented in terms of the convective number, Co, and several empirically determined constants, C_1 and C_2 for the convective term. The nucleate boiling term consists of the boiling number, Bo, several empirically determined constants, C_3 and C_4, and a fluid specific term, F_{fl}. This correlation consists of convective boiling and nucleate boiling terms as follows:

$$\frac{h_{tp}}{h_l} = \underbrace{C_1 Co^{C_2}}_{\substack{\text{convective} \\ \text{boiling term}}} + \underbrace{C_3 Bo^{C_4} F_{fl}}_{\substack{\text{nucleate} \\ \text{boiling term}}} \qquad (2.8)$$

where:

h_{tp} = two-phase heat transfer coefficient

C_1-C_4 = empirical constants (dimensionless)

Co = convective number = $\left(\dfrac{1-x}{x}\right)^{0.8}\left(\dfrac{\rho_v}{\rho_l}\right)^{0.5}$

Bo = boiling number = $\dfrac{q}{Gi_{fg}}$

h_l = single phase heat transfer coefficient with only the liquid fraction flowing in the tube

F_{fl} = fluid specific term

ρ = density, kg/m^3

q = heat flux, W/m^2

G = mass flux, kg/m^{2}s

i_{fg} = latent heat of vaporisation.

Table 2.1 - Constants in Kandlikar's correlation

Constants	Convective Region (Co<0.65)	Nucleate Boiling Region (Co>0.65)
C_1	1.1360	0.6683
C_2	-0.9	-0.2
C_3	667.2	1058.0
C_4	0.7	0.7

Initially, the data was divided into two regions as follows:

Co<0.65 - convective boiling region

Co>0.65 - nucleate boiling region.

A discontinuity at Co = 0.65 between two regions was presented by the Shah correlation. This discontinuity is eliminated in the Kandlikar correlation by allowing the transition from one region to another at the intersection of the respective correlations. The heat transfer coefficient at any given condition is evaluated using two sets of constants for the two regions. Since the transition from one region to another occurs at the intersection of the respective correlations, the higher of the two heat transfer coefficient values represents the predicted value from the proposed correlation. This method provides a continuity between the convective and nucleate boiling regions.

In the nucleate boiling region, the heat transfer is predominantly via the nucleate boiling mechanism. Similarly, in the convective region, the heat transfer is predominantly by a convective mechanism. The influence of heat flux in the two regions is explained as follows:

- **Nucleate boiling term**

  The constant C_4 in the Equation (2.8) is the exponent to the boiling number Bo in the nucleate boiling term. It is 0.7 for both convective and nucleate boiling regions. The nucleate boiling contribution to heat flux q is therefore proportional to $q^{0.7}$. The mechanism for the nucleate boiling in two-phase flow can be related to pool boiling. When a pool of liquid at saturated temperature is heated by electrically heated wires or a flat plate, the temperature of the region of pool boiling is usually lower than that of the partial film boiling. The heat transfer coefficient in pool boiling can be expressed as $h \propto q^n$. The value of the exponent n is 0.7 as given in two correlations recommended by Borishanski (1969) and Ratiani and Shekriladze (1972). It is seen that the nucleate boiling term shows dependence on q similar to the case of pool boiling.

- **Convective boiling term**

The dependence of the convective boiling term on quality is investigated in the two regions. In the convective boiling region, the exponent C_2 of Co is -0.9, and along with the $Re_l^{0.8}$ in the h_l expression, the convective boiling term varies as $x^{0.72}(1-x)^{0.08}$. However, this dependence should not be viewed in isolation, since the nucleate boiling contribution varies as $(1-x)^{0.8}$. Combining these two contributions may result in a

different dependence of h_{tp} on x depending on the fluid and other system and operating parameters. The exponent C_2 of Co in the nucleate boiling region is -0.2 which is much weaker than the value -0.9 found in the earlier work by Kandlikar (1983). This weak dependence on Co is to be expected in the nucleate boiling region where convection is not the dominant mechanism of heat transfer. As Bo increases, the percentage contribution due to convective boiling decreases. At high heat fluxes the heat transfer is predominantly by the nucleate boiling mechanism. However, at low heat flux values, the convective contribution may be quite significant.

Table 2.2 - Fluid parameter F_{fl} in Kandlikar's correlation

Fluid	F_{fl}	Fluid	F_{fl}
Water	1.00	R113	1.10
R11	1.30	R114	1.24
R12	1.5	R152a	1.10
R13B1	1.31	Nitrogen	4.70
R22	2.20	Neon	3.50
R134a	1.63		

The Kandlikar correlation is able to calculate the heat transfer coefficient for any given condition. Equation (2.7) is calculated using both sets of coefficients C_1-C_4 in Table 2.1 and fluid parameters in Table 2.2. The transition from nucleate boiling region to convective boiling region occurs at the intersection of the respective correlations.

However, Souza *et al* (1992) found that although Kandlikar's correlation predicted their data well, the effect of nucleate boiling on the heat transfer coefficients was overpredicted. The experimental heat transfer coefficients were accurately correlated

based on convective boiling effects alone, hence refuting the possibility of strong effects of nucleate boiling in the range of parameters considered in their study.

2.3.4 Eckels and Pate

Eckels and Pate (1990) compared the heat transfer coefficients of R134a and R12 in two-phase and single phase evaporation tests using existing correlations. They found that single heat transfer coefficients for R134a are significantly higher than those for R12. As compared to the heat transfer coefficient for R12, the prediction for the heat transfer coefficients for R134a is increased from 27% to 38% based on the liquid refrigerant temperature; the prediction for vapour is increased from 37% to 45%. These increases in heat transfer coefficients are mainly a result of the increased liquid and vapour thermal conductivity of R134a. Also, two-phase heat transfer coefficients for R134a are higher than those of R12 by 28% to 40% depending on the refrigerant temperature, the tube diameter and length. It was summarised that an increase of about 33% for heat transfer coefficients of R134a was observed when compared with R12 during evaporation. This increase can be slightly larger for longer tubes, small diameter tubes and higher temperatures. For evaporation, an increase in the tube length from 5 m to 30 m changed the R134a to R12 heat transfer coefficient ratio from 1.34 to 1.36. A decrease in outside diameters from 12.7 mm to 6.35 mm changed the ratio from 1.32 to 1.36. Temperature affected evaporation; by varying the ratio from 1.29 to 1.34 for a temperature range of -5°C to 10°C. As a design parameter, the ratio of the R134a and R12 heat transfer coefficients should be 1.33.

The heat transfer comparisons do not include the effect of lubricants that circulate in actual refrigeration systems. Specifically, the correlations used to estimate the R134a and R12 heat transfer coefficients were developed for pure refrigerants only. Research indicates that lubricants do have an effect on evaporation of refrigerants and therefore,

experimental studies are needed to determine the effect of lubricants on R12 and R134a heat transfer.

2.3.5 Summary of heat transfer correlations

The historic development of the correlations for two-phase heat transfer coefficients has been introduced. Different correlations are recommended for use in different applications - the following table summarises the details:

Table 2.3 - A summary of correlations for flow boiling heat transfer inside tubes. Mean deviations are derived from the comparisons of Jung and Radermacher's experimental data with their correlation, Chen's , Kandlikar's and Shah's correlations.

Correlation	Fluid	Test rig	Accuracy (mean deviation)	Limit of applicability
Jung and Radermacher (1989) $h_{tp} = Nh_{sa} + Fh_l$	Pure refrigerants	$\phi 8$ mm, 7.96m long, horizontal tube	7 %	Pure refrigerants only
Chen (1966) $h_{tp} = h_{nbc}N + h_l F$	Water, methanol, cyclolerane pentane	Vertical flow	12 %	Vertical pipe only
Kandlikar(1983) $\dfrac{h_{tp}}{h_l} = C_1 Co^{C2} + C_3 Bo^{C4} F_{fl}$	Water, R11, R12, R114, N_2, Ne	Vertical & horizontal flow	17.1 %	inaccuracy
Shah (1982) $h_{tp} = \psi h_l$	Water, R11, R12, R22 & R113	Vertical & horizontal tube	30 %	inaccuracy

2.3.6 Directions for this study

The above summary, shows that the Jung and Radermacher's correlation has the smallest deviation in predicting experimental results whilst the Shah correlation has the largest. This means that the Jung and Radermacher correlation is good for predicting two-phase heat transfer coefficients of pure refrigerants in horizontal tubes. The Jung and Radermacher correlation will be adopted in this computational scheme because it is the most updated and reliable for the requirements. Jung and Radermacher (1989a) reported that less than 10% deviations in predicting the heat transfer coefficients of refrigerants,R12 and R134a in a horizontal tube, therefore, their correlation is suitable to be used in AuCFD. The computational comparisons of the performance of Jung and Radermacher, Shah and Kandlikar 's correlations will be evaluated in Chapter 5.

2.4   Correlation for two-phase pressure drops

In horizontal tubes, the two-phase pressure drop during boiling flow is composed of two components, ΔP_f and ΔP_a which are the frictional and the accelerational pressure drops respectively. It is essential to know the void fraction (the ratio of gas flow area to total flow area) to compute the accelerational component. To compute the frictional component of the pressure drop, either the two-phase friction factor or the two-phase frictional multiplier must be known.

There have been two types of frictional pressure drop models in two-phase flow via homogeneous and separate flow models. In the homogeneous models, the flow of both gas and liquid velocities are assumed equal (slip ratio = 0). The frictional pressure drop is calculated as if the flow was single-phase, except for introducing modifiers to the properties inside the single-phase friction coefficient. In the separated flow model, the two phases are considered separate and the velocities may differ.

2.4.1 Homogenous models

The homogeneous models assume that both liquid and vapour phases move at the same velocity; consequently, it has also been called zero slip models. They consider the two-phase flow as a single phase flow having average fluid properties depending on quality. Thus, the frictional pressure drop is calculated by assuming an average friction coefficient between the inlet and the outlet.

The pressure drop correlation, based on a homogeneous model, is Pierre's (1955) semi-empirical correlation. The correlation, equation (2.9) was developed based on the measured pressure drop data for R12 and R22 flowing inside 12 and 18 mm diameter tubes:

$$\Delta P_{BP} = \left[f_{av} + \frac{(x_2 - x_1)D}{x_{av}L} \right] \frac{G^2 L}{D \rho_{av}}$$
(2.9)

where:

$$f_{av} = 0.0185 K_f^{0.25} \text{Re}^{-0.25}$$
(2.10)

$$\rho_{av} = \frac{\rho_v \rho_l}{x_{av}\rho_l + (1 - x_{av})\rho_v}$$
(2.11)

$$K_f = \frac{J \Delta x h_{fg}}{L}$$
(2.12)

where:

x_{av} = average vapour quality = $(x_1 + x_2)/2$

K_f = Pierre's boiling number (N/kg)

J = mechanical equivalent of heat: 1 in SI units

h_{fg} = heat of evaporation (J/kg)

L = tube length (m)

ρ_l = liquid density (kg/m^3)

ρ_v = vapour density (kg/m^3)

ρ_{av} = average density (kg/m^3).

Equation (2.9) is valid only when $(Re/K_f) > 1$. $(Re/K_f) > 1$ is the case when heat flux is high with a small mass flux and hence the quality of vapour between inlet and outlet,

Δx, is relatively large; therefore, the Pierre correlation is not suitable for application to the computational scheme developed here. The Pierre correlation is also inapplicable to the entire range of heat and mass fluxes considered in this study in that it would not provide accurate pressure drop estimation in the low mass flux range ($G < 1300$ kg/m^{2}s).

2.4.2 Separate models

The separate models consider the two phases to be divided into liquid and vapour streams and thus has been referred to as slip flow models. They originated from the work of Lockhart and Martinelli (1947), which was followed by Martinelli and Nelson (1948). Collier (1981) found the empirical correlation of Martinelli and Nelson (1948) as reliable as any annular flow (see section 2.2) pressure drop correlation. Jung and Radermacher (1990) modified the Martinelli and Nelson correlation for two-phase pressure drops in horizontal tubes. Recently, Souza *et.al.* (1995) developed a new correlation for two-phase pressure drop for pure refrigerants inside tubes by modifying the Lockhart and Martinelli (1947) and Martinelli and Nelson (1948) separated flow models.

2.4.3 Lockhart and Martinelli

Lockhart and Martinelli (1947) proposed a correlation of data for isothermal two-phase, two-component flow in pipes.

$$\Delta P_f = \Delta P_{fa} \phi_{fu}^2 \tag{2.13}$$

$$\Delta P_{fu} = 4f \left(\frac{L}{D} \right) \frac{G_l^2 V_l}{2g} \tag{2.14}$$

$$X^2 = \frac{Re_v^m}{Re_l^n} \frac{C_l}{C_v} \left(\frac{m_l}{m_v}\right)^2 \frac{\rho_v}{\rho_l} \qquad (2.15)$$

(X, ϕ, etc. are described below with the aid of Tables 2.4 and 2.5.)

They presented flow mechanisms, namely turbulent-turbulent, viscous-turbulent, turbulent-viscous and viscous-viscous, flow as governed by the Reynolds numbers in Table 2.4, for liquid flow only and for the vapour flow only in the pipe.

Table 2.4 – Determination of flow mechanism of fluid

Flow mechanism	Subscript	Re_l	Re_v
Liquid *Gas*			
Turbulent – Turbulent	t-t	>2000	>2000
Viscous – Turbulent	v-t	<1000	>2000
Turbulent – Viscous	t-v	>2000	<1000
Viscous – Viscous	v-v	<1000	<1000

Table 2.5 – Determination of coefficients for Equation 2.15

	t-t	v-t	t-v	v-v
n	0.2	1	0.2	1.0
m	0.2	0.2	1.0	1.0
C_l	0.046	16	0.046	16
C_v	0.046	0.046	16	16

The procedures for using Equations 2.13, 2.14 and 2.15, Tables 2.4 and 2.5 and Figure 2.3 to evaluate two-phase frictional pressure drops, ΔP_f are as follows:

1. Determine liquid and vapour Reynolds numbers and use Table 2.4 to find out the mechanism of the flow.

2. In Table 2.5, determine the coefficients, n, m C_l and C_v based on the flow mechanism and substitute into Equation. 2.15 to evaluate parameter, X.

3. In Figure 2.3, use parameter, X to find the pressure drop multiplier, ϕ.

4. Substitute the above parameters into Equation 2.14 and 2.13 to evaluate ΔP_{fa} and ΔP_f respectively.

where:

D = diameter of the tube (m)

L = length of the tube (m)

f = friction factor (dimensionless)

g = acceleration of gravity (m/s^2)

G = mass flux (kg/m^{2}s)

ρ = density (kg/m^3)

m = mass flow rate (kg/s)

Re   = Reynolds number

V = specific volume of liquid (m^3/kg)

X = Martinelli parameter

ϕ = Martinelli pressure drop multipliers to be obtained from Figure 2.3 and substituted into equations of the type of Equation. 2.13 (Dimensionless)

ΔP_f = friction pressure drops (Pa)

ΔP_{fa} = friction pressure drop with liquid only flowing at its mass velocity (Pa)

Subscripts

l = liquid phase

v = vapour state

t = turbulent

v = viscous.

2.4.4 Martinelli and Nelson

One of the basic assumptions made by Martinelli and Nelson (1948) was that the static pressure drop of the liquid phase was the same as that of the vapour phase. In bubbly and plug flow, when the liquid phase dominates the flow, the pressure drop of the liquid

is higher than that of the vapour. However, when the vapour quality becomes 80% to 90% in annular flow, the pressure drop of the vapour is increased due to an increased proportion of the total mass of the fluid. The pressure drop of the vapour is similar to that of the liquid; because of this assumption, their model is better suited to the annular flow regions in a Dx tube. Many modifications have been made to the basic Martinelli and Nelson model. Their correlations, with or without modifications, have been applied to conditions much different from those assumed in the original work with fairly good success.

The Martinelli and Nelson correlation is shown as follows:

$$\Delta P_{MN} = \frac{2f_{fo}G^2L}{D\rho_l}\left[\frac{1}{x}\int_0^x \phi_{fo}^2\,dx\right] + \frac{G^2}{\rho_l}\left[\frac{x^2\rho_l}{\alpha\rho_v} + \frac{(1-x)^2}{(1-\alpha)} - 1\right] \qquad (2.16)$$

where

α = void fraction

f_{fo} = friction coefficient

ϕ_{fo} = frictional multiplier

G = mass flux (kg/m^{2}s)

x = vapour quality

ρ = density (kg/m^3)

D = diameter of the tube (m)

L = length of the tube (m).

The following key parameters were defined by Lockhart and Martinelli to show the pressure drop in Equations 2.17, 2.18 and 2.19. Assuming turbulent flow in both liquid

and vapour phases, Martinelli's parameter, X_{tt} was obtained from Equation (2.20). Lockhart and Martinelli correlated ϕ_{lo}, ϕ_{vo} and α as a function of X_{tt} and presented their results in a graphical form as Figure 2.3. Their correlation, however, was only valid for the adiabatic flow of low pressure mixtures of air and liquid.
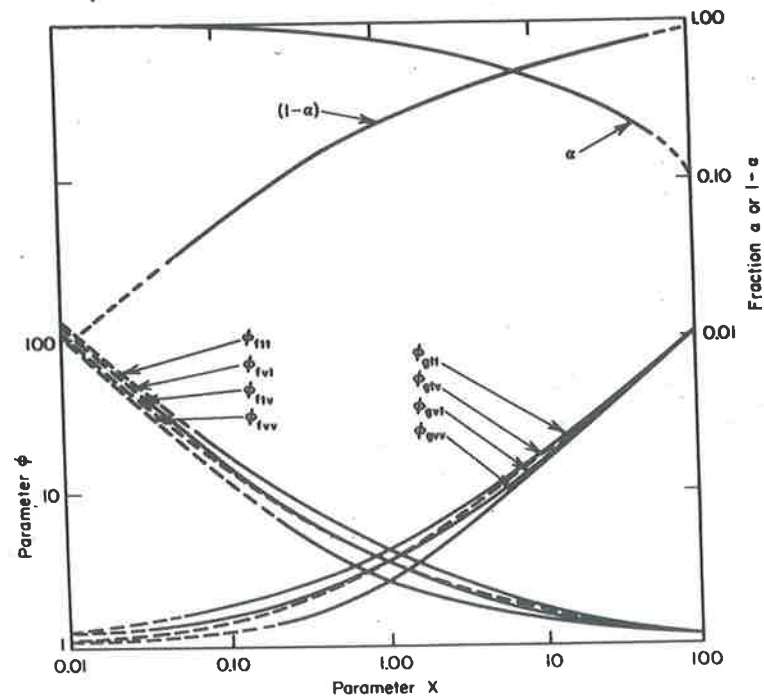
Figure 2.3 - *Void fraction and adiabatic friction multipliers for all fluids at about one atmosphere pressure*

$$\phi_{lo}^2 = \frac{\Delta P_f}{\Delta P_{fo}} \qquad (2.17)$$

$$\phi_{vo}^2 = \frac{\Delta P_f}{\Delta P_{vo}} \qquad (2.18)$$

$$X^2 = \frac{\Delta P_{lo}}{\Delta P_{vo}} \qquad (2.19)$$

$$X_{tt} = \left(\frac{1-x}{x}\right)^{0.9} \left(\frac{\rho_v}{\rho_l}\right)^{0.5} \left(\frac{\mu_l}{\mu_v}\right)^{0.1} \qquad (2.20)$$

where:

ΔP = pressure drop (Pa)

X = Martinelli parameter

ϕ = pressure drop multiplier

Subscripts

f = frictional

l = liquid

v = vapour

lo = liquid phase only flowing

vo = vapour phase only flowing

fo = total flow assumed as liquid

tt = turbulent-turbulent.

2.4.5 Jung and Radermacher

Jung and Radermacher (1989) measured 600 two-phase pressure drop data points during horizontal flow boiling of pure and mixed refrigerants of R12, R114, R12 and R152a. The range of heat flux was 10-45 kW/m^2 and mass flow rate was 16-46x10^{-3} kg/s. Jung and Radermacher compared their results with the well-known Pierre correlation and Martinelli and Nelson correlation. Pierre's correlation failed to predict half of their experimental data while Martinelli and Nelson's correlation overpredicted it by 20%. From the measured data, they found the accelerational pressure drop was determined to

be always less than 10% of the measured pressure drop. Thus, the frictional pressure drop would constitute most of the two-phase pressure drop in evaporators. Jung and Radermacher developed the correlation for two-phase pressure drops as follows:

$$\Delta P_{tp} \approx \Delta P_f \qquad (2.21)$$

$$\Delta P_{tp} = \frac{2 f_{fo} G^2 L}{D \rho_l} \left[\frac{1}{\Delta x} \int_{x_1}^{x_2} \phi_{tp}^2 dx \right] \qquad (2.22)$$

$$\phi_{tp}^2 = 30.78 x^{1.323} (1-x)^{0.477} pr^{-0.7232} \qquad (2.23)$$

where:

ΔP_{tp} = two-phase pressure drop (Pa)

ΔP_f = frictional pressure drop (Pa)

f_{fo} = friction factor

G = mass flux (kg/m^{2}s)

L = tube length, (m)

D = diameter (m)

ρ = density (kg/m^3)

x = vapour quality

Δx = quality change between inlet and outlet = x_2-x_1

ϕ_{tp} = two-phase pressure drop multiplier

Pr = reduced pressure = critical pressure / saturated pressure.

They developed a simple correlation with a chart (Figure 2.4) to aid the estimation of pressure drop during flow boiling.
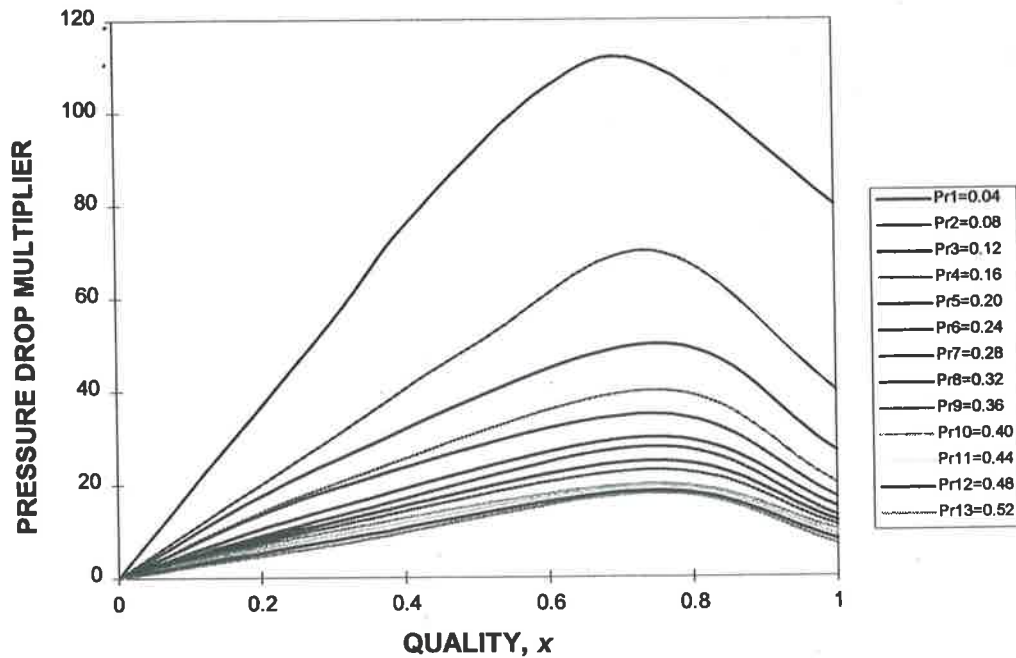
Figure 2.4 - *Two-phase pressure drop multiplier, ϕ_{tp}, as a function of quality for various reduced pressures.*

2.4.6 Souza *et al*

Souza *et.al.* (1993) developed a new correlation for two-phase frictional pressure drop for pure refrigerants inside smooth tubes by modifying the Lockhart and Martinelli (1947) and Martinelli and Nelson (1948) separated flow models to include a Froude number, Fr_l. The Froude number plays an important role in the correlation when body forces and inertia forces are significant in the flow, i.e. for stratified or wavy flow regimes. As in the case of two-phase flow, a strong influence of the mass flow rate was represented by the Froude number. From their test results, the correlation predicted the frictional pressure drop of R12 and R134a data as a function of X_{tt} and Fr_l with a mean deviation of 4.6%. Also, with the proposed frictional pressure drop correlation and a suggested acceleration model in flow boiling, the correlation predicted the experimental data well with a mean deviation of 6.2%. The total pressure drop during two-phase flow inside a horizontal tube is developed as follows:

$$\Delta P_{tp} = \Delta P_f + \Delta P_a \qquad (2.24)$$

$$\Delta P_f = \Delta P_{lo}\left(\frac{1}{\Delta x}\int \phi_{lo}^2 dx\right) \qquad (2.25)$$

$$\phi_{lo}^2 = (1.376 + C_1 X_{tt}^{-c_2})(1-x)^{1.75} \qquad (2.26)$$

where:

For $0 < \mathrm{Fr}_l \Leftrightarrow 0.7$

$\qquad C_1 = 4.172 + 5.480 \ \mathrm{Fr}_l - 1.564 \ \mathrm{Fr}_l^2$

$\qquad C_2 = 1.773 - 0.169 \ \mathrm{Fr}_l$

For $\mathrm{Fr}_l > 0.7$

$\qquad C_1 = 7.242$

$\qquad C_2 = 1.655$

$$\Delta P_a = G^2\left\{\left[\frac{x_o^2}{\rho_o \alpha_o} + \frac{(1-x_o)^2}{\rho_l(1-\alpha_o)}\right] - \left[\frac{x_l^2}{\rho_l \alpha_l} + \frac{(1-x_l)^2}{\rho_l(1-\alpha_l)}\right]\right\}. \qquad (2.27)$$

The overall pressure drop due to acceleration can be obtained by the application of a simplified momentum equation, in which the vapour and liquid velocities are assumed to be uniform in each phase.

2.4.7 Souza and Pimenta

Souza and Pimenta (1995) developed a new correlation for two-phase frictional pressure drop inside horizontal straight tubes for pure and mixed refrigerants using the separated flow model, the Lockhart-Martinelli parameter, X_{tt} and an adequate property index, τ. The Froude number in Souza *et.al.*'s previous correlation was good for stratified or

wavy flow regimes with lower mass fluxes. As the predominant flow pattern observed for most of the tests with higher mass fluxes was the annular flow pattern, the Froude number was replaced by the property index, τ. The final correlation for two-phase flow multiplier has the following form:

$$\phi_{lo}^2 = 1 + \left(\tau^2 - 1\right)x^{1.75}\left(1 + 0.9524\tau X_{tt}^{0.4126}\right) \tag{2.28}$$

$$\tau = \left(\frac{\rho_l}{\rho_v}\right)^{0.5}\left(\frac{\mu_v}{\mu_l}\right)^{0.125}. \tag{2.29}$$

When their results from the new correlation in equations (2.24) to (2.29) were compared with the obtained experimental data from Souza *et.al.*, the mean relative error or mean deviation for the frictional pressure drop correlation was 8.2%.

2.4.8 Summary of Pressure Drop Correlations

The historic development of the correlations for two-phase pressure drops has been introduced. The researchers used different models to develop their own correlations which were summarised as follows:

Table 2.6 - A summary of correlations for two-phase pressure drops

Researcher	Correlation	Comments
Lockhart and Martinelli (1947)	Refer to Equations (2.13) to (2.15)	First separate model - correlation used four flow mechanisms as governed by Reynolds numbers.
Martinelli and Nelson (1948)	Refer to Equations (2.16) to (2.20)	Separate model - correlation modified from Lockhart and Martinelli and the graph for frictional multiplier as a function of pressure and vapour quality developed.
Pierre (1964)	Refer to Equations (2.9) to (2.12)	Homogenous model - correlation failed to predict half of the Jung's experimental data
Jung and Radermacher (1989b)	$\Delta P_{tp} \approx \Delta P_f$	Separate model -correlation modified from Martinelli and Nelson but accelerational pressure drop was excluded.
Souza *et al* (1993)	$\Delta P_{tp} = \Delta P_f + \Delta P_a$	Separate model - correlation modified from Martinelli and Nelson and accelerational pressure drop was included. Froude number was used.
Souza and Pimenta (1995)	$\Delta P_{tp} = \Delta P_f + \Delta P_a$	Separate model - correlation modified from Martinelli and Nelson and accelerational pressure drop was included. The property index was used.

2.4.9 Directions of this study

Due to limitations in Pierre's correlation, namely a requirement for high heat flux and low mass flux, this homogenous model (the only accepted) is not suitable for two-phase

model development. Of the separate flow models; Jung and Radermacher (1989b) presented that the correlation for pressure drop had a 8.4% mean deviation of their test results, therefore their correlation is tested in Chapter 5 to establish whether it is suitable for the computational scheme developed as part of this study. Souza *et al* modified Martinelli and Nelson's graphical method into a numerical equation using the Froude number, Fr_l however, the number was not suitable for the higher mass flux flow in most of their tests. With the use of property index, τ, Souza and Pimenta's (1995) correlation was better for the higher mass flow which was the same separate model as Jung and Radermacher. Both correlations from Jung and Radermacher and Souza and Pimenta are also concerned with the two-phase heat transfer coefficients of refrigerants R12 and R134a flowing in a horizontal tube, therefore these correlations were used for this study.

2.5 Equations for refrigerant properties

Chan and Haselden (1981) presented the basic equations for refrigerant transport properties. They developed their computer-based refrigerant thermodynamics properties in three parts: basic equations, program listing and use of the program in the computation of standard refrigeration cycles. Part 1 described a set of computer-based methods for calculating densities, vapour pressures, enthalpies, internal energies and entropies of refrigerants. They also presented the derivations of the basic equations for refrigerants R11, R12, R13, R13B1, R14, R22, R113, R114, and R502 as used by the IIR (International Institute of Refrigeration) in its latest charts. In part 2, listings were presented for a set of computer subroutines to enable specific volume, vapour pressure, internal energy, enthalpy and entropy to be calculated for ten different refrigerants. The values were based on the IIR equations. In part 3, the first program listed provides for the user to call up the thermodynamic properties of one of the stored refrigerants at a specified temperature (and pressure). The second program calculates the performance of a vapour compression refrigeration cycle for the specified refrigerant operating between given values of the evaporator and condenser temperatures. The computer routines developed by Chan and Haselden for evaluation of refrigerant thermodynamic properties, whilst widely used, were not suitable for some types of refrigeration computer programs due to large computation time requirements. Cleland (1986) proposed an alternative in the form of curve-fitted equations with greater computer speed. A possible application was in the area of dynamic simulation where many thousands of property evaluations must be made in every program execution. The proposed equations cover R12, R22, R502, R717, over a wide range of practical

conditions. The accuracy of the property estimated from the proposed equations should be adequate for most practical situations, but the equations should not be seen as a general replacement for the Chan and Haselden routines.

Jung and Radermacher (1991) presented a compilation of experimental data and predictive methods for viscosities, thermal conductivities, and surface tension of halogenated pure and mixed refrigerants. A variety of estimating methods was tested against the reliable measured data. Their results indicated that more fundamental theory was needed, especially to predict transport properties of liquids. A large scatter was observed among various thermal conductivity data, and more accurate data needed to be measured to develop a general predictive method for this property. Finally, the combination of experimental data and prediction methods would be sufficient to help engineers and researchers in the refrigeration field design and develop new equipment using ozone-safe pure and mixed refrigerants.

The equations for saturated pressure, saturated temperatures, liquid and vapour enthalpies of the refrigerants, R12 and R134a from Cleland will be used in the computational scheme developed because of their simplicity and accuracy. On the other hand, Jung and Radermacher (1991) recommended that equations 2.30, 2.31, 2.32 and 2.33 for R12 and R134a developed by the other researchers be used for calculating transport properties in a horizontal tube. In 1986, Nagaoka *et al* developed a general empirical correlation for the viscosity of gaseous fluorocarbon refrigerants. They have

tested Equation 2.30 against 116 data points of 16 halogenated refrigerants. The mean and maximum deviations found were 1.62% and 4.97%.

$$\mu\xi = (0.5124 T_r - 0.0517)^{0.82} z_c^{-0.81}$$ (2.30)

$$\xi = T_c^{1/6} M_w^{-1/2} P_c^{-2/3}$$ (2.31)

where:

μ = gas viscosity GPa s

ξ = viscosity parameter characteristic to each component

T_c = critical temperature K

T_r = reduced temperature K

P_c = critical pressure MPa

M_w = molecular weight

z_c = compressibility factor at critical point.

In 1970, Phillips and Murphy measured the liquid viscosity of 21 commonly used halocarbon refrigerants using a capillary viscometer. Their experimental data for pure components have been compared with other investigators' data and have shown to be in good agreement. Phillips and Murphy fitted their data to a four-constant equation with a deviation of 0.5%:

$$\log_{10} \mu = A + B/T + CT + DT^2$$ (2.32)

where temperature T, and viscosity, μ, are in Kelvin (K) and centiPoise (cP), respectively.

Yata $et\ al$ (1984) measured liquid thermal conductivities of 10 halogenated refrigerants in the temperature range of 204 K to 450 K. The accuracy of their results was estimated

to be better than 1.5%. They accounted for the effect of temperature by using a linear curve:

$$k_l = A + BT + CT^2 \qquad (2.33)$$

where k_l and T are in mW/m K and K respectively.

2.5.1 Summary of refrigerant properties used

The following Table 2.7 shows R12 and R134a properties used Phillips, Yata, and Nagaoka *et al*'s equations for calculating liquid viscosity, liquid thermal conductivity and vapour viscosity. The data for equations of R134a liquid viscosity and liquid thermal conductivity are provided by Shankland (1990). Most of the refrigerant properties are available from the existing literature. However, liquid densities of R12 and R134a are in tabulated form which cannot be used in computational studies. It is necessary to develop the polynomial equations for R12 and R134a's properties in Chapter 3. The equations used are summarized as follows:

Table 2.7 - Summary of the property correlations used

Property	R12	R134a
Liquid thermal conductivity	Yata (1984)	Shankland (1990)
Liquid viscosity	Phillips (1970)	Shankland (1990)
Liquid density	Au (see Chapter 3)	Au (see Chapter 3)
Liquid enthalpy	Cleland (1986)	Cleland (1986)
Liquid specific heat capacity	Au (see Appendix II)	Au (see Appendix III)
Vapour thermal conductivity	Au (see Appendix II)	Au (see Appendix III)
Vapour viscosity	Nagaoka *et al* (1986)	Nagaoka *et al* (1986)
Vapour density	Au (see Appendix II)	Au (see Appendix III)
Vapour enthalpy	Cleland (1986)	Cleland (1986)
Vapour specific heat capacity	Au (see Appendix II)	Au (see Appendix III)
Saturated pressure	Cleland (1986)	Cleland (1986)

CHAPTER 3

METHODOLOGY

This chapter contains three main themes. Firstly, different techniques which may be used for determining the equations of refrigerant properties and correlations for two-phase heat transfer coefficient and pressure drop, are reviewed to select suitable techniques for this study. Secondly, three issues in the validation of computational fluid dynamics codes namely empirics, round-off and discretization (order of solution) are presented. The solution technique for AuCFD is also determined here. Finally, an overall structure of the algorithm in the computational scheme, developed (AuCFD) as part of this study, is described.

3.1 Review of computational fluid dynamics and experimental techniques

The performance of a Dx-coil with refrigerant is based on many criteria - one crucial set of criteria is the fluid mechanical characteristics of the refrigerants. There are many approaches used for solving transport properties of refrigerants; generally, these approaches are divided into two categories: computational and experimental. Each approach has distinct advantages and unique disadvantages. Wendt (1991) indicated that the first generation of computational fluid dynamics solutions appeared during the 1950s and early 1960s spurred by the simultaneous advent of efficient, high-speed computers and the need to solve the high-velocity, high-temperature re-entry body problem in space flight. Such physical phenomena generally cannot be modelled analytically and numerical solutions of the governing equations on a high-speed digital computer were an absolute necessity.

Experimental techniques are considered to be extremely important and reliable. They are able to deal with different flow problems and flow in complicated geometries. They

can give accurate data at points where probes are inserted to take measurements. However, the aim of this research project is to design a computational scheme which can provide a quicker technique for solving two-phase flow problems in a Dx- coil for use as a design tool; computational fluid dynamics (CFD) can provide this tool. The transport properties, two-phase heat transfer coefficients and pressure drops of refrigerants can be easily estimated at any location within the Dx tube using CFD. Computational fluid dynamics also demonstrates some advantages and disadvantages as compared with experimental technique as follows:

Advantages:

- Computational techniques can be performed in a small space.

- A full picture of the two-phase flow of refrigerant inside a horizontal tube can be obtained.

- CFD is relatively cheap and provides a preliminary design stage for heat exchanger.

- CFD lends itself to the development of a design tool.

Disadvantages:

- Boundary and initial conditions - the results of CFD are only as valid as the physical models incorporated in the governing equations and boundary conditions, and hence are subject to errors.

- Truncation errors as well as round-off error are associated with the particular algorithm are used to obtain a numerical solution.

Both of these sources of errors combine to compromise the accuracy of CFD results. It is important to minimise these and to establish their numerical significance.

3.2   General CFD techniques

Basically, computational fluid dynamics is used to calculate the governing partial differential equations of fluid flow, and obtain a final numerical description of the complete flow field. The end product of CFD is a collection of numbers which is a

quantitative description of the characteristics of fluid flow. There are three main issues in computational fluid dynamics about which the techniques pivot via empirics, round-off and discretization (order of solution). Empirics rely on experiment or experience. In this study, a finite difference method is used to develop a unique empirical equation for solving the problems of two-phase heat transfers. Round-off and discretization are concerned with the accuracy of the empirical equation which depends on the number of iterations, the grid spacing and the order of solutions.

The finite difference method uses the fundamental governing equations of fluid dynamics. All dynamics of the fluid is based on the mathematical statements:

1. mass is conserved

2. $F = m\,a$

3. energy is conserved.

To obtain the basic equations of fluid motion, the following philosophy is always followed:

1. Select the appropriate fundamental physical principles from the laws of physics.

2. Apply these physical principles to a suitable model of the flow.

3. Extract the mathematical equations from the application which embody such physical principles.

3.2.1 Finite difference method

The finite difference method is widely used in CFD. The philosophy of the finite difference method is to replace the partial derivatives appearing in the governing equations of fluid dynamics with algebraic difference quotients. The numerical solutions of finite equations can give answers only at discrete points in the domain, called gridpoints. Figure 3.1 shows a section of a discrete grid in the xy plane. The spacing of the gridpoints in the x direction, Δl_x is uniform as is the spacing of the grid points in the y direction, Δl_y. The grid spacings are not required to be uniform in both or either direction and they may vary non-uniformly from one gridpoint to the next in either direction. In Figure 3.1, the gridpoints are identified by an index i which runs in the x direction. Therefore, if (i, j) is the index for any fluid dynamic parameter, θ, the immediate point to the right of (i, j) is labelled as $(i+1,j)$, the point to the left is $(i-1,j)$, the point directly above is $(i,j+1)$, and the point directly below is $(i,j-1)$. If θ represents a fluid parameter at gridpoint (i, j), the fluid parameter will be changed through the domain at various gridpoints based on the computational equations.
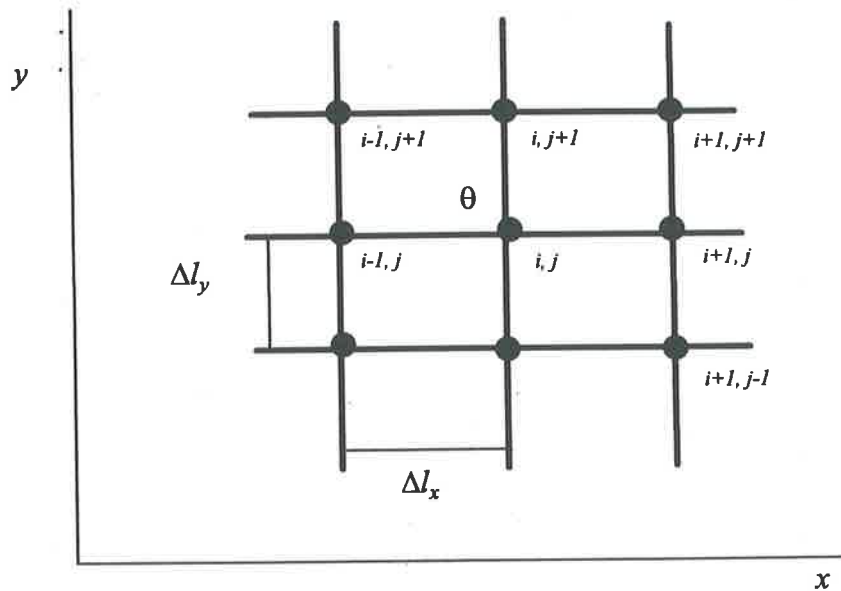
Figure 3.1 - General discrete grid points

Finite difference representations of derivatives may be based on a Taylor's series expansion about a point; if $\theta_{i,j}$ indicates the fluid property (θ) at point (i, j), the fluid property, $\theta_{i+1,j}$ at point ($i+1, j$) can be expressed as a Taylor series expanded in terms of the value of θ at point (i, j) as below:

$$\theta_{u+1,j} = \theta_{i,j} + \Delta l \frac{d\theta}{dl}\bigg|_{i,j} + \frac{(\Delta l)^2}{2} \frac{d^2\theta}{dl^2}\bigg|_{i,j} + \frac{(\Delta l)^3}{6} \frac{d^3\theta}{dl^3}\bigg|_{i,j} + \frac{(\Delta l)^4}{24} \frac{d^4\theta}{dl^4}\bigg|_{i,j} + \cdots \quad (3.1)$$

This assumes that θ varies with spatial co-ordinate x. θ may be used to represent any fluid parameter in Equation 3.1. For numerical computations, it is not practical to carry an infinite number of terms in Equation 3.1, so it is truncated. If terms of order $(\Delta l)^3$ and higher are omitted, Equation 3.1 becomes:

$$\theta_{u+1,j} \approx \theta_{i,j} + \Delta l \frac{d\theta}{dl}\bigg|_{i,j} + \frac{(\Delta l)^2}{2} \frac{d^2\theta}{dl^2}\bigg|_{i,j}. \quad (3.2)$$

Equation 3.1 will become 3.2 which is referred to as second order accurate.

46

3.2.2 Discretization

Equation 3.2 is of second-order accuracy because terms of $(\Delta l)^3$ and higher order have been omitted. If terms of order $(\Delta l)^2$ and higher order are omitted, Equation (3.2) reduces to one of first order accuracy:

$$\theta_{u+1,j} \approx \theta_{i,j} + \Delta l \frac{d\theta}{dl}\Big|_{i,j} \qquad (3.3)$$

In Equations 3.2 and 3.3, the omitted higher-order terms represent the truncation error in the finite series representation. The truncation error is the difference between the partial derivative and its finite difference representation.

3.2.3 Solution technique

In general, Hoffmann (1989) stated that there are two method of solution for the system of simultaneous linear algebraic equations. These schemes are classified as direct and iterative methods. The composite Simpson rule, Cramer's rule and Gaussian elimination are some familiar direct methods. The major disadvantage of these method is the huge amount of arithmetic operations required to produce a solution. Some advanced direct methods have been proposed which require moderate computation time, but almost all of them have disadvantages. Usually these methods are limited by one or more restrictions such as the Cartesian co-ordinate system, a rectangular domain, the size of the coefficient matrix, a large storage requirement, boundary conditions, or difficulty of programming. An alternative iterative approach can solve a system of linear algebraic equations and is simple and easy to program. The idea behind this method is to obtain the solution by iteration; usually an initial solution is guessed and new values are computed based on the finite difference equations which describe the domain. Based on

47

the newly computed values, a new solution is sought and the procedure is repeated until a specified convergence criterion has been reached. Five popular iteration methods are the Jacobi iteration method, the point Gauss-Seidel iteration method, the line Gauss-Seidel iteration method, point successive over-relaxation method and line successive over-relaxation method. The discussion of these methods is beyond the scope of this chapter because these methods are not appropriate for the one-dimensional AuCFD model, but essentially each aims to accelerate convergence beyond that given by the Jacobi iteration method. Based on the nature of the correlation for two-phase pressure drops, a numerical integration method such as the composite Simpson rule will be used and discussed later in this Chapter and Chapter 4.

3.3   AuCFD technique

The main difference between normal CFD and the AuCFD code developed in this study is that only a one-dimensional scheme is needed and the Navier-Stokes equations (the basis of most commercial CFD codes) are not solved. Due to these requirements, a unique computational scheme must be developed rather than using an existing CFD package. The new scheme (AuCFD) uses energy balancing, refrigerant transport properties, empirical, two-phase heat transfer and pressure drop correlations and finite difference methods to develop numerical equations for modelling Dx evaporator tubes.

3.3.1 AuCFD technique - energy balance

The technique of energy balancing was used to develop the unique computational fluid dynamic model which is illustrated as follows:
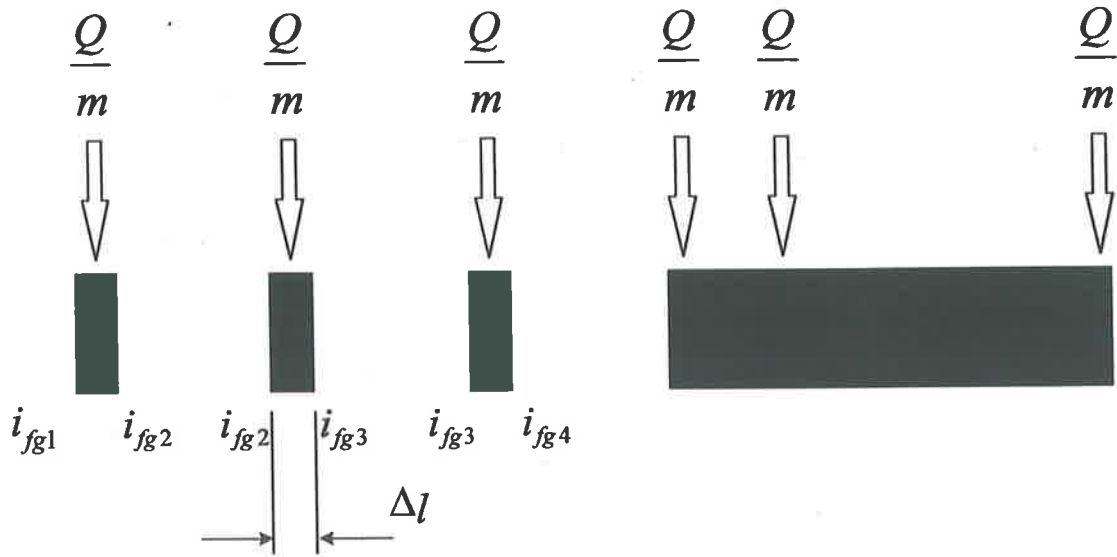
Figure 3.2 - Example for energy balance in horizontal tubes

where:

Q = constant heat flux (W)

m = mass flow rate (kg/s) (= mdot)

i_{fg1} = refrigerant enthalpy (i_fg1) at grid point 1 (J/kg).

The pipe is sub-divided into sections on which an energy balance is carried out. The heat energy entering any given section in the refrigerant through walls must be equal to the energy leaving the section in the refrigerant. If refrigerant properties are ascertained at the inlet to the section, properties at the outlet of the section can be found using equations of state in the computer routine. These will become properties at the next section's inlet. The above Figure 3.2 provides a description of the finite difference method applied to the AuCFD approach.

Figure 3.2 shows that the refrigerant enthalpy, i_{fg1} at point 1, is changed to those at point $n+1$ when heat energy, Q ($q \times \Delta l \times D \times \pi$) is input into the pipe. The outlet conditions of the refrigerants $i_{fg,n+1}$, in the first section will become the inlet conditions of those in the second section and so on. The outlet refrigerant properties from the pipe end, the average two-phase heat transfer coefficients and the total pressure drops can be calculated using this method. The inlet and outlet parameters of the system are referred to here as the geometry of the pipe (length, L in the x direction, and diameter, D) , constant mass flow rate (kg/s) and the applied constant heat flux, q (W/m^2) to the pipe. The outlet vapour quality, the saturated temperature, the two-phase heat transfer coefficients and pressure drops of the refrigerants vary with the initial conditions. As the mass flow rate of the refrigerants is constant, there will be no change in kinetic energy of the refrigerants through the pipe.

The equations used to illustrate how to apply the energy balance for the outlet of the new liquid enthalpy of the refrigerants flowing inside a horizontal heat pipe are:

$$\text{(inlet wet enthalpy)} \qquad i_{fgn} = x_n (i_{gn} - i_{fn}) + i_{fn} \qquad (3.4)$$

$$\text{(outlet wet enthalpy)} \qquad i_{fgn+1} = \frac{Q}{\dot{m}} + i_{fgn} \qquad (3.5)$$

where:

Q = heat energy (W) = $q \times \Delta l \times D \times \pi$

q = heat flux (W/m^2)

D = diameter of tube (m)

Δl = grid spacing (m)

m = mass flow rate (*mdot*) of refrigerant (kg/s)

i_{fg} = wet-enthalpy (J/kg)

i_f = liquid enthalpy (J/kg)

i_g = vapour enthalpy (J/kg)

Subscripts

n = inlet to a section

$n+1$ = outlet from a section.

In Equation 3.4, before the wet enthalpy i_{fgn} is determined, the liquid enthalpy i_{fn}, the vapour enthalpy i_{gn} and the vapour quality x_n, have to be calculated using the numerical equations for refrigerant properties (refer to AII and AIII). With the use of Equation 3.5 and Figure 3.2, the wet-enthalpy i_{fg2} or i_{fgn+1} can be calculated by the sum of the wet-enthalpy i_{fgn} and rate of heat energy, Q/m applied to the pipe. The outlet conditions of the first section will become the inlet conditions to the second section. Then, as the refrigerant continues on to the outlet of the second section, the wet enthalpy i_{fg3} is the sum of wet-enthalpy i_{fg2} and heat energy, Q/m applied to the pipe. The outlet condition of the second section will become the inlet condition of the third section and so on.
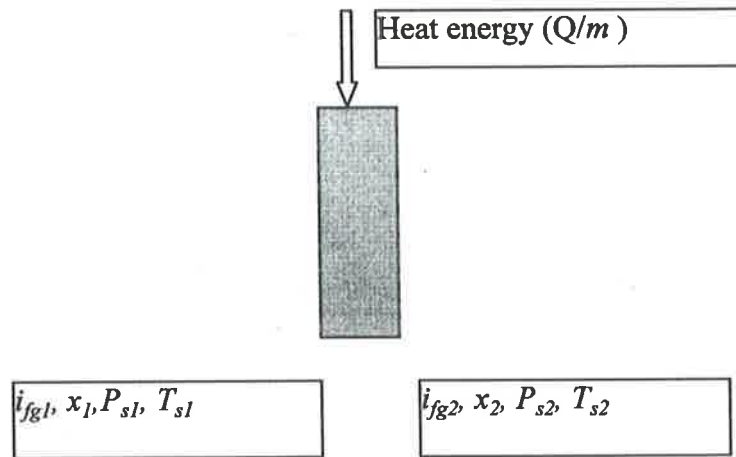
Figure 3.3 – Section of a horizontal tube

The amount of heat energy gained by the refrigerant is based on the mass flow rate through each section of the pipe. When a section of the pipe is considered in Figure 3.3, the outlet wet enthalpy of the refrigerants, i_{fg2} is worked out from Equation 3.5 and the outlet saturated pressure, P_{s2}, is equal to the inlet saturated pressure minus the two-phase pressure drop. Then, the outlet saturated temperature, T_{s2}, can be calculated using Equation 3.6. which shows the relationship between saturated pressure and temperature of refrigerants, R12 from Cleland (1986).

$$Ts = \left(\frac{-2033.5646}{\log Ps - 20.82963} \right) - 248.3 \qquad (3.6)$$

The other physical properties of the refrigerant are dependent on the saturated temperature. If the saturated pressure decreases inside the tube, the saturated

temperature is decreased accordingly. This affects the transport properties of refrigerant. As the liquid and vapour enthalpy are also dependent on the outlet saturated temperature of refrigerant, the outlet liquid and vapour enthalpy and the outlet vapour quality can be determined. This heat transfer mechanism will continue until the end of the tube.

In this study, a finite difference method is used to investigate and analyse the characteristics of the two-phase boiling flow of refrigerants inside horizontal tubes. Physical properties, heat transfer coefficients and pressure drops can be determined at any particular length of the tube. They are based on the input of inlet vapour quality, mass flux and saturated temperature of refrigerants and heat flux applied to the tube. The energy balance technique used in the scheme played an important role in determining the refrigerant transport properties at any stage. The details of the solution procedures of the computational scheme (AuCFD) for two-phase heat transfer coefficients and pressure drops is shown in Chapter 3.7 and Figure 3.7.

3.3.2 AuCFD technique - correlations used

The semi-empirical correlations used in AuCFD for two-phase heat transfer coefficient and pressure drop calculations are obtained from Jung and Radermacher's (1989a) Souza and Pimenta's (1995) papers respectively. The Jung and Radermacher correlation (1989a) - Equations 3.7 to 3.9, based on R12, R152a, and R114, were validated by comparing them with experimental data for R11 and R134a. The Souza and Pimenta correlation - Equations (2.24) to (2.27) are used for the higher mass flux of fluid where the region is dominated by annular flow.

- **Jung and Radermacher (1989a):**

$$h_{tp} = N h_{sa} + F h_{lo} \tag{3.7}$$

$$h_{sa} = 207 \frac{k_l}{bd} \left(\frac{qbd}{k_l T_s} \right)^{0.745} \left(\frac{\rho_v}{\rho_l} \right)^{0.581} Pr_l^{0.533} \tag{3.8}$$

$$h_l = 0.023 \frac{k_l}{d} Re_l^{0.8} Pr_l^{0.4} \tag{3.9}$$

where:

$$N = 4048 X_{tt}^{1.22} Bo^{1.33} \qquad \text{for } X_{tt} \le 1$$

$$N = 2.0 - 0.1 X_{tt}^{-0.28} Bo^{-0.33} \qquad \text{for } 1 < X_{tt} \le 5$$

$$bd = 0.0146\beta (2\sigma / (g(\rho_l - \rho_v)))^{0.5} \qquad \text{with a contact angle } \beta = 35^{\circ}$$

$$F = 2.37 \left(0.29 + \frac{1}{X_{tt}} \right)^{0.85}$$

$$X_{tt} = \left(\frac{1-x}{x} \right)^{0.9} \left(\frac{\rho_v}{\rho_l} \right)^{0.5} \left(\frac{\mu_l}{\mu_v} \right)^{0.1}.$$

- **Souza and Pimenta (1995)**

$$\Delta P_{tp} = \Delta P_f + \Delta P_a \tag{(2.24)}$$

$$\Delta P_f = \Delta P_{lo} \left(\frac{1}{\Delta x} \int \phi_{lo}^2 dx \right) \tag{(2.25)}$$

$$\phi_{lo}^2 = 1 + \left(\tau^2 - 1 \right) x^{1.75} (1 + 0.9524 \tau X_{tt}^{0.4126}) \tag{(2.28)}$$

$$\tau = \left(\frac{\rho_l}{\rho_v} \right)^{0.5} \left(\frac{\mu_v}{\mu_l} \right)^{0.125}. \tag{(2.29)}$$

$$\Delta P_a = G^2 \left\{ \left[\frac{x_o^2}{\rho_o \alpha_o} + \frac{(1-x_o)^2}{\rho_i (1-\alpha_o)} \right] - \left[\frac{x_i^2}{\rho i_i \alpha_i} + \frac{(1-x_i)^2}{\rho_i (1-\alpha_i)} \right] \right\}. \tag{(2.27)}$$

where:

Bo = boiling number

F = heat transfer enhancement factor

N = factor due to nucleate boiling

k_l = thermal conductivity (W/m)

Re_l = Reynolds number

Pr_l = Prandtl number

d = diameter of tube (m) = D

h_l = single phase heat transfer coefficient (W/m^2 K)

ΔP_{tp} = two-phase pressure drop (Pa)

ΔP_f = frictional pressure drop (Pa)

ΔP_a = accelerational pressure drop (Pa)

G = mass flux (kg/m^{2}s)

L = tube length, (m)

ρ = density (kg/m^3)

x = vapour quality

Δx = quality change between inlet and outlet = $x_2\text{-}x_1$

X_{tt} = Martinelli parameter

ϕ_{tp} = two-phase pressure drop multiplier

τ = property index

α = void fraction

Subscript

v vapour state

l liquid state

i test section inlet

o test section outlet

lo   liquid only.

$$Q = q \times \Delta l \times D \times \pi$$

$$(h_{tp} , \Delta P_{tp})_n \qquad (h_{tp} , \Delta P_{tp})_{n+1}$$

$$\Delta l$$
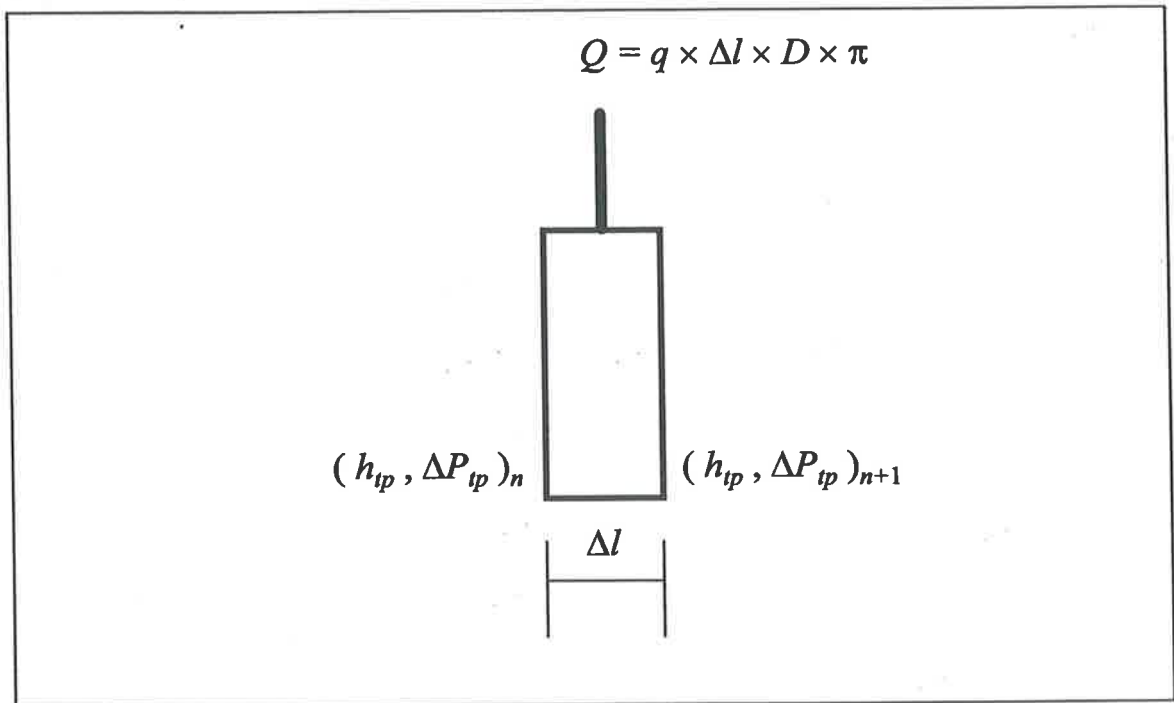
Figure 3.4 - A coupled system of equations in a grid spacing, Δl

where:

Q = constant heat flux (W) = $q \times \Delta l \times D \times \pi$

h_{tp} = two-phase heat transfer coefficient (W/m^2 K)

ΔP_{tp} = two-phase pressure drop (Pa)

Δl = grid spacing.

The correlations for the two-phase heat transfer coefficient, h_{tp} and the pressure drop, ΔP_{tp} are a coupled system of equations. This means that the pressure drop, ΔP_{tp} affects the heat transfer coefficient, h_{tp}, due to the changes in saturated pressure and temperature of the refrigerant. With the aid of the finite difference method, the two-phase heat transfer coefficients and pressure drops could be calculated accurately.

3.3.3 AuCFD technique – finite difference method

The following is the solution technique of finite difference method using the composite

Simpson rule for the correlation of two-phase pressure drop in horizontal tubes.
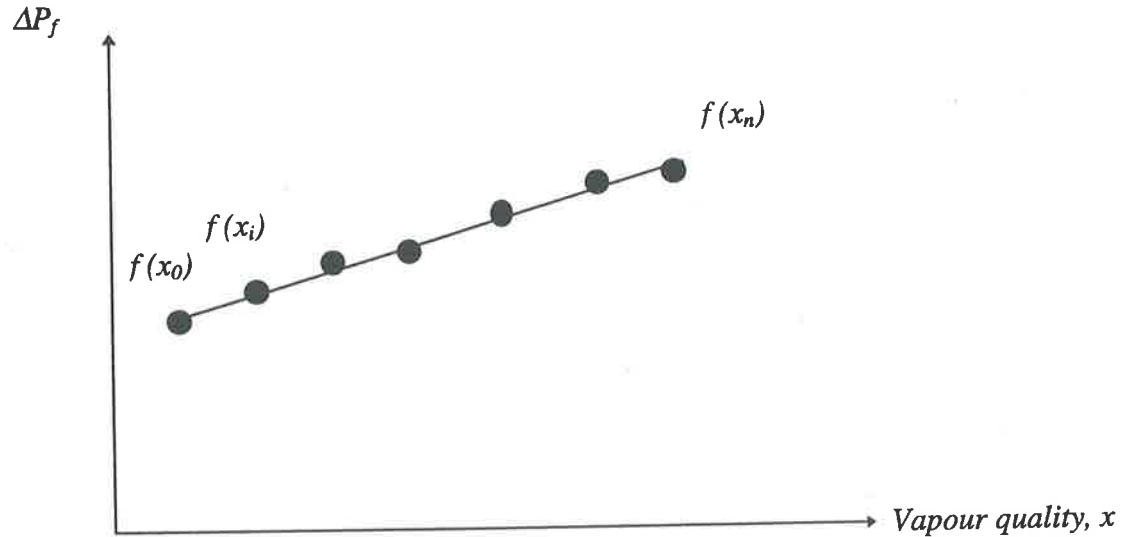
Figure 3.4 - *Discrete grid points for two-phase pressure drops*

$$\theta = \frac{\Delta l}{6}\left[f(x_0) + f(x_n) + 2\sum_{i=1}^{n-1} f(x_i) + 4\sum_{i=1}^{n} f(x_{i-1/2}) \right] \qquad (3.10)$$

where:

Δl = grid spacing (m)

n   = number of iterations

i = 1,2,...n

θ = arbitrary variable used in composite Simpson rule & Taylor series (Eqt. 3.1).

Basically, numerical integration such as the composite Simpson Rule, in contrast to differentiation, is a stable process which can derive the correlations for two-phase pressure drops. The implementation of Equations (2.25) and (2.28) in the AuCFD scheme will use the composite Simpson rule to transform the correlations into a

numerical equation which came from Souza and Pimenta's (1995) correlation for two-phase pressure drops of refrigerants. The model implemented was a first-order accurate representation of Souza and Pimenta's work.

$$\Delta P_f = \Delta P_{lo} \left(\frac{1}{\Delta x} \int \phi_{lo}^2 dx \right) \qquad ((2.25))$$

$$\phi_{lo}^2 = 1 + \left(\tau^2 - 1 \right) x^{1.75} (1 + 0.9524 \tau X_{tt}^{0.4126}). \qquad ((2.28))$$

Equations ((2.25)) and ((2.28)) will become Equations (3.11) and (3.12)

$$\Delta P_f = \int C \phi_{lo}^2 dx \qquad (3.11)$$

$$f(x) = \phi_{lo}^2 = 1 + \left(\tau^2 - 1 \right) x^{1.75} (1 + 0.9524 \tau X_{tt}^{0.4126}). \qquad (3.12)$$

where:

C   = constant to be assumed for $\Delta P_{lo} / \Delta x$

$f(x)$ = function of numerical equation.

$$\Delta P_f = CS = \frac{C\Delta l}{6} \left[f(x_0) + f(x_n) + 2\sum_{i=1}^{n-1} f(x_i) + 4\sum_{i=1}^{n} f(x_{i-1/2}) \right]. \qquad (3.13)$$

To order to apply Equation 3.13 to the AuCF scheme, the relationship between grid spacing, Δl and vapour quality, Δx should be found. With the use of Equation 3.5

$$i_{fgn+1} = \frac{Q}{\dot{m}} + i_{fgn} \qquad ((3.5))$$

$$i_{fg2} = \frac{q\pi D\Delta l}{\dot{m}} + i_{fg1} \qquad (3.14)$$

As q, D and m are assumed to be constant, Equation 3.14 can be written as Equation 3.15.

$$i_{fg2} - i_{fg1} = K\Delta l \tag{3.15}$$

$$i_{fg2} = x_2(i_{fg2} - i_{f2}) + i_{f2} \tag{3.16}$$

$$i_{fg1} = x_1(i_{fg1} - i_{f1}) + i_{f1} \tag{3.17}$$

Subsitute Equations 3.16 and 3.17 into 3.15,

$$x_2(i_{g2} - i_{f2}) + i_{f2} - x_1(i_{g1} - i_{f1}) + i_{f1} = K\Delta l. \tag{3.18}$$

As can be seen from Equation 3.18, the grid spacing, Δl is dependent on the input of the vapour quality, liquid and vapour enthaply and K (heat flux, mass flux and diameter of the pipe). K is the relationship of input parameters ($q\pi D/m$) for two-phase heat transfer in this numerical method.

3.4   Summary of general CFD and AuCFD

The following table shows a comparison of the analogies and differences between general CFD and AuCFD. As can be seen from Table 3.1, existing equations, models and orders of accuracy are always used in general CFD rather than in AuCFD. Hence, the model for two-phase heat transfer coefficients and pressure drop in one-dimensional computational fluid dynamics was established in AuCFD. With the use of thermal energy balance technique and first-order accurate formulations, the solution algorithm was developed in section 3.6.

Table 3.1 - Summary of general CFD and AuCFD

	General CFD	AuCFD
Governing equations	Navier-Stokes equations continuity energy balancing	Continuity energy balancing equations of state
Empirics	k - e turbulence modelling interphase slip chemical reactions	Pressure drop multiplier Two-phase heat transfer coefficient and pressure drop
Discretization	Finite difference or finite element method 2- and 3-dimensions Second or third orders of accuracy(dependent on node position within the domain)	Finite difference method 1 dimension First order accurate
Solution Technique	Jacobi, Gauss-Seidel, SOR or similar iterative technique	piecewise, forward marching, non-iterative

3.5 Equations for refrigerant transport properties

Some equations for determining refrigerant properties presented in Chapter 2 can be readily adopted into a computational scheme, however other refrigerant properties do not translate easily into numerical equations. Although the physical properties of R12 and R134a can be easily obtained from the tables in the ASHRAE handbook and the chemical manufacturers' data sheets, the physical properties of refrigerant are tabulated against the saturated and superheated temperatures of the refrigerants. The data cannot be transferred directly into the computer program. It was therefore necessary to derive polynomial equations to describe the variation of these properties with temperature and pressure. As mentioned in Chapter 2 - section 2.5, a polynomial equation for density, ρ is developed here and is typical of the method used for other such parameters.

The equation for liquid density, ρ, of R12 is assumed as Equation 3.19:

$$\rho = A + BT_{mn} + CT_{mn}^2 \tag{3.19}$$

$$T_{mn} = \left(1 - \frac{T_s}{T_c}\right)^{1/3} \tag{3.20}$$

where:

A   = constant

B   = constant

C   = constant

T_s = saturated temperature of liquid (K)

T_c = critical temperature of liquid (K)

ρ = density of liquid (kg/m^3)

T_{mn} = mean temperature (K).

Then, the polynomial equation for R12 liquid density was defined as Equation 3.21 below:

$$\rho = 1463.63 - 1888.14 \times T_{mn} + 2687.14 \times T_{mn}^2. \tag{3.21}$$

Equation 3.21 is a typical polynomial which is used for calculating density of R12 with the input of a saturated temperature. For transport properties of the other refrigerants, a list of developed polynomial and existing equations for R12 and R134a is shown in Appendices AII and AIII.

3.6   *Additional calculations*

So far, this work has concentrated on its main objective - that of developing and testing a model for calculating heat transfer coefficients and pressure drops through the convecting boiling region of a Dx heat evaporator tube. In fulfilling the secondary aim of developing a design tool for heat exchangers it is necessary also to calculate heat exchange between the fluid in cross-flow (in this case air) and performance of the Dx tube in the superheated region. The bases for these calculations is explained here.

3.6.1 Airside calculations

As mentioned in Chapter 1, the design tool Dx heat exchanger is a cross-flow type in which two different fluids, air and refrigerant transfer heat energy to each other through the tube wall. As an example, the following figure and correlations for circular finned-tube heat exchanger are based on findings by Briggs and Young (1965).
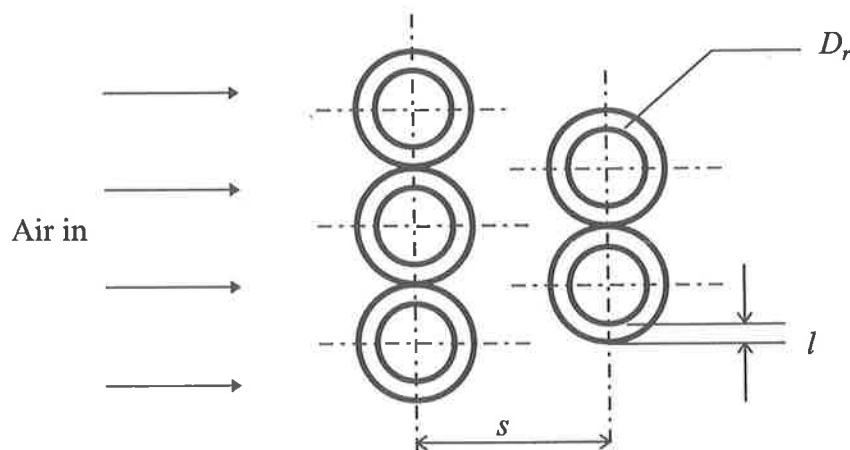
Figure 3.5 - Model for circular finned-tube heat exchanger

$$\frac{h_a D_r}{k} = 0.134\left(\frac{D_r G_{\text{max}}}{\mu}\right)^{0.681}\left(\frac{C_p \mu}{k}\right)^{1/3}\left(\frac{s}{l}\right)^{0.2}\left(\frac{s}{t}\right)^{0.113} \quad\quad (3.22)$$

where:

C_p = Specific heat capacity of air (kJ/kg K)

D_r = root diameter of tube (m)

G_{max} = mass rate flow at minimum cross section (kg/m^{2}s)

h_a = mean heat transfer coefficient of air (W/m^2 K)

k = thermal conductivity of air (W/m K)

l = fin height

s = distance between adjacent fins

t = fin thickness

μ = viscosity at bulk temperature (Pa s).

This is only one possible fin/tube configuration, other fin/tube configurations are easily programmed. A good source of reference for this augmentation is Kays and London (1955).

3.6.2 Superheat calculations

The major difference between the superheated and saturated regions of the tube is the vapour quality of the refrigerant. When the vapour quality of the refrigerant is equal to 1, it means that the region is superheated and no more liquid refrigerant should be present. However, the refrigerant is commonly superheated by around 6 K to ensure no "slug" of liquid in a heterogeneous flow enter and damage the compressor. Refrigerant properties used in this region are dry vapour state - since such a small degree of

superheat is modelled, this approximation is sufficiently accurate. The equations used from Dittus-Boelter (1930) for the calculation of superheated heat transfer coefficients are shown in Equation 3.23.

$$h_{sh} = 0.023\,\mathrm{Re}_g^{\,0.8}\,\mathrm{Pr}_g^{\,0.4} \qquad (3.23)$$

where:

h_{sh} = superheated heat transfer coefficient (W/m^2 K)

Re_g = vapour Reynolds number = Re_g and Re$_v$

Pr_g =vapour Prandtl number = Pr_g and Pr$_v$.

3.7 *Implementation of AuCFD*

A flowchart describes how the computer programs work out the two-phase heat transfer coefficients and pressure drops using the finite difference method. This section lists the steps involved in accomplishing each task within the computational scheme. The scheme uses software programs written in the Turbo C++ language for calculating the thermophysical properties of refrigerants and the correlations for heat transfer coefficients and pressure drops. The algorithm can be defined in programming terms which the flowcharts were developed to describe the processes for producing the desired output from the given input.

The solution procedures for two-phase heat transfer coefficient and pressure are shown schematically in the flowchart of Figure 3.6. It describes the processes for dealing with input and output parameters and calculations of two-phase heat transfer coefficients, pressure drops and refrigerant properties.

```
┌─────────────────────────────────┐
│  Define constants and variables │
└─────────────────────────────────┘
                │
                ▼
┌─────────────────────────────────┐
│  Input design parameter for tube│
│        and flow conditions      │
└─────────────────────────────────┘
                │
                ▼
┌─────────────────────────────────┐
│  Tubeside - refrigerant transport│
│      properties calculation     │
└─────────────────────────────────┘
                │
                ▼
┌─────────────────────────────────┐
│  Jung correlation for two-phase │
│     heat transfer coefficient   │
└─────────────────────────────────┘
                │
                ▼
┌─────────────────────────────────┐
│  Souza correlation for two-phase│
│          pressure drops         │
└─────────────────────────────────┘
                │
                ▼
┌─────────────────────────────────┐
│  Calculate two-phase htc and pd │
│   of refrigerant and htc of air │
└─────────────────────────────────┘
                │
                ▼
┌─────────────────────────────────┐
│  Calculate average htc and pd of│
│ refrigerant and average htc of air│
└─────────────────────────────────┘
                │
                ▼
         No  ◇ Is $x > 1$? ◇
                │ Yes
                ▼
┌─────────────────────────────────┐
│  Superheat - refrigerant transport│
│      properties calculation     │
└─────────────────────────────────┘
                │
                ▼
┌─────────────────────────────────┐
│  Dittus & Boelter's correlation │
│     for heat transfer coefficient│
└─────────────────────────────────┘
                │
                ▼
┌─────────────────────────────────┐
│   Correlation for pressure drops│
└─────────────────────────────────┘
```

Selecting parameters

Tubeside region calculation

Decision making based on vapour quality, x

Superheated region calculation

Figure 3.6 - Solution procedures for computational scheme of two-phase heat transfer coefficient and pressure drop.

3.7.1 Selecting parameters

The computational scheme, AuCFD consists of a main program and three sub-routines for air and refrigerant properties. The main program is used to control and implement the three sub-routines and deal with all the necessary requirements. The sub-routines for the transport properties of R12 and R134a were written to suit the saturated temperature range from -10°C to 15°C. All the various names for the transport properties of refrigerants and air and the physical size of horizontal tube were created and built into the sub-routines. As the computational scheme, AuCFD is executed, it will require the user to input the values of length, internal and external diameters of a horizontal tube, saturated temperature, mass flow rate, inlet vapour quality of the refrigerant, velocity and temperature of air and constant heat flux applied to the tube.

3.7.2 Tubeside region calculation

As all the input data is put into the scheme, the program, R12.cpp or R134a.cpp, calculates all the related refrigerant properties. Some equations for liquid viscosity, liquid thermal conductivity and vapour viscosity of the refrigerants were presented in Chapter 2. Some polynomial equations for liquid density, liquid specific heat capacity, vapour density, vapour conductivity and vapour specific heat capacity of the refrigerant were developed in section 3.5.

As the refrigerants flow through the tubeside, the saturated temperature of the refrigerant will be changed due to a constant or variable heat input which affects the physical properties of the refrigerant. Since the tube has been divided into several sections, the parameters used for the two-phase heat transfer coefficient and the pressure drop correlations can be calculated at each section outlet. The values of the two-phase total heat transfer coefficient and the total pressure drops will be accumulated until the refrigerants exit the tube. As can be seen from Chapter 2, the two-phase heat transfer coefficients of the refrigerants are determined by the sum of convective boiling and nucleate boiling heat transfers while the two-phase pressure drops are added by frictional and acceleration pressure drops along the tube. The heat transfer coefficient of air is also evaluated using the input of air temperature, air velocity and heat flux parameters in the tubeside region.

3.7.3 Decision making based on quality, x

A control structure's WHILE loop is used to repeat a set of statements automatically while a certain condition is true. The WHILE loop is set to control a number of intervals, n for calculating tube side conditions. The number of intervals, n depends on a vapour quality, x. In other words, the loop will continue until x is greater 1. The refrigerant vapour quality is based on the mass flow rate itself and the amount of heat transfer to the refrigerant. If the refrigerant becomes superheated ($x > 1$), the solution procedure will forward to the next step.

3.7.4 Superheated region calculation

In this section, as the refrigerant becomes superheated, all the relevant refrigerant transport properties, vapour density, vapour conductivity, vapour viscosity etc. will be calculated again using the programs, R12.cpp and R134a.cpp. Then, the average heat transfer coefficient and pressure drop of the refrigerants are determined using Dittus and Boelter's correlation and Souza *et al*'s correlation. Also, the average heat transfer coefficient of air is calculated with the use of air temperature, air velocity and heat flux parameters.

3.7.5 Iteration

The present WHILE loop is set to control a number of intervals, n for calculating superheated conditions. The number of intervals, n depends on a grid spacing, Δl and pipe length, L. In other words, if the pipe length is known, the number of intervals is

equal to the pipe length divided by the grid spacing.. As soon as the iteration number equals to the number of intervals, the solution procedure will forward to the next step.

3.7.6 Compute the test results

This step will print input and output data on the user screen to ensure that the data is input correctly. The main output data of average heat transfer coefficients and total pressure drops of the refrigerants and average heat transfer coefficient of the air are calculated as follows:

- **Refrigerant side (Tubeside)**

$$htc\_t = htc\_t + h\_tp \qquad (3.24)$$

$$htc\_av = \frac{htc\_t \times A}{L \times ID \times \pi} \qquad (3.25)$$

$$dp\_t = dp\_t + dp + dp\_a \qquad (3.26)$$

- **Air side**

$$h\_airt = h\_airt + h\_air \qquad (3.27)$$

$$h\_airav = \frac{h\_airt \times A}{L \times OD \times \pi}. \qquad (3.28)$$

where:

IA = sectional surface area of tube, $\Delta l \times ID \times \pi$ (m^2)

OA = sectional surface area of tube, $\Delta l \times OD \times \pi$ (m^2)

ID = internal diameter of tube (m) = D

OD = outside diameter of tube (m)

L = length of tube (m)

h_air = heat transfer coefficient of air (W/m^2 K) = h_a

h_airt = total of heat transfer coefficient of air (W/m^{2}K)

h_airav= average heat transfer coefficient of air (W/m^{2}K)

h_tp = two-phase heat transfer coefficient of refrigerant (W/m²K) = h_{tp}

htc_t = total two-phase heat transfer coefficient of refrigerant (W/m²K)

htc_av = average two-phase heat transfer coefficient of refrigerant (W/m²K)

dp = two-phase frictional pressure drops (Pa)

dp_a = two-phase accelerational pressure drops (Pa)

dp_t = total two-phase pressure drops (Pa) = ΔP_{tp}

Δl = grid spacing (m).

For the refrigerant side, in Equation 3.24, the two-phase heat transfer coefficient at each grid point will be added to the total two-phase heat transfer coefficient. The the average two-phase heat transfer coefficient multiplied by the total inside surface area of the tube is equal to the total two-phase heat transfer coefficient multiplied by the sectional area of the tube. The average two-phase heat transfer coefficient can be determined in Equation 3.25. The two-phase pressure drops of the refrigerant at each grid point will be added up to the total two-phase pressure drop in Equation 3.26.

Similarly, for the air, the heat transfer coefficient of air at each grid point will be added to the total heat transfer coefficient of air. The average heat transfer coefficient multiplied by the total outside surface area of the tube is equal to the total two-phase heat transfer coefficient multiplied by the sectional area of the tube. The average heat transfer coefficient of air can be determined in Equation 3.28.

3.8   Summary

Computational fluid dynamics and experimental techniques for this project have been reviewed. The comparison of the general CFD and AuCFD method have also been made in section 3.4. AuCFD is a unique one-dimensional analysis of two phase heat transfer coefficients and pressure drops of refrigerants in horizontal evaporator tubes

which estimates the transport properties of refrigerants. With the use of flowcharts, the solution procedures for AuCFD were shown and explained progressively.

Chapter 4

VALIDATION

4.1 Introduction

This chapter describes the validation of the AuCFD code developed and a first-order accurate finite difference approach applied to the scheme. The validation of the AuCFD code is achieved by using error analysis to check the accuracy and stability of the computer programs under all flow conditions. The round-off error is investigated to establish how it affects the computational results. Under different flow conditions, the independence of grid spacings, Δl, is tested to obtain six-decimal-place accuracy of pressure drops, with the use of different numbers of iterations, n and pipe lengths, L where $L = \Delta l \times n$.

Finally, in this chapter, the independence of the grid spacing is recommended which minimises the errors in the AuCFD code.

4.2 Grid independence

The independence of grid spacing can be derived using a theoretical approach shown in Chapter 3, which minimises the computational errors. The curve of grid spacing, Δl, versus the computational error is plotted as follows:
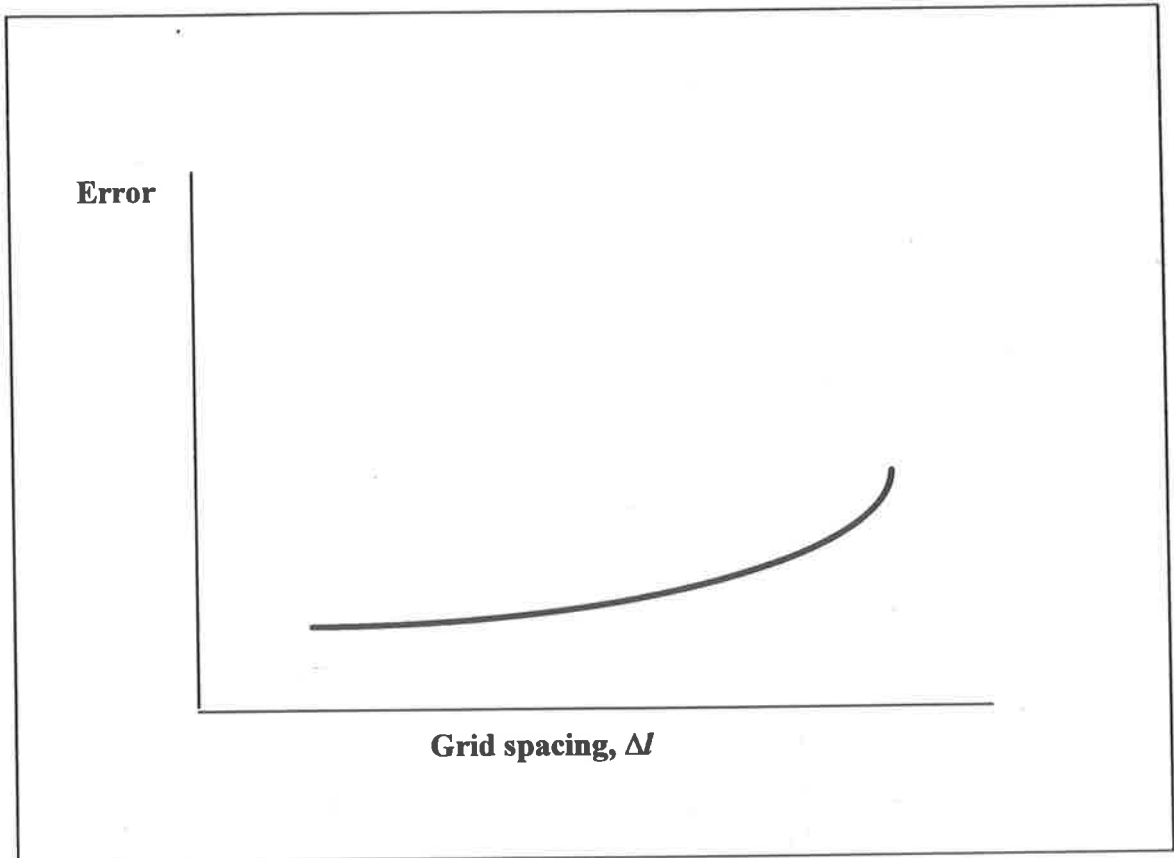
Figure 4.1 -*Relationship between round-off error and grid spacing,* Δl

In Figure 4.1, it can be seen that the round-off error is increasing as the grid spacing is increased and the number of iterations is decreased. The grid spacing varies with the inputs of vapour quality, liquid and vapour enthaply, heat flux, mass flux, the number of iterations, and diameter and length of the pipe. Further validation of the grid spacing will be shown after the round-off error is discussed.

4.2.1 Experimental results

The following table is extracted from Souza *et al* (1995) where R12 refrigerant was used in a horizontal tube 1.2954 m long and 10.92 mm diameter. The results of the total pressure drops are compared with the computational results with independent grid spacings derived in the next section.

Table 4.1 - Validation models used - from Souza et al (1995)

Test no.	Mass flux ($kg/m^2.s$)	Heat flux (kW/m^2)	Inlet vapour quality	Saturated temperature (°C)	Total pressure drop (Pa)
1	198.8	9.93	0.797	4.7	3550
2	296.6	30.09	0.201	4.8	4150

4.2.2 Computational results

The computational results are shown in the following Table 4.2. The input parameters are obtained from Table 4.1 in accordance with the test numbers. With the use of Equation 3.18 and Souza *et al*'s data, the independence of grid spacing can be determined as follows:

$$\Delta l = \left[\frac{x_2(i_{g2} - i_{f2}) + i_{f2} - x_1(i_{g1} - i_{f1}) + i_{f1}}{K} \right]$$

((3.18))

Table 4.2 - Validation Results

Grid spacing (m)	Test no.1 (Compare with 3550 Pa)		Test no. 2 (Compare with 4150 Pa)	
	Pressure drops (Pa)	% of error	Pressure drops (Pa)	error (%)
0.086	3713.3413	4.6	4821.8850	16.19

4.3   Round-off error

The round-off error is the numerical error introduced during a repetitive number of calculations, in which the computer is constantly rounding the numbers to some significant figure.   In some calculations, the magnitude of the round-off error is proportional to the number of grid points in the problem domain. In these cases, refining the grid may decrease the truncation error but increase the round-off error. The round-off error is defined by Lewis *et al* (1983) as follows:

$$\varepsilon = \frac{-f^{IV}(\xi)\left(\dfrac{\Delta l}{2}\right)^4 L}{180} \qquad 0 < \xi < L \qquad\qquad (4.1)$$

where:

ε = round-off error

L = pipe length, (m)

ξ = value between 0 and pipe length (m)

Δl = grid spacing, (m)

f^{IV} = fourth order accuracy.

The aim of this section is to analyse the round-off error which exists in the scheme with a relationship between grid spacing, tube length and number of iterations. The round-off error is mainly influenced by the number of iterations undertaken when running the program. In order to test the significance of the round-off error, a calculated grid spacing, Δl from Equation 3.18 was used in the models with various tube length, heat flux and different numbers of iterations. Using a first order accuracy finite difference method as shown in Chapter 3 (Section 3.3), a suitable grid spacing Δl of the pipe is used in the

scheme. The relationship between the number of iterations n, the grid spacing Δl and the total pipe length, L is shown below:

$$L = \Delta l \times n.$$

If the number of iterations is changed, the grid spacing will be changed to balance the equation. In order to use Equation 4.1 for calculating round-off errors, Equation 3.12 is differentiated to $f^{IV}(x)$.

$$f(x) = \phi_{lo}^2 = 1 + \left(\tau^2 - 1\right)x^{1.75}\left(1 + 0.9524\tau X_{tt}^{0.4126}\right) \qquad ((3.12))$$

Differentiate Equation 3.12,

$$f^I(x) = 1.75\left(\tau^2 - 1\right)x^{0.75} + A \qquad (4.2)$$

Assume A is approaching to 0 and elminated, then differentiate Equation (4.2) to the fourth derivatives where τ is the property index (see Eqt. 2.29) developed by Souza et al (1995).

$$f^{IV}(x) = 0.40625x^{-2.25}\left(\tau^2 - 1\right). \qquad (4.3)$$

4.3.1 Testing procedure for round-off estimation model

Two different flow conditions from Table 4.1 are used to determine the iterations, n so that the composite Simpson rule can give the value of two-phase pressure drops correct to six digits after the decimal point, assuming that correlations for two-phase pressure drops can be calculated accurately.

In test no. 1, as $f(x) = \phi_{lo}^2 = 1 + (\tau^2 - 1)x^{1.75}(1 + 0.9524\tau X_{tt}^{0.4126})$, $L = 1.2954$, Δl =1.2954/n; hence Equation 4.1 can be used to calculate the error in the composite Simpson rule.

$$\varepsilon = \frac{-f^{IV}(\xi)\left(\dfrac{\Delta l}{2}\right)^4 L}{180} \qquad 0 < \xi < L \qquad\qquad ((4.1))$$

The absolute error is maximum in Equation 4.3, $f^{IV}(x) = 0.40625x^{-2.25} = 0.6769$ when x is 0.797 (minimum). Equation 4.1 will become Equation 4.4 as

$$\max \frac{0.6769 \times 0.22798}{180n^4} \qquad\qquad (4.4)$$

As the six-place accuracy is used, n can be determined as follows:

$$\frac{0.6769 \times 0.22798}{180n^4} < 5 \times 10^{-7} \qquad\qquad (4.5)$$

$$n \gg\approx 6. \qquad\qquad (4.6)$$

Similarly, in test no.2, with the use of the six-place accuracy, n can also be found as follows:

$$\frac{15.0177 \times 0.22798}{180n^4} < 5 \times 10^{-7} \qquad\qquad (4.7)$$

$$n \gg\approx 14. \qquad\qquad (4.8)$$

4.3.2 Test results for the round-off estimation model

The test results for two different flow conditions using the above parameters are shown. The results of two-phase pressure drops in test numbers 1 and 2 for various values of n are:

Table 4.3 – Two-phase pressure drops versus iterations in test no.1

Iteration, n	Two-phase pressure drops (kPa), ΔP_{tp}
6	3.7136413
15	3.7136833
30	3.7136921
45	3.7137013
60	3.7137521
100	3.7138733
200	3.7139733

Table 4.4 – Two-phase pressure drops versus iterations in test no.2

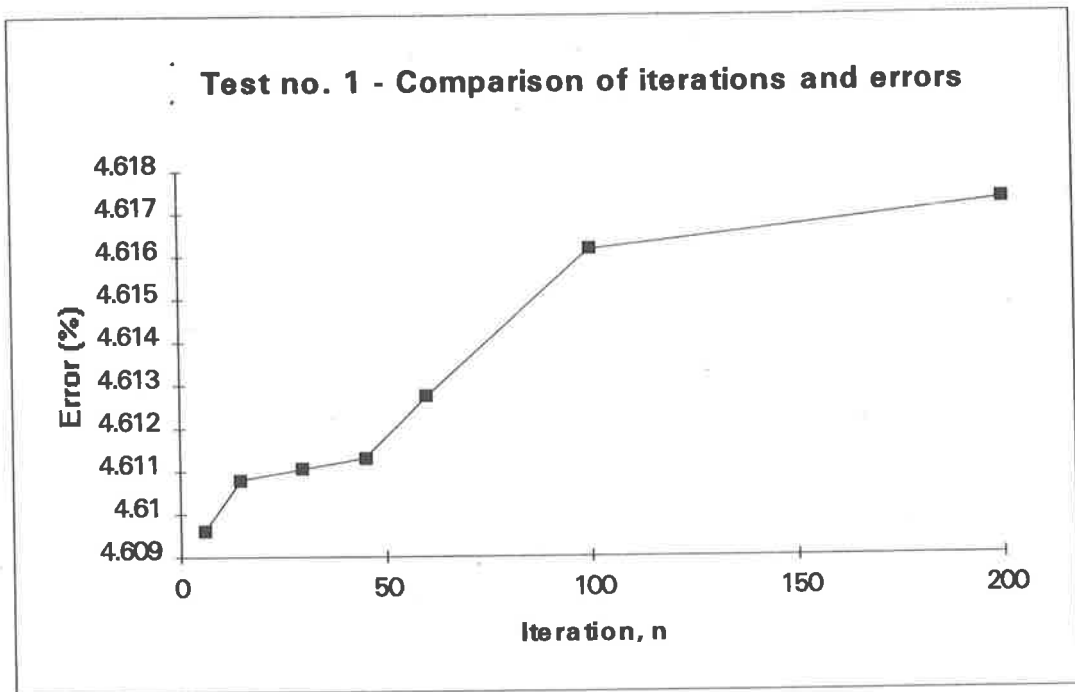| Iteration, n	Two-phase pressure drops (kPa), ΔP_{tp}
15	4.8218850
30	4.82171356
45	4.82172165
60	4.82173177
100	4.82174155
200	4.82178193
300	4.82188121

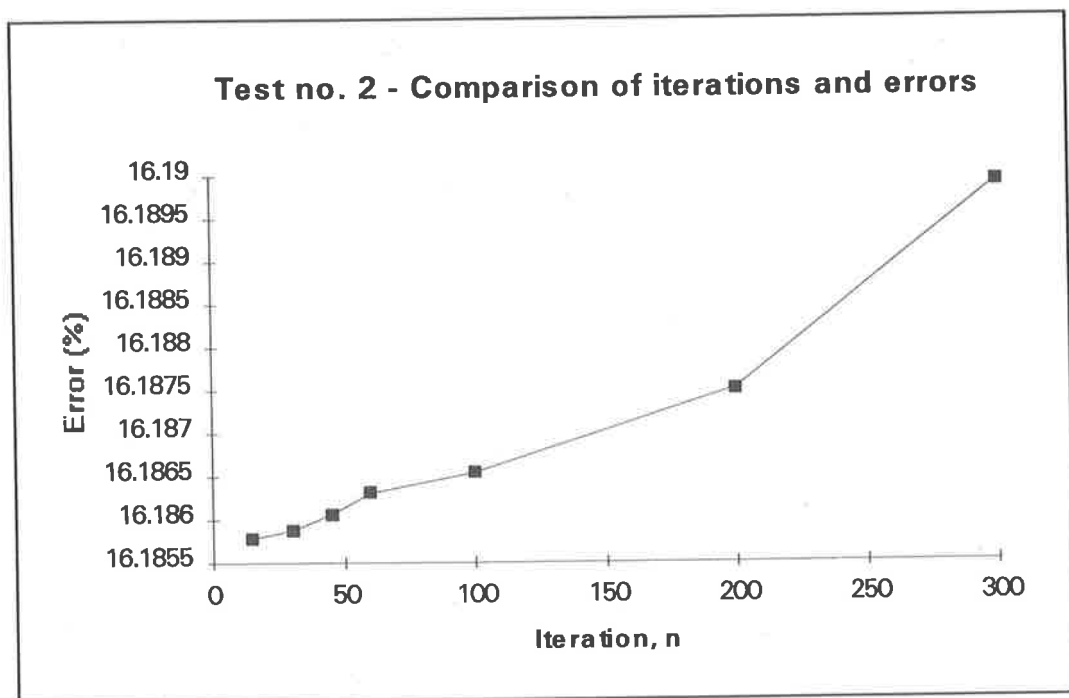*Figure 4.2 - Round-off errors versus iterations*

Figure 4.3 - Round-off errors versus iterations

From the plotted graphs in Figures 4.2 and 4.3, it appears that the trends of both curves are similar to each other and converging to a minimum computational error with the use of the calculated iterations (n = 6 and 15 , in test numbers 1 and 2 respectively on page 78). It is obvious when the iteration is increased, the round-off error is increased gradually. The number of iterations is dependent on the vapour quality of refrigerants, the pipe length and the number of decimal place accuracy.

From the results of Tables 4.3 and 4.4, with the use of independent grid spacings, 0.2159m and 0.08636, it is found that the scheme can show six decimal place accuracy. However, due to the characteristic of two-phase pressure drops from Sozau *et.al.* (1995), the percentage of computational error in test no.2 is higher than test no.1. This phenomenon will be discussed in Chapter 5.

4.4   Verification of independence of grid spacing

In order to obtain an independence of grid spacing, Δl within the pipe model, various input configurations are used in this Chapter. The results of two-phase pressure drops using the independence of grid spacing, Δl are compared with the experimental results from Souza *et al* (1995). With the use of Equation 3.15 and Souza's data, the independence of grid spacing can be determined as follows:

$$\Delta l = \left[\frac{x_2(i_{g2} - i_{f2}) + i_{f2} - x_1(i_{g1} - i_{f1}) + i_{f1}}{K} \right] \qquad ((3.18))$$

As the grid spacing Δl varies, the number of iteration n will be changed because it is equal to the specified pipe length L divided by the number of sub-divisions which represent grid spacing Δl. The experimental and computational results are tabulated below.

4.4.1 Testing procedure for the independent grid spacing model

These tests assume no pressure drops across the horizontal tube. The various ranges of the heat flux q (W/m^2) and the total length of the tube L (m) are used to obtain the same total heat transfer, Q (W) for different lengths of the tube. This means that in order to maintain the same heat transfer, Q (W), the highest heat flux, $q\times8$ (W/m^2), will match with the shortest length of tube, 0.161925 m with minimum surface area, whilst the lowest heat flux, $q/8$ (W/m^2), will match with the longest length of tube, 10.3632 m, with maximum surface area. The combinations of the heat flux and the length of tubes are $q\times8$ (W/m^2), $q\times4$ (W/m^2), $q\times2$ (W/m^2), q (W/m^2), $q/2$ (W/m^2), $q/4$ (W/m^2) and $q/8$ (W/m^2), and 0.161925 m to 10.3632 m respectively. The numbers of iterations are 6 and 15 for test no.1 and 2 respectively.

4.4.2 Test results for grid independence

The test results for two different flow conditions using the above parameters were tabulated. The graphs in all tests were plotted as the total heat transfer Q (W) versus the grid spacing, Δl.

Table 4.5 - *Independent grid spacing models as test no. 1 and 2 at calculated iterations*

Length, L (m)	Test no. 1 (n = 6)			Test no. 2 (n = 15)		
	Grid spacing (m)	Heat flux, q (W/m^2)	Total heat transfer, Q (W)	Grid spacing (m)	Heat flux, q (W/m^2)	Outlet wet ehthalpy, i_{fg} (J/kg)
10.36	1.727	1241 (q/8)	441.496	0.691	3761 (q/8)	279786.5
5.18	0.863	2483	441.496	0.345	7522.5	279768.9
2.59	0.432	4965	441.496	0.173	15045	279760.4
1.30	0.216	9930 (q)	441.496	0.087	30090(q)	279758.9
0.65	0.108	19860	441.496	0.043	60180)	279758.4
0.33	0.055	39720	441.496	0.022	120360	279758.1
0.16	0.027	79440(8q)	441.496	0.011	240720 (8q)	279758.1
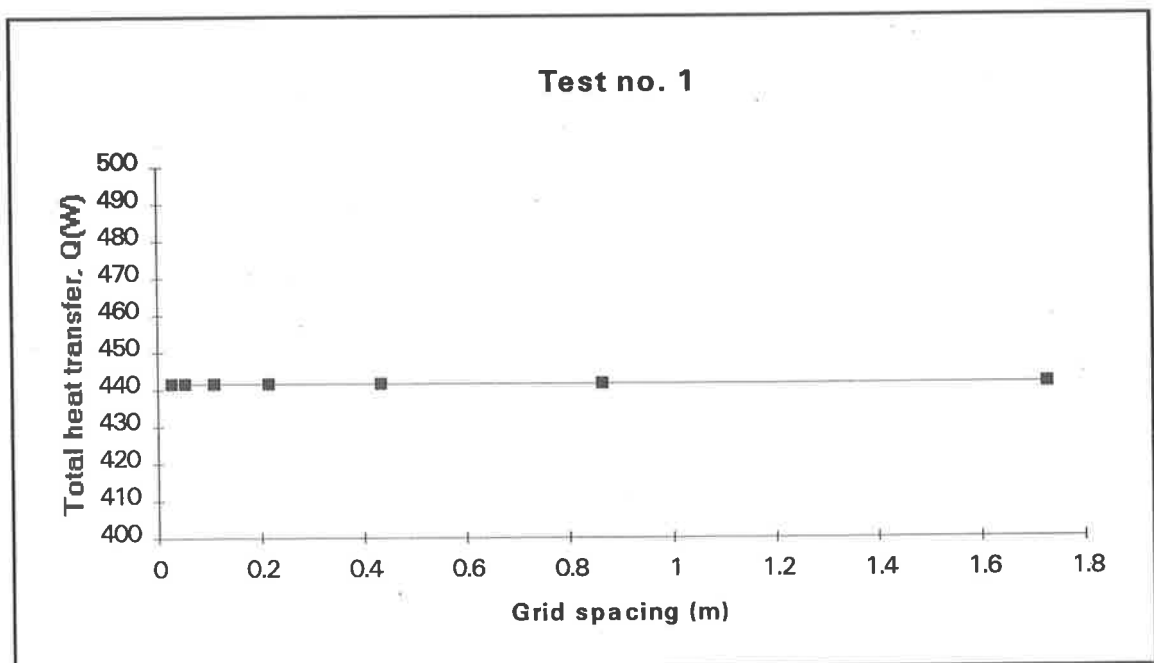
Figure 4.4 - *Test results for independence of grid spacing model at calculated iteration*
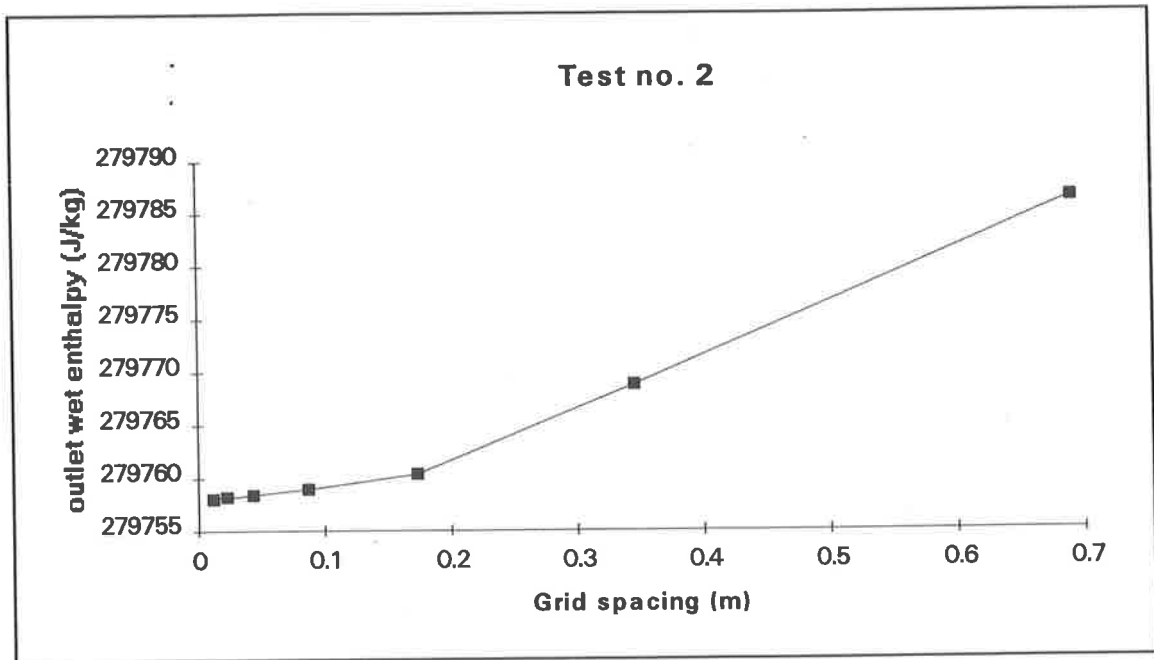
Test no. 2

Figure 4.5 - Test results for independence of grid spacing model at calculated iteration

In test no.1, the total heat transfer , Q (W) is a function of the pipe diameter and total length. The heat flux, q (W/m^2) multiplied by the total surface area of the pipe is equal to a constant value for total heat transfer , Q (W) (see Chapter 3). Since the total heat transfer, Q (W) is not a function of the distance, the composite Simpson Rule will not vary the total heat transfer, Q (W) with the grid spacing. The straight horizontal line in Figure 4.4 verifies that the physics of the total heat transfer, Q (W) is intrinsically not grid dependent and grid spacing, Δl is not critical.

However, in test no. 2, the results are different from test no. 1 because wet enthalpy , i_{fg} (J/kg) is not constant with distance. Wet enthalpy i_{fg} (J/kg) varies with distance and therefore with grid spacing within the composite Simpson's Rule. In Figure 4.5, as the grid spacing is increased, the error is increased accordingly. It also shows a classic

convergence curve. Once a sufficiently fine spacing (0.011m to 0.086m) is used, an acceptable error is attained. An error of 0.01% is considered acceptable here indicating that a grid spacing of 0.086m should be used.

It is concluded that test no. 1 is inherently grid independent. A grid spacing of 0.086m in test no.2 is established and validated in the AuCFD code. As grid dependence will vary from model to model, a convergence curve for grid independence should be plotted for each case . For each of the tests in this thesis, the results have been verified to be independent of the grid. If the differences in vapour quality, mass flux, and heat flux are not significant between the tests, re-plotting the convergence curve is not be required.

4.5   Summary

Validation of the AuCFD was obtained by testing different grid spacings and refrigerant flow and heat flux conditions. It is found that the round-off error is not significant with the use of an independent grid and double-precision accuracy. With the use of the composite Simpson's rule, a first-order implementation of the finite difference equations yields an acceptably accurate computational model for evaporating fluid flow in a Dx tube.

It is also validated that grid independence can be demonstrated through the convergence zone where the error is decreased uniformly to a small value. In other words, the correct grid size should be used in the numerical method (composite Simpson's Rule) and the AuCFD code does converge to a solution with acceptable errors.

The justification for using a first-order accuracy solution instead of second-order for pressure drop is that second order would not improve the accuracy of the solution beyond the 20% deviation already accepted between the correlation used and published pressure drop data. It is currently the best possible correlation for two-phase pressure drops available in heat transfer field.

These considerations have been adhered to in building models of Dx evaporators. Round off errors can be minimised to within acceptable levels in the AuCFD code developed here to make it a useful tool in the design of Dx evaporators.

Chapter 5

RESULTS AND DISCUSSION

This chapter describes the computational results for the correlations for two-phase heat transfer coefficients and pressure drops of refrigerants . Firstly, the correlations for two-phase heat transfer coefficients with or without pressure drops against compared to the published data. Secondly, the correlations for two-phase pressure drop are also compared to the published data. Finally, suitable correlations are adopted for two-phase heat transfer coefficients and pressure drops in the scheme.

5.1   Comparative study

The purpose of the comparative study was to verify suitability of the correlations for two-phase heat transfer coefficient and pressure drops of pure refrigerants, R12 and R134a. This study uses a computational technique rather than an experimental one. Hence the published data of the other authors were reviewed and used to test against different correlations under the same input conditions. The computational results indicated that an appropriate correlation could be found to predict the data from Jung and Radermacher (1989), Johnson and Chaddock (1964) and Souza *et al* (1995) accurately. These results could then be used in a computational design tool for Dx evaporators.

In these results, the heat transfer coefficient and pressure drop comparisons do not take into account the effect of lubricants that circulate in actual refrigeration systems. The correlations adopted to determine the R134a and R12 heat transfer coefficient and pressure drops were developed for pure refrigerants only. The results of the computational scheme can predict the published (experimental) data with some deviations due to the experimental errors involved. After the comparative tests, the

correlations for two-phase heat transfer coefficient and pressure drops were finally determined and used in the computational design tool.

5.2   Correlations for two-phase heat transfer coefficient

In order to evaluate the suitability of the correlations for two-phase heat transfer coefficients in the computational design tool, comparative tests were conducted and are reported in this section. The first test was for the two-phase heat transfer coefficients without pressure drops R12 and R134A and the second test was for the two-phase heat transfer coefficients with pressure drops of R12 and R134A.

5.2.1 Test results for two-phase heat transfer coefficient without pressure drops

For the prediction of two-phase heat transfer coefficients, the Jung and Radermacher (1989), Shah (1982) and Kandlikar (1990) correlations were used and compared with the published data of Jung and Radermacher (1989) and Panek (1992). Under the same geometry of tubing, refrigerant and flow conditions from Jung and Radermacher's and Panek's published data, the test results of each correlation were compared with its corresponding published data.

The test conditions from Jung and Radermacher's paper are listed in Table 5.2 where the saturated temperatures, the inlet qualities and the mass flow rates of R12 and R134A can be found. An inner diameter of 8 mm and length of the evaporator tube of 7.96 m is used for these tests. An average heat flux of 20 kW/m^2 is also applied to the tube to provide 4 kW cooling capacity. The computational results are plotted in Figures 5.1 and 5.2. The mean deviations of different correlations (from experimental data) and the percentage of the nucleate and convective boiling contributions are tabulated in Table 5.2.

Figure 5.1 - *Comparison of experimental and computational results for HTC of R134a. Exp-J&R are experimental data from Jung and Radermacher, J&R are calculated data points using Jung and Radermacher's correlation, and Kandlikar and Shar are calculated data points from these authors' correlation.*

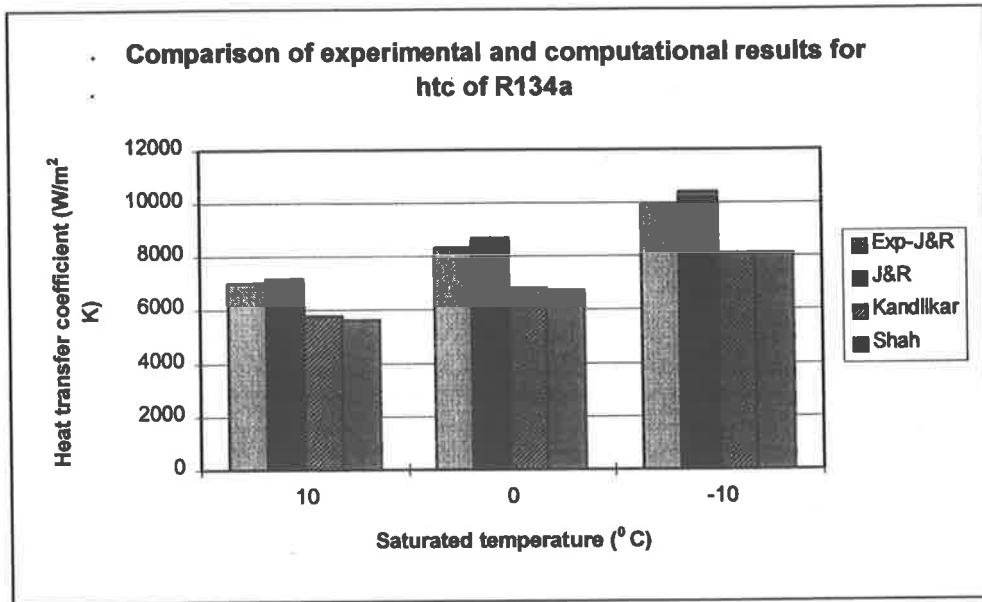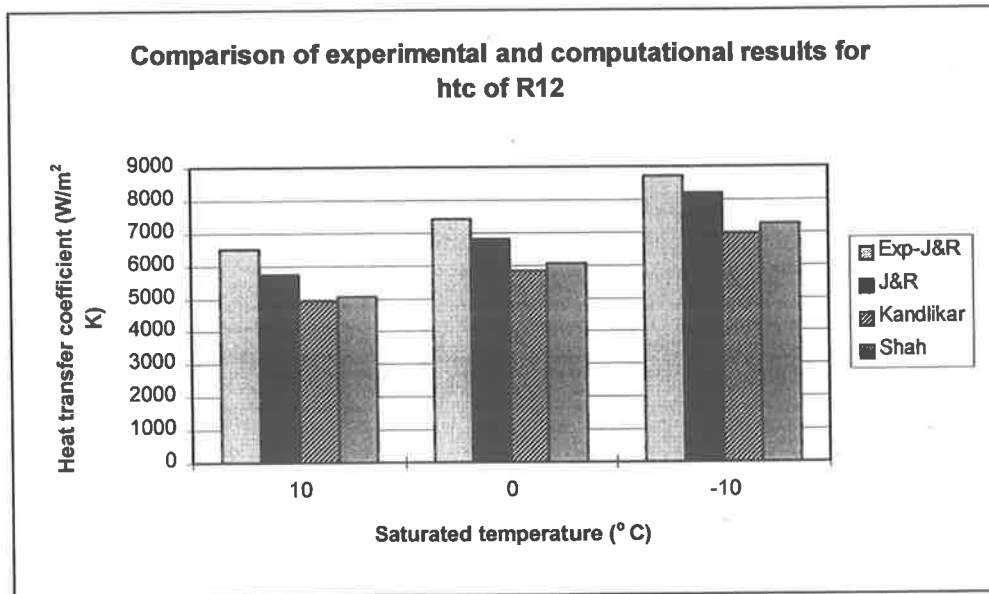**Figure 5.2** - *Comparison of experimental and computational results for HTC of R12. Exp-J&R are experimental data from Jung and Radermacher, J&R are calculated data points using Jung and Radermacher's correlation, and*

*Kandlikar and Shar are calculated data points from these authors'
correlations.*

Table 5.1 - Conditions for the comparative tests

Fluid	Saturated temperature -10°C		Saturated temperature 0°C		Saturated temperature 10°C	
	mass flow rate (g/s)	inlet quality(%)	mass flow rate (g/s)	inlet quality(%)	mass flow rate (g/s)	inlet quality(%)
R134a	28.74	33.0	27.49	27.6	26.38	21.8
R12	36.91	31.0	35.48	25.8	34.20	20.3

Table 5.2 - Test results for mean deviation of heat transfer coefficient of R134a

Correlation	Mean deviation from Jung & Radermacher's' experimental data points	Nucleate boiling contribution	Convective boiling contribution
Jung & Radermacher	+5%	5%	95%
Kandlikar	-19.6%	27%	73%
Shah	-18.8%	Not applicable	Not applicable

5.2.2 Discussions of two-phase heat transfer coefficients without pressure drops

For the prediction of two-phase heat transfer coefficient, Figures 5.1 and 5.2 suggest that Jung and Radermacher's correlation was the best in these tests with 5% mean deviation. The test results indicated that the total heat transfer coefficient consisted of 5% nucleate boiling contribution and 95% convective evaporation contribution.

The following Figures, 5.3 and 5.4, show that the nucleate boiling contribution decreased with increasing vapour quality. The nucleate boiling contribution was

affected by the product of a boiling suppression factor, N and a pool boiling heat transfer coefficient h_{sa}. When the vapour quality is increased, the boiling suppression factor is decreased due to a decreasing Martinelli's parameter, X_{tt}. On the contrary, the convective evaporative contribution was increased with the increasing vapour quality and was affected by the two-phase enhancement factor, F and single-phase heat transfer coefficient, h_{lo}. When the vapour quality is increased, the two-phase enhancement factor was increased more than the decreasing single-phase heat transfer coefficient. Hence the convective evaporative contribution became dominant.

Kandlikar's correlation predicted the experimental data with an averaged deviation of 19.6%. This correlation was selected for testing due to its generalised nature, being developed for databases from several researchers that use R12 as one of the primary fluids. However, R12 will be phased out by the year of 2000 completely and R134a will become a substitute; therefore, the correlation developed from R12 databases cannot be used as a long-term and practical resources.

Shah's correlation predicted the experimental data with a mean deviation of 18.8%. Shah did not break up his correlation into nucleate boiling and convective boiling terms. It should be noted that of the 60 experimental points, only 6 are found to be in the bubble suppression regime with the others in the convective boiling regime. This means that Shah's correlation was suitable for the bubble suppression regime with a lower vapour quality.
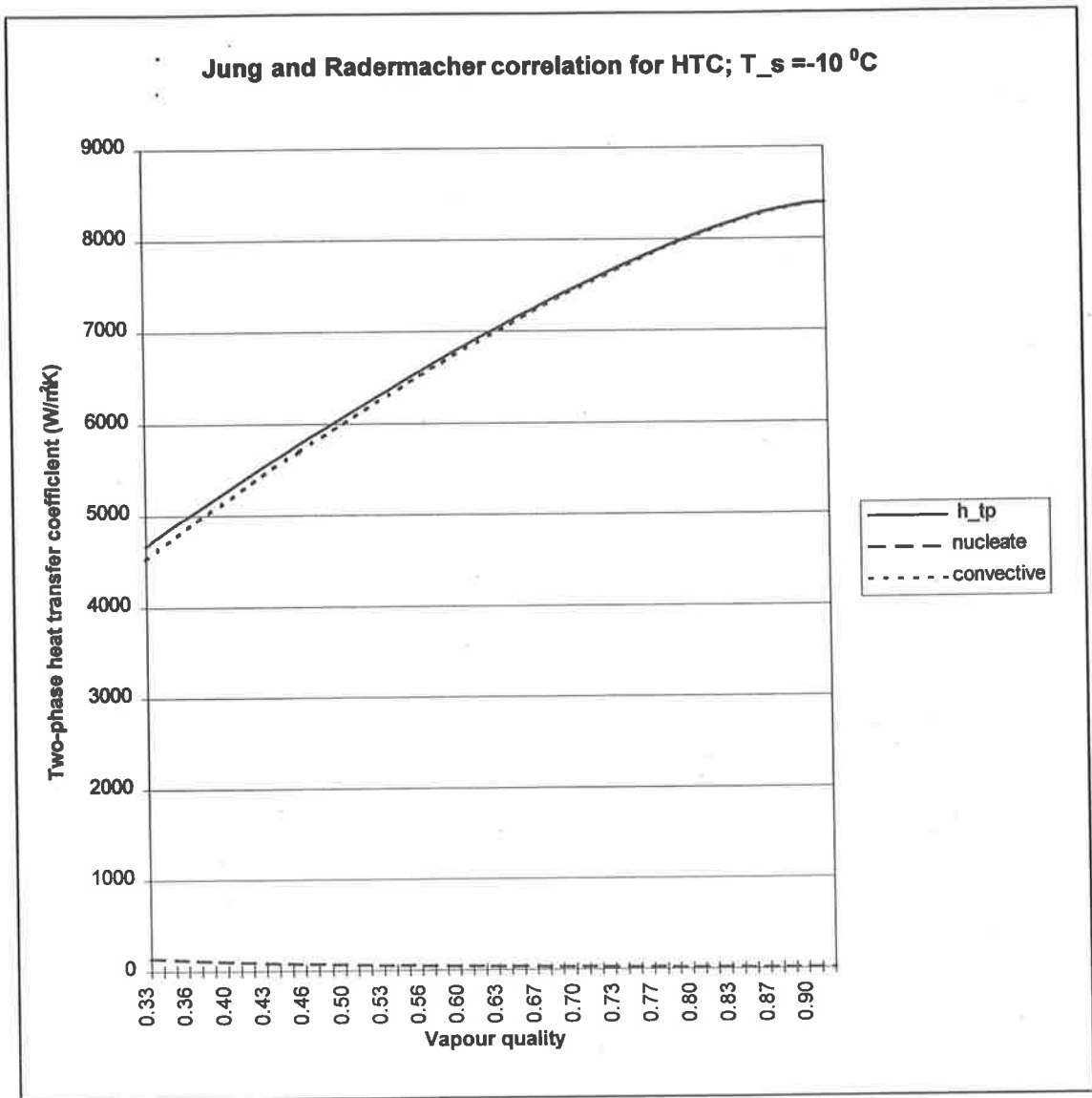
Figure 5.3 - *Nucleate boiling and convective evaporation contributions in two-phase heat transfer coefficient*
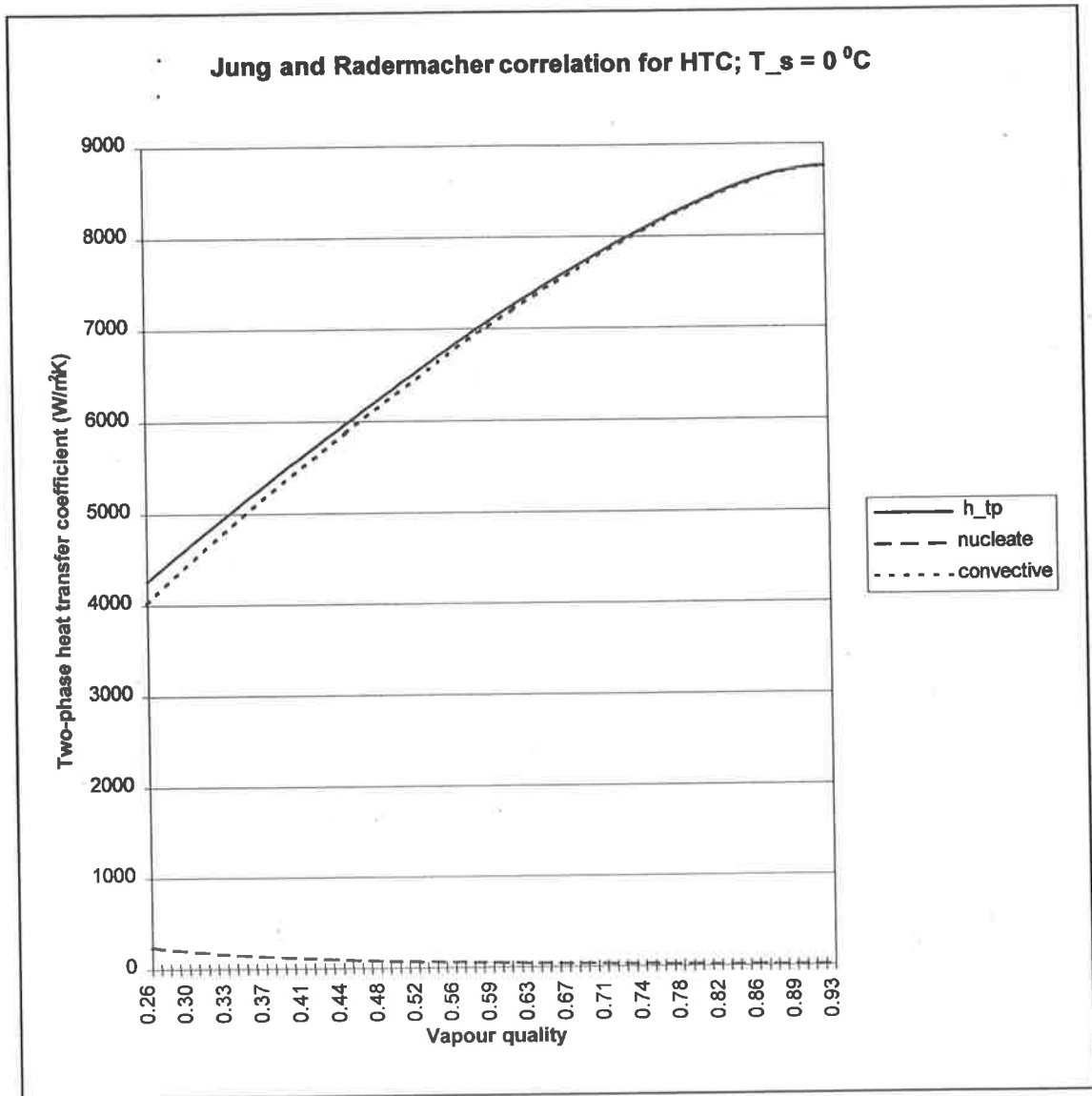
Figure 5.4 - *Nucleate boiling and convective evaporation contributions in two-phase heat transfer coefficient.*

5.2.3 Test results for two-phase heat transfer coefficient with pressure drops

For the prediction of two-phase heat transfer coefficients with pressure drops, the test conditions from Panek's paper (1992) were used to compare with the computational results of Souza *et. al's* correlation (1995) for pressure drops and Jung and Radermacher's correlation (1989a) for heat transfer coefficient. The results are detailed

in Table 5.3.   A horizontal tube of diameter 10.211mm and length 2.642m was modelled. The computational results are plotted in Figure 5.5.

The experimental data from Johnson and Chaddock (1964) was tested against the computational results from Jung and Radermacher's correlation (1989a)for heat transfer coefficients to demonstrate the applicability of Jung and Radermacher's correlation to data of other investigations.   A comparison between experimental and computational data is shown in Figure 5.6.

Table 5.3 - Conditions and results of R134a tests

Test no.	Heat flux (kW/m^2)	Mass flux (kg/s)	Inlet vapour quality (%)	Experimental heat transfer coefficient (W/m^2K)	Computational heat transfer coefficient (W/m^2K)
1	5.2	0.0246	21.1	2833	2282
2	5.0	0.025	39.3	3594	3318
3	10.1	0.044	19.7	4241	3572
4	19.3	0.0245	59.3	2816	4561
5	24.4	0.04076	49.4	3458	6267
6	30.9	0.0413	39.3	3972	5929
7	4.9	0.00802	24.8	1318	1259
8	10.2	0.0407	59.5	6333	6415
9	10.2	0.0411	39.7	5151	5056
10	10.2	0.0409	20.1	3776	3485
11	10.2	0.0418	19.5	3778	3481
12	10.2	0.0329	20.4	3631	3059

Figure 5.5 - *Results of R134a tests. Exp-Panek are experimental data from Panek, Comp-J&R are calculated data from Jung and Radermacher's (1990) correlation.*

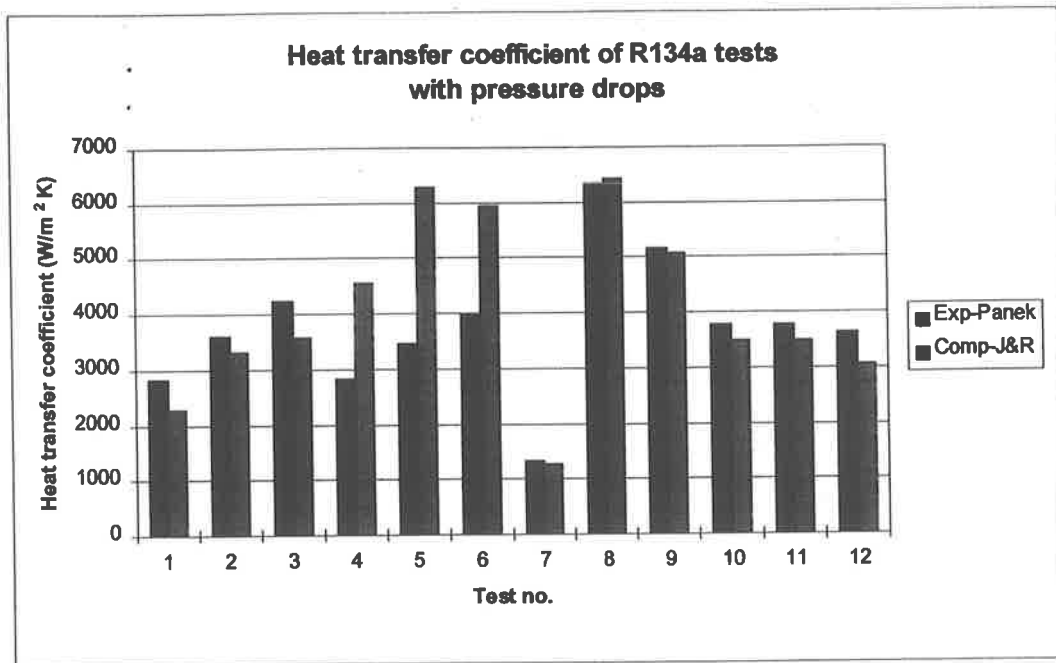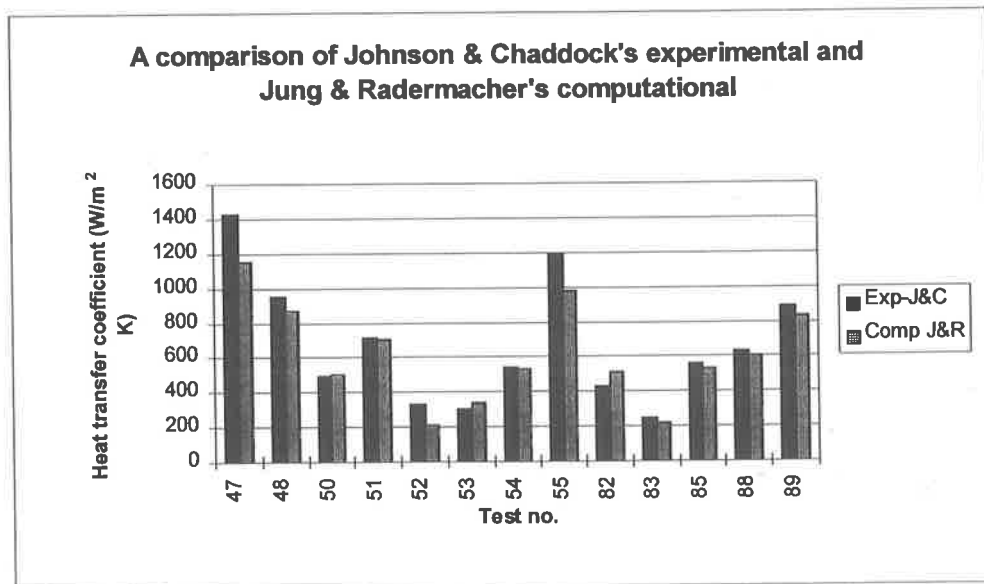**Figure 5.6** - *Comparison of experimental and computational results for HTC of R12. Exp-J&C are experimental data from Johnson and Chaddock, Comp-J&R are calculated data from Jung and Radermacher's (1990) correlation.*

5.2.4 Discussion of two-phase heat transfer coefficient with pressure drops

From Figure 5.5, it can be seen that the computational results have a good prediction of the experimental data with less than 10% variation except test numbers. 4, 5. and 6. Due to the overprediction of two-phase pressure drops of the refrigerants in test numbers 4, 5 and 6, the saturated temperature of refrigerants was also decreased accordingly. The heat transfer coefficients were therefore increased with the decreasing saturated temperature as the vapour quality was increased. This implied that the application of Souza *et al*'s correlation for two-phase pressure drops could not well predict the heat exchanger with over 20kW/m^2 cooling capacity. Some inaccurate predictions of the above results were caused by the over-predicted pressure drops which could affect the value of the heat transfer coefficient of the tube. In Figure 5.6, the computational data from Jung and Radermacher's correlation and the experimental data of Johnson and Chaddock are compared to verify that Jung and Radermacher's correlation could predict the two-phase heat transfer coefficients consistently under different flow conditions of the refrigerant, R12.

As a generalisation, Jung and Radermacher's correlation for two-phase heat transfer coefficient is reliable for predicting heat transfer of boiling flow within tubes.

5.3   Correlations for two-phase pressure drops

The aim of these tests was to find a suitable correlation for two-phase pressure drops for use in the computational scheme (AuCFD) - the results of comparative tests are reported in this section. Firstly, computational results from Jung and Radermacher's and Souza and Pimenta's correlations were compared with the experimental data points from Johnson and Chaddock (1964). Secondly, one of the above correlations was selected to be used based on the test results from section 5.3.1. Finally, the computational results

of the selected correlation were compared with Souza *et al*'s experimental data as an independent check of the correlation's general applicability The test conditions and test results are illustrated as follows.

5.3.1 Test results for two-phase pressure drops of R12

The test conditions from Johnson and Chaddock are shown in Table 5.4. and the comparative test results are plotted in Figure 5.7. The test results of Souza *et al*'s experimental and computational data are presented in Figures 5.8 and 5.9.

Table 5.4 - Test results for two-phase pressure drops of R12

Test no.	Saturated temp. ($^\circ$C)	Mass flow rate (kg/s)	Inlet vapour quality	Heat flux (W/m^2)	Experimental (Pa)	Jung & Radermacher (Pa)	Souza & Pimenta (Pa)
1	-24.2	0.010973	0.043	16151.4	1228	732	813
2	-29.7	0.008766	0.045	11924.3	690	534	593
3	-41.7	0.006048	0.028	6129.34	345	270	307
4	-51.7	0.003764	0.054	3290.22	207	118	183
5	-50.8	0.004338	0.085	6271.29	680	370	443
6	-49.5	0.00345	0.111	6192.43	414	292	362
7	-26.2	0.004198	0.096	6176.66	207	169	190
8	-19.06	0.004708	0.088	6176.66	207	152	162
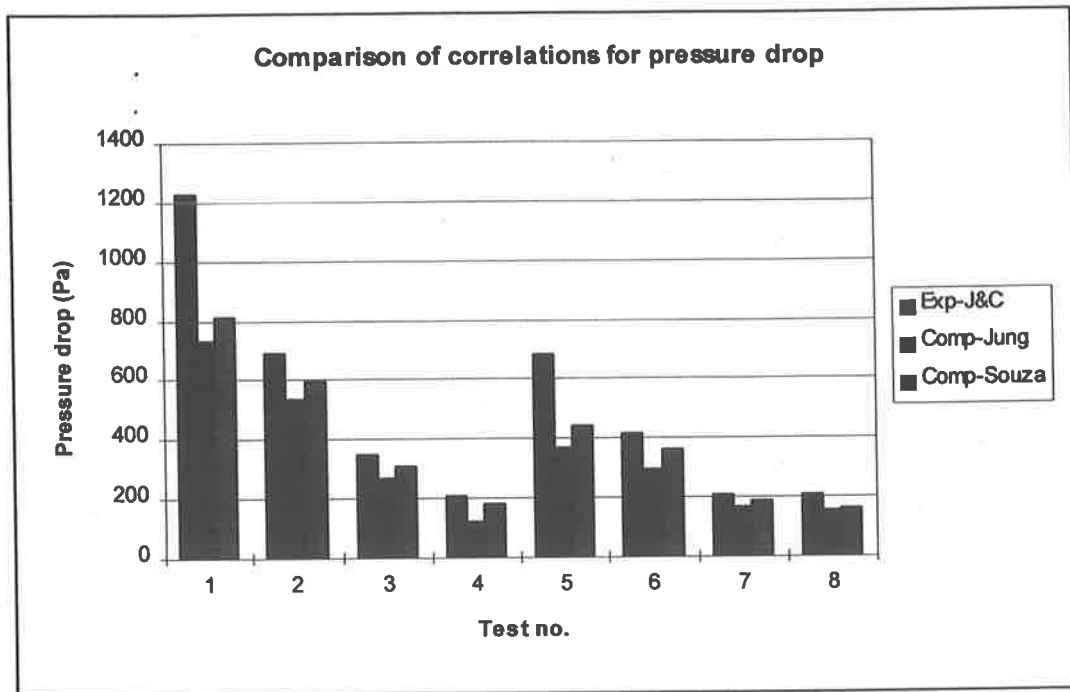
Figure 5.7 - *two-phase pressure drops of R12 (not available in the literature for R134a). Exp-J&C are experimental data points from Johnson and Chaddock (1964), Comp-Jung are calculated data points from Jung and Radermacher's (1990) correlation and Comp-Souza are computational data points from Souza and Pimenta's correlation.*

5.3.2 Discussion of two-phase pressure drops of R12

Table 5.4 and Figure 5.7 indicate that the computational data scheme based on Souza and Pimenta's correlation for two-phase pressure drops predicted Johnson and Chaddock's experimental data much better than the computational scheme based on Jung and Radermacher's correlation. However, if the heat flux is larger than 20 kW/m^2, Souza and Pimenta's correlation does not yield a good prediction of pressure drops. Souza and Pimenta (1995) presented that the trends of the frictional pressure drops changes sharply around a quality of 85% which is called the peaking effect. The flow changes from annular to spray regime. A physical explanation for a such variation of pressure drop is that this change means a sizeable drop of shear stress at the wall, as the

liquid viscosity is 20 times the vapour viscosity. At around vapour quality of 85%, specially if the evaporator tube is heated, the wall tends to dry up. Further testing has been carried out to verify Souza and Pimenta's correlation.

5.3.3 Test results of two-phase pressure drops of R12 and R134a

The following test results used the experimental data from Souza *et al* (1993) to verify whether Souza and Pimenta's correlation for two-phase pressure drops can be applied to any flow conditions in horizontal Dx tubes.

Table 5.5 - Input conditions for two-phase pressure drops of R12 and R134a

Refrigerant	Tube length	Tube diameter	Mass flux	Heat flux
R12	1.2954 m	10.92 mm	200 -500 kg/m^2s	5 - 30 kW/m^2
R134a	1.2954 m	10.92 mm	200 -500 kg/m^2s	5 - 30 kW/m^2
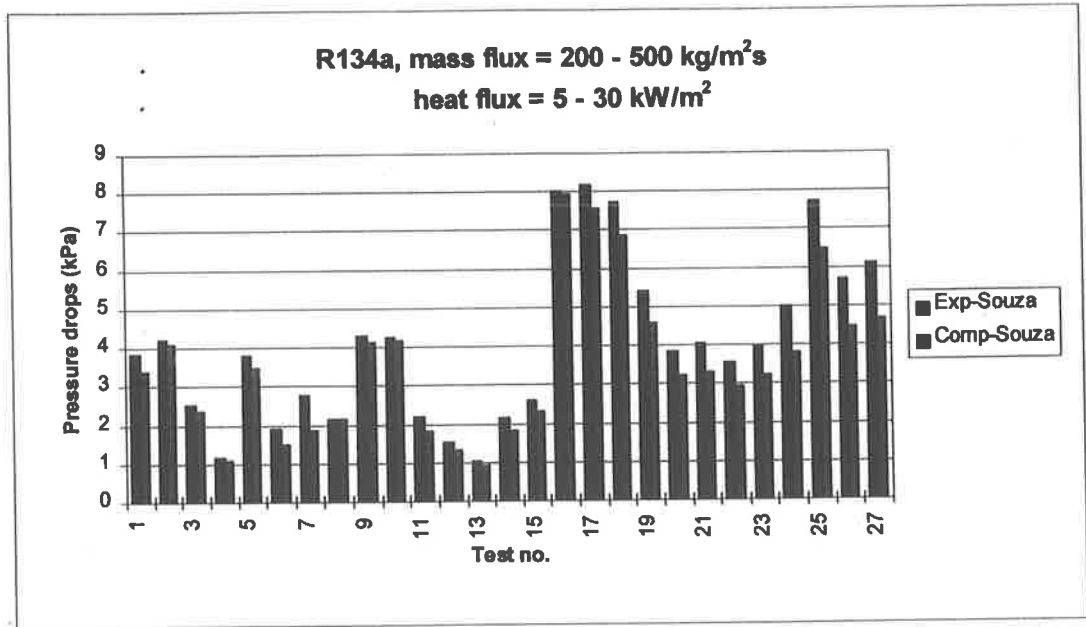
Figure 5.8 - *two-phase pressure drops of R134a. Exp-Souza are experimental data points from Souza et.al. and Comp-Souza are calculated data points form Souza and Pimenta's correlation.*
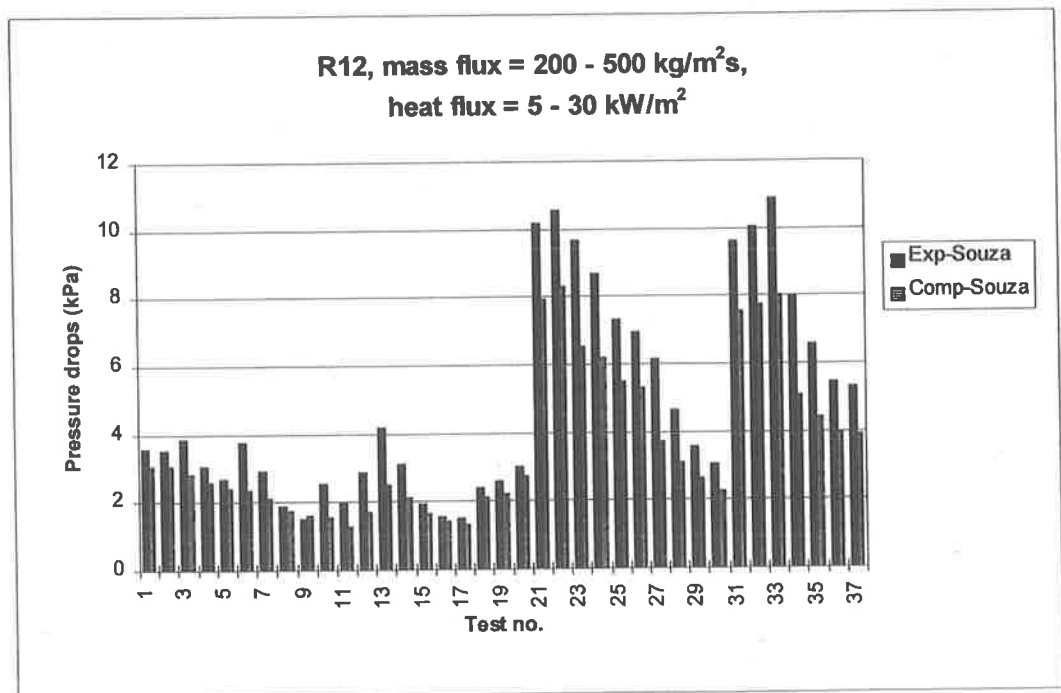
Figure 5.9 - *two-phase pressure drops of R12. Exp-Souza are experimental data points from Souza et.al. and Comp-Souza are calculated data points form Souza and Pimenta's correlation.*

5.3.4 Discussion of two-phase pressure drops of R12 and R134a

In Figures 5:8 and 5.9, Souza and Pimenta's correlation performed well in predicting two-phase pressure drops of refrigerant R12 and R134a with less than 20% mean deviation. R134a is a potential replacement of R12 and, the results of two-phase pressure drops of R134a were better than R12. The computational results of R134a in Figure 5.8 were similar to those in Souza *et. al*'s published data. Souza and Pimenta's correlation is the best for predicting two-phase pressure drops in the present research field and reliable enough to be used in the AuCFD.

5.4 Summary of the test results

As can be seen from the above test results, Jung and Radermacher's (1990) correlation for two-phase heat transfer coefficients and Souza and Pimenta's (1995) correlation for two-phase pressure drops predicted well the experimental data from the other researchers. The mean deviations for the computational results were acceptable, therefore, these correlations were used as the empirical bases in the AuCFD computational scheme developed here. In general, heat transfer coefficient correlations were seen to better predict experimental data points (~7%) than did pressure drop correlations (~20%).

Chapter 6

FINAL MODEL FOR AuCFD

6.1 Introduction

This chapter will describe how to use the final model for a Dx tube, its applications and limitations. The Dx tube is a direct heat exchanger where incoming fluids will be heated or cooled as they pass through the tubes. The final model calculated the two-phase and superheated heat transfer coefficients and pressure drops of refrigerants and heat transfer coefficients of air. As mentioned in Chapter 1, the main aim of this scheme is to develop a unique model for calculating two-phase heat transfer coefficients and pressure drops of refrigerant in horizontal tubes. The addition of the superheated region and airside calculations are simple augmentations to the design tool. The model is an air to refrigerant heat exchanger where constant or variable heat flux is transferred from the air flow through the tube wall to the refrigerant. The following will show how to build the model and use the execution files of the model.

6.2 A big picture of the model

The model includes three different regions, tubeside, airside and superheated. The tubeside region is mainly concerned with the two-phase flow of the refrigerant inside the tube calculating heat transfer coefficients, vapour quality, transport properties and pressure drops. The airside region only manipulates heat transfer coefficients of cross-flowing air. After the refrigerant has become 100% vapour inside the tube, the superheated region takes over from the tubeside region and starts to calculate superheated heat transfer coefficients.
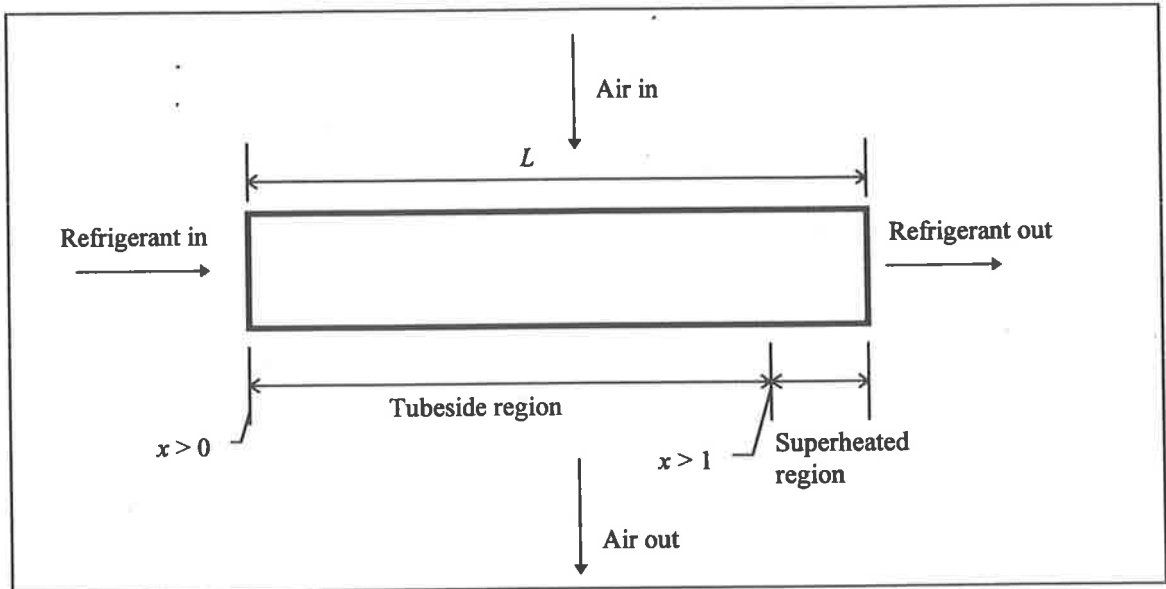
Figure 6.1 - Model with superheated region
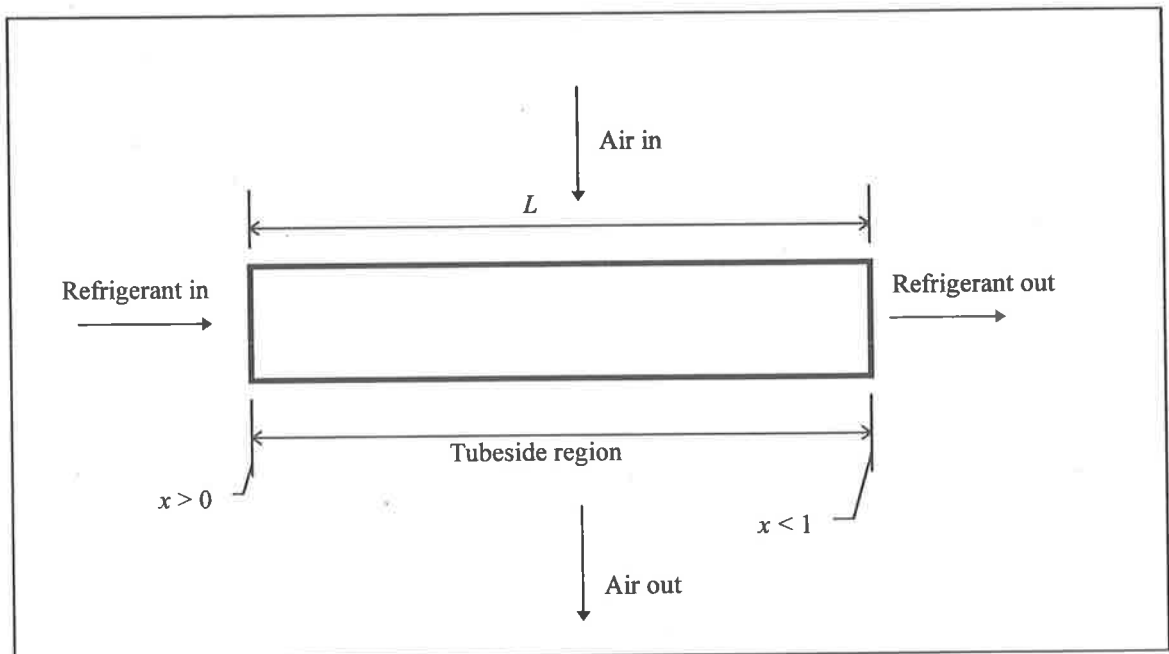
Figure 6.2 - Model without superheated region

where:

L = total length of tube (m)

x = vapour quality of refrigerant.

Figure 6.1, shows the case where superheating occurs; in the tubeside region, the inlet vapour quality x of refrigerant increases as it passes through the tube gaining heat energy from the hot airside Then, in the superheated region, the vapour quality of refrigerant becomes greater than 1 before it comes out of the tube. On the other hand, in Figure 6.2, no superheated region is modelled because the vapour quality of the refrigerant was less than 1 when it reached the tube end. The model, with or without superheated region, depends on the variables such as inlet vapour quality, mass flow rate, saturated temperature of refrigerant and quantity of heat flux applied to the tube.

To control whether the region is superheated, a control loop for the tubeside region is used to monitor the vapour quality of refrigerant. If the quality is still less than 1, the control loop will continue to execute the tubeside functions. If the quality is greater than 1, the control loop for Tubeside region will jump into the other control loop for the superheated region. The control loop for the superheated region lapses when the interval n is greater than the total-length. The total-length is equal to $n+1$, where $n = L/\Delta l$.

6.2.1 Tubeside region

In this region , the main task is to determine the two-phase heat transfer coefficients and pressure drops of the refrigerant under various flow conditions which is the main focus of this thesis. With the use of the control loop for tubeside region, the functions for transport properties of the refrigerant at any saturated temperature or iteration number are extracted from the specified refrigerant property program. As all the required refrigerant properties are calculated, the two-phase heat transfer coefficients and pressure drops will be found out. When the refrigerant exits the tubeside region, the average two-phase heat transfer coefficient and the total two-phase pressure drops are calculated within the control loop. Equations, 6.1, 6.2 and 6.3 from Souza *et al* (1993)

---

are shown below. Equation 6.1 is used to accumulate the two-phase heat transfer coefficient of the refrigerant. With Equation 6.2 the average two-phase heat transfer coefficient of the refrigerant can be determined. The total two-phase pressure drop is also accumulated by the frictional and accelerational pressure drops in Equation 6.3.

$$*htc\_t = *htc\_t + h\_tp \qquad (6.1)$$

$$htc\_av = \frac{*htc\_t \times AI}{L \times PI \times ID} \qquad (6.2)$$

$$*dp\_t = *dp\_t + dp + dp\_a \qquad (6.3)$$

where:

AI = internal surface area of tube (m^2)

ID = internal diameter of tube (m)

dp = two-phase frictional pressure drops (Pa)

dp_a = two-phase accelerational pressure drops (Pa)

$*dp\_t$ = total two-phase pressure drops (Pa) = ΔP_{tp}

htc_av = average two-phase heat transfer coefficients (W/m^2 K)

$*htc\_t$ = total two-phase heat transfer coefficients (W/m^2 K)

h_tp = two-phase heat transfer coefficients (W/m^2.K) = h_{tp}

L = length of tube (m)

PI = represent circle constant π

Superscript

$*$ = coefficient evaluated at saturated temperature of refrigerant.

6.2.2 Airside region

As the air passes over outside of the tubes, the heat transfer coefficient of air is calculated using Equations 3.29. In Equation 3.29, the heat transfer coefficient of air, h_air is calculated using Brigg and Young's correlation (1965) which is based on a configuration of finned tube heat exchanger using velocities in the minimum flow cross-sectional area. The equations for calculating the average heat transfer coefficient of air in the heat exchanger are shown in Equations, 6.4 and 6.5. The equation for calculating the heat transfer rate between the air and the refrigerant is also expressed as Equation 6.6 where T_s and T_air are the refrigerant and air temperatures respectively on each side of the wall.

$$*h\_airt = *h\_airt + h\_tp \qquad (6.4)$$

$$h\_airav = \frac{*h\_airt \times AO}{L \times PI \times OD} \qquad (6.5)$$

$$Q = \frac{T\_air - *T\_s}{\dfrac{1}{h\_tp \times AI} + \dfrac{\log(OD/ID)}{2PI \times k\_cu \times l} + \dfrac{1}{h\_air \times AO}} \qquad (6.6)$$

where:

AO = external surface area of tube (m^2)

AI = internal surface area of tube (m^2)

ID = internal diameter of tube (m)

OD = external diameter of tube (m)

k_cu = conductivity of copper tube (W/m K)

h_air = heat transfer coefficients of air = h_a (W/m^2 K)

h_airt = total heat transfer coefficients of air (W/m^2 K)

h_airav = average heat transfer coefficients of air (W/m^2 K)

L = length of tube (m)

PI = represent circle constant π

T_air = air temperature (°C)

T_s = refrigerant temperature (°C)

Q = heat transfer rate (W)

Superscript

*   = coefficient evaluated at saturated temperature of refrigerant.

6.2.3 Superheated region

The major difference between the superheated and tubeside regions is the vapour quality of the refrigerant. When the vapour quality of the refrigerant is greater than 1, it means that the region is superheated and no more liquid refrigerant exist in those areas. Also, all the refrigerant properties are referred to the vapour state only. The refrigerant is commonly superheated by around 6 K to ensure no "slugs" of liquid in a heterogeneous flow enter and damage the compressor.

The main task of this part of the program is to determine the superheated heat transfer coefficients of the refrigerant. As the control loop is transferred from tubeside region to superheated region, due to $x>1$, AuCFD starts to calculate the superheated heat transfer coefficients of the refrigerant. Since only low superheat occurs, the saturated temperature of the refrigerant is assumed valid for calculating the refrigerant properties. The equations used from Dittus-Boelter (1930) for the calculation of superheated heat transfer coefficients are developed in section 3.5and shown as Equation 6.7 below.

$$h\_SH = 0.023 \, Re\_g^{0.8} \, Pr\_g^{0.4} \qquad (6.7)$$

where:

h_SH = superheated heat transfer coefficient (W/m^2 K)

Re_g = vapour Reynolds number $= Re_g = Re_v$

Pr_g =vapour Prandtl number $= Pr_g = .Pr_v$.

6.3 Installing and Starting 'AuCFD'

There are two different AuCFD executable files available for users: Au-R134a.exe and Au-R12.exe which are used for calculating two-phase heat transfer coefficients and pressure drops of refrigerant, R134a and R12 and heat transfer coefficients of air. Using the Turbo C++ software package, these two files can be copied into a sub-directory of Turbo C++ and are ready to be used.

To run the files directly, double click either Au-134a.exe or Au-R12.exe icons from File Manager or enter the Turbo C++ environment and edit the execution file.

6.4 Input of variables

Under the heading of "Computational Scheme for HTC and Pressure drops", the computer will require the user to type in relevant data and press "Enter". The following shows the questions as they appear on the screen.

Computational Scheme for HTC and Pressure drops

Enter a length of a horizontal tube (m)...

Enter an internal diameter of a horizontal tube (m)...

Enter an external diameter of a horizontal tube (m)...

Enter a saturated temperature (^{0}C) of refrigerant at inlet...

Enter a mass flow rate (kg/s), mdot...

Enter a vapour quality, x...

Enter a air temperature(^{0}C) passing over a heat exchanger...

Enter a air mass flow rate (m/s) passing over a heat exchanger...

Enter fin height (m)...

Enter fin thickness (m)...

Enter distance between adjacent fins (m)...

Enter heat flux condition: constant=0, variable =1...

Enter a heat flux of air (W/m^2)...

Ensure all input data is correct before pressing the 'Enter' key. If wrong data is entered, make the constant heat flux value '0' and press the 'Enter' key. The program then reinitialise the user input routine. If all values were entered correctly, the program will execute and print all input and output data on the screen.

6.5   Output of variables

If the execution is successfully completed, the screen will show reiterate the input values and list the output variables as follows:

<u>Input Data</u>

The length of a horizontal tube (m) is

The diameter of a horizontal tube (m) is

The saturated temperature (^{0}C) of refrigerant at inlet is

The mass flow rate (kg/s), mdot is

The inlet vapour quality, x is

The air temperature(^{0}C) passing over heat exchanger is

The air velocity (m/s) passing over heat exchanger is

The fin height (m) is

The fin thickness (m) is

The distance between adjacent fins (m) is

The heat flux condition is

The heat flux of air (W/m^2) is

<u>Output Data</u>

The total two-phase pressure drops : dp_t =

The two-phase average heat transfer coefficient: htc_av =

The superheated heat transfer coefficient: h_SH =

The heat transfer coefficient of air: h_air =.

As can be seen from above, all the input data can be checked to ensure that the input data is entered correctly.

6.6   Error Codes

If the execution is unsuccessful, the most common messages are:

Floating point error: Divide by 0

"Divide by 0" means the result is infinitive, such as 1.0/0.0.

Floating point error: Domain

"Domain" means the result is not a number, like 0.0/0.0.

Floating point error: Overflow

"Overflow" means the result is infinitive with complete loss of precision, such as assigning 1e200*1e200 to a double.

The messages indicate that some input data is inappropriate or some typing errors were made during the data input.

6.7   Printing input and output data

When the input and output data are shown on the screen, it is easy to print the data by pressing the 'Print Screen' button on the keyboard.

6.8   Summary of final model for AuCFD

The AuCFD code is a useful design tool for calculating the heat capacity (W) of air conditioning or refrigeration units by using the values of two-phase and superheated heat transfer coefficients, pressure drops of refrigerants and heat transfer coefficient of air. Any user, even with little computational experience, should be able to use the

package. A limitation of the AuCFD package is that the execution files of the model should be run in a Turbo C++ environment.

Chapter 7

CONCLUSIONS AND RECOMMENDATIONS

7.1   Introduction

This chapter draws conclusions about two major achievement of this research work. Firstly, the development of a computational scheme, AuCFD for calculating two-phase heat transfer coefficients and pressure drops in direct expansion heat exchangers. The second major work was the investigations of other researchers' empirical correlations for heat transfer coefficients and pressure drops in general application for heat exchanger design.

Finally, some recommendations will be made for the future development of the present work.

7.2   Development of a computational scheme

Using the scheme developed here, a design engineer can estimate the size of a heat exchanger needed using various input parameters, such as the tube diameter and length, the saturated temperature, the mass flow rate of the refrigerants and the constant heat flux applied to the tube. The scheme contains two separate R12 and R134A refrigerants' execution files for the engineer to compare the performance of R12 with R134A under the same test conditions. The scheme can be used in the following applications:

- **Theoretical estimation** of two-phase heat transfer coefficient and pressure drops of R12 or R134a flowing through a horizontal tube are achieved using the scheme. Heat

exchanger size can be optimised for any particular power output (kW) requirement in air conditioning or refrigeration plants.

- **Comparative tests** of two-phase heat transfer coefficients and pressure drops of R12 and R134a can be done under the same conditions. This will allow re-design and retrofitting of existing R12 systems with R134a.

7.2.1 Verification of the scheme

As can be seen in Chapter 4, the AuCFD code has been validated under different flow conditions with grid independence. The main technique used in the scheme is a finite difference method which can be applied to the equations for the energy balance of refrigerants flowing in a horizontal tube. The composite Simpson rule is used to calculate the values for two-phase pressure drops. Using a numerical error analysis, the round-off errors were found to be insignificant in the scheme and a first order of accuracy is used in the correlations.

As can be seen from the test results in Chapter 5, with a first order scheme, the prediction of heat transfer coefficients of the refrigerants was better than the prediction of pressure drops. Also, the prediction of pressure drops of R134a was better than the pressure drops of R12. It can be explained as follows:

- The correlations for two-phase heat transfer coefficients and pressure drops were developed particularly for some new working fluids in the industry such as R134a.

- As R134a becomes more popular and R12 has phased out, more accurate correlations for R134a transport properties are available in the industry.

7.3   *Comparison of correlations*

A comparison of the researchers' empirical correlations for heat transfer and pressure drop were made in Chapter 2. Most of the researchers stated that their correlations were derived from the empirical data and predicted two-phase flow mechanisms. However, their correlations were developed from their own specific tube configurations and flow conditions. The deviations between the correlations for predicting the data were significant, therefore the selection of a suitable correlation must be conducted carefully. The tube size, flow conditions, and applications of the coefficients are considered as a selection criteria. After Jung and Radermacher's (1989a) and Souza and Pimenta's (1995) correlations for two-phase heat transfer coefficients and pressure drops have been investigated, their correlations were validated in Chapter 4 and were selected to be used in the AuCFD code. In Chapter 5, a series of comparisons between the correlations and the published data were carried out, Jung and Radermacher's (1989a) and Souza and Pimenta's (1995) correlations were selected to be used in the AuCFD scheme.

7.4   *Recommendations for AuCFD*

For future development of the current work, there are some recommendations to be made:

- General correlations for two-phase pressure drops need to be developed to suit all applications for different fluids.

- Two-phase pressure drops due to bend losses should be investigated.

- Experimental data is required to confirm computational data.

- Using computational and experimental techniques, further investigations for correlation for two-phase heat transfer coefficients are required for different refrigerants.

- Various heat fluxes and oil lubricants in the system should be studied.

- Vertical tube arrangement and bends should be added to the tubeside calculations.

- More airside models should be added to increase the applicability of AuCFD to industrial applications.

REFERENCES

Abdelsalam, M., and Stephan, K., 1980. Heat transfer correlation for natural convection boiling, *Journal of Heat and Mass Transfer,* **23** 73-87.

ASHRAE, 1989. ASHRAE Handbook in Fundamentals, *American Society of Heating, Refrigerating and Air-Conditioning Engineers, Inc.,* Atlanta., chapter 4

ASHRAE, 1990. ASHRAE Handbook in Refrigeration Systems & Application, *American Society of Heating, Refrigeration and Air-Conditioning Engineers, Inc.,* Atlanta, chapter 3.

Altma, M., Norris, R.H. and. Staub, F.W., 1960. Local and average heat transfer and pressure drops for refrigerants evaporating in horizontal tube, *ASME Journal of Heat Transfer,* August 1960, 189-198.

Alves, G.E., 1954. Co-current liquid-gas flow in a pipeline contactor, *Chem. Process Eng.,* 50 (9), 449-456.

Borishanski, V.M., 1969. Correlation of the effect of pressure on the critical heat flux and heat transfer rates using the theory of thermodynamics similarity, *Problems of heat transfer and hydraulics of two phase media,* Z.Z. Kutateladze, ed., Pregamon, Oxford, United Kingdom, 67-72.

Briggs, D.E. and Young, E.H., 1965. Convective heat transfer and pressure drop of air flowing across triangular pitch banks of finned tubes, *Chemical Engineering Program. Symposia . Series No.* 41 and 59.

Chan, C.Y. and Haselden, G.G., 1981. Computer-based refrigerant thermodynamic properties. Part 1: Basic equations, *Int. J. Refrigeration,* **4,** 7-12.

Chen, J. C., 1966. Correlation for boiling heat transfer to saturated fluids in convective flow. *Ind. Eng. Chem. Process Design Develop.,* **5** (3).

Cleland, A.C., 1986. Computer sub-routine for rapid evaluation of refrigerant thermodynamic properties, *Int. J. Refrigeration,* **9,** 346-351.

Collier, J.G., 1972. *Convective Boiling and Condensation,* McGraw Hill Book Co. Ltd.

Dittus, F.W. and Boelter, L.M.K., 1930. *Publ. Eng.*, University of California at Berkeley, **2** ,443.

Eckels, S.J. and Pate, M.B., 1990. A comparison of R134a and R12 in tube heat transfer coefficients based on existing correlations, *ASHRAE Transaction*, **96** (1),256-265.

Fukushima, T and Koudou, M., 1990. Heat transfer coefficients and pressure drop for convective boiling and condensation of R134a. Proceedings USNC/IIR Purdue Refrigerant Conference, 196-204.

Gouse, S.W. and Coumou, K.G., 1965. Heat transfer and flow inside a horizontal tube evaporator : Phase I, *ASHRAE Transaction*, **71** (1), 152-160.

Hoffmann, K.A.,1989. *Computational fluid dynamics for engineers*. A publication of engineering education system.

Holman, J.P.,1992. *Heat Transfer*. McGraw-Hill book company.

Johnston, R.C. and Chaddock, J.B., 1964. Heat transfer and pressure drop of refrigerants evaporating in horizontal tubes, *ASHRAE Transaction*, **70**, 163-172.

Jung, D.S. and Radermacher, R., 1989a. Prediction of heat transfer coefficients of various refrigerants during evaporation, *ASHRAE Transaction*, **95** (2), 48-53.

Jung, D.S. and Radermacher, R., 1989b. Prediction of pressure drop during horizontal annular flow boiling of pure and mixed refrigerants, *Int. J. Heat Mass Transfer*, **32** (12), 2435-2446.

Jung, D.S. and Radermacher, R., 1991. Transport properties and surface tension of pure and mixed refrigerants, *ASHRAE Transaction*, **97** (1), 90-99.

Kandlikar, S.G., 1990. A general correlation for saturated two-phase flow boiling heat transfer inside horizontal and vertical tubes, *ASME Journal of Heat Transfer*, **112**, 219-228.

Katarina, H., 1990. Heat transfer coefficients, two-phase flow boiling of R134a, *Proceedings USNC/IIR Purdue Refrigeration. Conference*, 205-214.

Kays, W.M., and London, A.L.,1955. *Compact heat exchangers*. The National Press, Palo Alto, California.

Lazarek, G.M. and Black, S.H., 1982. Evaporative heat transfer, pressure drop and critical heat flux in a small vertical tube with R-113, *Int. J. Heat Mass Transfer*, **25**, (7), 945-966.

Launder, B.E. and Spalding, D.B., 1972. *Lectures in Mathematical Models of Turbulence*, Academic Press, London.

Lewis, R.W., Morgan, K and Schrefler,B.A.,1983. *Numerical methods in heat transfer*, Chichester, J.Wiley, New York.

Lockhart, R.W. and Martinelli, R.C., 1947. Proposed correlation of data for isothermal two-phase two-component flow in pipes, *Chemical Engineering Progress*, **45**, 39 - 48.

Martinelli, R.C. and Nelson, B., 1948. Prediction of pressure drop during forced-circulation boiling water, *Transaction of ASME*, **70**, 695-702.

Nagaoka et al ,1986. A new correlation for the viscosity of gaseous fluorocarbon refrigerants. *Int. J. Thermophysics*, 7 (5), 1023-1031.

Panek, J.S., 1992. *Evaporation heat transfer and pressure drop in ozone-safe refrigerants and refrigerant-oil mixtures*, Masters thesis, Dept. of mechanical engineering, University of Illinois at Urbana-Champaign.

Pierre, B., 1955. The coefficient of heat transfer for boiling freon-12 in horizontal tubes, *SF Review 2(1)*. Svenska Flaktfabriken A.B., Stockholm, Sweden.

Ratiani, G.V. and Shehriladze, I.G., 1972. Study of the process of fully developed boiling of liquids, *Heat Transfer - Soviet Research*, 4 (4), 126-141.

Rohsenow and Hartnett, 1973. *Handbook of heat transfer*, McGraw-Hill Book Company.

Shah, M.M., 1976. A new correlation for heat transfer during boiling flow through pipes, *ASHRAE Transactions*, **82** (2) 66-86.

Shankland I. R., 1990. Private Communication Allied Signal Inc., Genetron Products Laboratory, Buffalo, New York.

Souza, *et al.*, 1992.Experimental evaluation of convective boiling of refrigerants HTC-134a and CFC-12. *ASME, HTD, Two phase flow and heat transfer*, **197**, 121-127.

Souza, A.L., Chato, J.C., Wattelet J.P. and Christoffersen, B.R., 1993. Pressure drop during two-phase flow of pure refrigerants and refrigerant-oil mixtures in horizontal smooth tubes. *ASME, HTD, Heat transfer with alternate refrigerant*, **243**, 35- 41.

Souza, A.L. and Pimenta, M.M., 1995. Prediction of pressure drop during horizontal two-phase flow of pure and mixed refrigerants, *ASME, FED*, **210**, Cavitation and multiphase flow.

Torikoshi, K. and Ebisu, T., 1993. Heat transfer and pressure drop characteristics of R134a, R32, and a mixture of R32/R134a inside a horizontal tube, *ASHRAE Transaction*, 90-96.

Takamatsu, H., Momoki, S. and Fujii, T., 1991. A comparison of evaporation heat transfer coefficients and pressure drop in a horizontal smooth tube for R134a and R12, *XVIII International Congress of Refrigeration*, 444-448.

Turaga, M. and Guy, R.W., 1985. Refrigerant side heat transfer and pressure drop estimates for direct expansion coils. A review of works in North America use, *International Journal of Refrigeration*, **8** (3), 134-142.

Wendt, J.F.,1992. *Computational fluid dynamics*. Springer-Verlag.

Yata *et al* ,1984. Measurement of thermal conductivity of liquid fluorocarbons, *Int. J. Thermophysics*, **5** (2).

APPENDIX I

The following is a list of the main program, 97comp.cpp, which contains all major equations for calculating two-phase and superheated heat transfer coefficient and pressure drop and heat transfer coefficient of air. The requirements of input and output parameters and the control loops for the Tubeside, Superheated and Airside regions are also included.

```
// ------------------------------------------------------------------
// Computational scheme for two phase HTC & pressure drops.
// Program name : 97comp1.cpp
// Author: Edwin AU
// Date: 24/11/1997
//------------------------------------------------------------------

#include<math.h>
#include<iostream.h>
#include<stdio.h>
#include<conio.h>

// global (external) constants

   const double PI = 3.1415927;
   const double g =9.81;

// global function definition - R12 properties
   double liquid_conductivity(double);
   double liquid_density(double);
   double liquid_enthalpy(double);
   double liquid_Prandtl(double);
   double liquid_viscosity(double);
   double saturated_pressure(double);
   double surface_tension(double);
   double saturated_temperature(double);
   double vapour_density(double);
   double vapour_enthalpy(double);
   double vapour_Prandtl(double);
   double vapour_viscosity(double);
   double wet_enthalpy(double,double);
```

```cpp
// global fucction definition - Air properties
   double air_viscosity(double);
   double air_density(double);
   double air_conductivity(double);
   double air_specific_heat(double);
   double air_Prandtl(double);

// global function definition - HTC & pressure drop
   double boiling_number(double,double,double,double);
   double laminar_coeff(double,double,double,double);
   double Martinelli(double,double);
   double mass_velocity(double,double);
   double ht_factor(double,double);
   double nb_factor(double,double,double,double,double);
   double nb_coeff(double,double);
   double Jung_coeff(double,double,double,double,double);
   double press_drop(double,double,double,double,double);
   double press_drop_acc(double,double,double,double);
   double phys_property_index(double);
   double press_drop_super(double,double,double,double);

// Air_side heat transfer coefficient and superheated region of refrigerant
   double compact (double,double,double,double);
   double HTC_super(double,double,double);

// input variables from published data
   void read(double&,double&,double&,double&,double&,double&,double&,double&,
             double&,double&);

// output file declaration
   FILE *dfp;

main()
{  // output parameter
   void tubeside(double*,double*,double*,double,double,double,double,double,
                 double, double*,double*,double*,int,double,double, double*);
   void superheat(double*, double*, double*, double, double,doublc,double,
                  double,double, double,double*, int,double);

   // input variables

   double L,
          ID,
          OD,
          T_s,
          mdot,
```

```c
               T_air,
               V_air,
               flux;
               x,
                 q,
                 A,
                 l=0.02,
               htc_av;

        read(L,ID,OD,T_s,mdot,x,T_air, V_air, flux,q);

        int interval;

        double quality,
               enthalpy,
               freon_temp,
               q_sum,
               total_length,
               dp_t,
               htc_t,
               h_airt,
               wall_temp,
               air_temp,
               i_g,
               air_velocity,
               h_air,
               h_SH,
                h_tp;

          double length=0.02;

// open data file
   dfp = fopen("c:\compsch.xls","w");
   fprintf(dfp,"x\t  h_tp\t  dp\n");

// initialization for loop on function tubeside
     interval = 0;
     q_sum = 0;
     dp_t =0;
     htc_t=0;
     h_airt=0;

     freon_temp = T_s;
     air_temp = T_air;
     air_velocity =V_air;
     quality = x;
     enthalpy = wet_enthalpy(freon_temp,quality);
```

```cpp
total_length=L/l+1.0;

    while (quality<1.0)
{
cout<<"\n\nITERATION NO. "<<interval<<endl;
cout<<"MAIN: x =  "<<quality<<endl;
cout<<"MAIN: freon_temp = "<< freon_temp<<endl;
cout<<"MAIN: enthalpy =  "<<enthalpy<<endl;
cout<<"MAIN: cumulative heat transfer = "<<q_sum<<endl;
tubeside(&freon_temp,&quality,&enthalpy,length,mdot,q,ID,OD,L,
        &q_sum,&dp_t,&htc_t,flux,air_temp, air_velocity,&h_airt);
interval++;
} //end of while loop

//Initialization and loop for superheated region

wall_temp = freon_temp +2.1;

cout<<"\nSuperheated Region"<<endl;
while (interval < total_length)
{ cout<<"\n\nITERATION NO. "<<interval<<endl;
cout<<"MAIN: x =  "<<quality<<endl;
cout<<"MAIN: freon_temp = "<< freon_temp<<endl;
cout<<"MAIN: enthalpy =  "<<enthalpy<<endl;
cout<<"MAIN: cumulative heat transfer = "<<q_sum<<endl;
superheat(&freon_temp,&i_g, &wall_temp,ID,OD,q,air_temp, length,mdot,
        h_air,&q_sum,flux,air_velocity);
interval++;}

cprintf("\nInput and Output Data\r\n");
cprintf("---------------------\r\n");
cprintf("The length of a horizontal tube (m) is ");
cout<<L<<endl;
cprintf("The internal diameter of a horizontal tube (m) is ");
cout<<ID<<endl;
cprintf("The external diameter of a horizontal tube (m) is ");
cout<<OD<<endl;
cprintf("The saturated temperature (oC) of refrigerant is ");
cout<<T_s<<endl;
cprintf("The mass flow rate(kg/s),mdot is ");
cout<<mdot<<endl;
cprintf("The inlet vapour quality,x is ");
cout<<x<<endl;
cprintf("The air temperature (oC) across heat exchanger is ");
cout<<T_air<<endl;
cprintf("The air velocity (m/s) across heat exchanger is ");
cout<<V_air<<endl;
```

```cpp
      cprintf("The constant heat flux (W/m2),q is ");
      cout<<q<<endl;
      cprintf("\nTHE TOTAL FRICTIONAL PRESSURE DROPS: dp_t = ");
      cout<<dp_t<<endl;
      A=PI*ID*l;
      htc_av = htc_t*A/(L*PI*ID);
      cprintf("THE TWO PHASE AVERAGE HEAT TRANSFER COEFFICIENT:
htc_av = ");
      cout<<htc_av<<endl;
      cprintf("THE SUPERHEATED HEAT TRANSFER COEFFICIENT: h_SH = ");
      cout<<h_SH<<endl;
      cprintf("THE HEAT TRANSFER COEFFICIENT OF AIR: h_air = ");
      cout<<h_air<<endl;

      return 0;
}


void tubeside(double *T_s,double *x,double *i_fg,double l,double mdot, double q,
            double ID,double OD, double L,double *q_sum,double *dp_t,double *htc_t,
            int flux,double T_air, double V_air,double *h_airt)

{// start tubeside

      double AI,
            AO,
            Q,
            m_factor,
            F,
            h_l,
            h_tp,
            htc_av,
            h_airav,
            h_air,
            i_f,
            i_g,
            P_s,
            dp,
            dp_a,
            N,
            k_cu = 386.0,
            h_sa;

      AI=PI*ID*l;
      AO=PI*OD*l;

      dp = press_drop(ID,*T_s,mdot,*x,l);
      cout<<"TUBESIDE: dp = "<<dp<<endl;
```

```cpp
dp_a=press_drop_acc(ID,*T_s,mdot,*x);
cout<<"TUBESIDE: dp_a = "<<dp_a<<endl;
m_factor = Martinelli(*T_s,*x);
cout<<"TUBESIDE: Xtt = "<<m_factor<<endl;
F = ht_factor(*T_s,*x);
cout<<"TUBESIDE: F = "<<F<<endl;
h_l = laminar_coeff(ID,*T_s, mdot,*x);
cout<<"TUBESIDE: h_l = "<<h_l<<endl;
N = nb_factor(ID,*T_s, mdot,*x,q);
cout<<"TUBESIDE: N = "<<N<<endl;
h_sa = nb_coeff(*T_s,q);
cout<<"TUBESIDE: h_sa = "<<h_sa<<endl;
h_tp = Jung_coeff(ID,*T_s,mdot,*x,q);
cout<<"TUBESIDE: h_tp = "<<h_tp<<endl;
cout<<"TUBESIDE: x = "<<*x<<endl;

    if (flux==0)
    Q=q*AI;
    else if (flux==1)
    Q = (T_air - *T_s)/((((1.0/h_tp*AI))+
(log(OD/ID)/(2.0*PI*k_cu*l))+(1.0/(h_air*AO))));
    else
    cout<<"TUBESIDE ERROR: FLUX CONDITION NOT SPECIFIED"<<endl;

    cout<<"TUBESIDE: Q = "<<Q<<endl;
    *q_sum=*q_sum+Q;
    fprintf(dfp,"%g\t %g\t %g\n",*x,h_tp,dp);

// output conditions
    *i_fg = (Q/mdot) + *i_fg;
    cout<<"TUBESIDE: *i_fg = "<<*i_fg<<endl;
    P_s= saturated_pressure(*T_s)-dp-dp_a;
    cout<<"TUBESIDE: P_s = "<<P_s<<endl;
    *T_s=saturated_temperature(P_s);
    cout<<"TUBESIDE:*T_s = "<<*T_s<<endl;
    i_f= liquid_enthalpy(*T_s);
    cout<<"TUBESIDE: i_f = "<< i_f<<endl;
    i_g= vapour_enthalpy(*T_s);
    cout<<"TUBESIDE: i_g = "<<i_g<<endl;
    *x = (*i_fg-i_f)/(i_g-i_f);
    h_air=compact(T_air,V_air,*T_s,OD);
    cout<<"AIRSIDE: h_air = "<<h_air<<endl;
    *h_airt =*h_airt+h_air;
    h_airav=*h_airt*AO/(L*PI*OD);
    cout<<"\nAVERAGE HTC OF AIR: h_airav ="<<h_airav<<endl;
    *htc_t = *htc_t+h_tp;
    htc_av = *htc_t*AI/(L*PI*ID);
```

```cpp
        cprintf("TWO PHASE AVERAGE HTC OF REFIGERANT : htc_av=");
        cout<<htc_av<<endl;
        *dp_t = *dp_t +dp+dp_a;
        cout<<"TOTAL PRESSURE DROPS OF REFRIGERANT: dp_t =
"<<*dp_t<<endl;
    } // end tubeside


void superheat(double *T_s, double *i_g, double *T_w,double ID, double OD,double q,
            double T_air, double l,double mdot, double h_air, double *q_sum,
            int flux, double V_air)

{//Start superheat: heat transfer in the superheated region

        double AO,     //outside heat transfer area
            AI,        //inside heat transfer area
            k_cu=386.0, // thermal conductivity of pure copper tubing
            h_SH,      //heat transfer coefficient due to boiling & convective

            Q,
            dp_SH,
            P_s;

        AO = PI*OD*l;
        AI = PI*ID*l;

        h_SH = HTC_super(*T_s, mdot,ID);
        cout<<"SUPERHEAT: h_SH ="<< h_SH<<endl;
        dp_SH = press_drop_super(ID,*T_s,mdot,l);
        cout<<"SUPERHEAT: dp_SH ="<< dp_SH<<endl;

        if (flux==0)
        Q=q*AI;
        else if (flux==1)
        Q = (T_air - *T_s)/(((1.0/h_SH*AI))+
(log(OD/ID)/(2.0*PI*k_cu*l))+(1.0/(h_air*AO))));
        else
        cout<<"SUPERHEAT ERROR: FLUX CONDITION NOT
SPECIFIED"<<endl;
        cout<<"SUPERHEAT: Q ="<< Q<<endl;
        *q_sum = *q_sum+Q;
        *T_w = (Q/h_SH*AI) + *T_s ;
        cout<<"SUPERHEAT: *T_w ="<< *T_w<<endl;

    // output conditions
        *i_g = (Q/mdot) + *i_g;
        cout<<"SUPERHEAT: i_g ="<< i_g<<endl;
        P_s = saturated_pressure(*T_s) - dp_SH;
```

```cpp
        cout<<"SUPERHEAT: P_s ="<< P_s<<endl;
        *T_s = saturated_temperature(P_s);
        cout<<"SUPERHEAT: *T_s ="<<*T_s<<endl;
        h_air=compact(T_air,V_air,*T_s,OD);
        cout<<"AIRSIDE: h_air="<<h_air<<endl;

} //end superheat

void read(double& L, double& ID, double& OD, double& T_s,double& mdot,
          double& x, double& T_air, double& V_air, double& flux,double& q)
{
  // text color
  clrscr();
  textcolor(GREEN);
  textbackground(BLUE);

  cprintf("\n\nComputational scheme for HTC and Pressure drops\r\n");
  cprintf("-------------------------------------------------\r\n");
  cprintf("Enter a length of a horizontal tube (m)...");
  cin>>L;
  cprintf("Enter an internal diameter of a horizontal tube (m)...");
  cin>>ID;
  cprintf("Enter an external diameter of a horizontal tube (m)...");
  cin>>OD;
  cprintf("Enter a saturated temperature (oC) of refrigerant...");
  cin>> T_s;
  cprintf("Enter a mass flow rate(kg/s),mdot...");
  cin>>mdot;
  cprintf("Enter a vapour quality,x...");
  cin>>x;
  cprintf("Enter air temperature (oC) across heat exchanger...");
  cin>> T_air;
  cprintf("Enter air velocity (m/s) across heat exchanger...");
  cin>> V_air;
  cprintf("Enter heat flux condition, constant = 0, variable = 1...");
  cin>>flux;
  cprintf("Enter a heat flux (W/m2), q...");
  cin>>q;
}

double boiling_number(double ID,double T_s,double mdot,double q)
{// start boiling_number:calulation of J&R boiling number

        double Bo,            // boiling number
               i_f,           // liquid enthalpy
               i_g,           // vapour enthalpy
               G;             // mass velcoity
```

```
        i_f = liquid_enthalpy(T_s);
        i_g = vapour_enthalpy(T_s);
        G =mass_velocity(ID,mdot);

        Bo = q/(G*(i_g-i_f));
        return Bo;
}

double laminar_coeff(double ID,double T_s,double mdot,double x)
{//start laminar_coeff: to determine the laminar heat transfer coefficient
//              at saturated temperature and vapour quality.

        double h_l,      // laminar heat transfer coefficient
               Re,       // Reynold number
               k_f,      // thermal conductivity of liquid
               mu_f,     // dynamic viscosity of liquid
               Pr_f;     // Prandtl number

        k_f = liquid_conductivity(T_s);
        mu_f= liquid_viscosity(T_s);
        Pr_f = liquid_Prandtl(T_s);

        Re = (mdot*4.0)/(mu_f*PI*ID);
        h_l = 0.023*(k_f/ID)*pow((Re*(1.0 -x)),0.8)*pow(Pr_f,0.4);
        return h_l;
}

double Martinelli(double T_s,double x)
{// start Martinelli:"function to determine the Martinelli parameter

        double X_tt,     // Martinelli<parameter
               rho,      // liquid density
               mu_f,     //dynamic viscosity of liquid
               rhov,     // vapour density
               mu_g;     // dynamic viscosity of vapour

    mu_f = liquid_viscosity(T_s);
     mu_g = vapour_viscosity(T_s);
    rho=liquid_density(T_s);
    rhov=vapour_density(T_s);

    X_tt=pow(((1.0-x)/x),0.875)*pow((mu_f/mu_g),0.125)*pow((rhov/rho),0.5);

    return X_tt;
}
```

```cpp
double mass_velocity(double ID,double mdot)
{// start mass_velocity: calculation of mass velocity (kg/m2s)

    double G;
    G = 4.0 * mdot/(PI*pow(ID,2.0));
    return G;
}


double ht_factor(double T_s, double x)
{// start ht_factor: function to determine J&R (F)

    double F,          // heat transfer enjancement factor
        X_tt;

    X_tt = Martinelli(T_s,x);

    F=2.37*pow((0.129+ 1.0/X_tt),0.85);
    return F;
}

double nb_factor(double ID,double T_s, double mdot, double x,double q)
{// start nb_factor: function to determine J&R (N)

    double N,          // nucleate boiling factor
        Bo,
        X_tt;

    Bo = boiling_number(ID,T_s,mdot,q);
    X_tt=Martinelli(T_s,x);

    if (X_tt<=1.0)
        N=4048.0*pow(X_tt,1.22)*pow(Bo,1.13);
    else if (X_tt<=5.0)
        N=2.0-0.1*pow(X_tt,-0.28)*pow(Bo,-0.33);
    else
        cout<<"NUCLEATE: X_tt out of range"<<endl;
    return N;
}

double nb_coeff(double T_s,double q)
{// start nb_coeff: function to determine J&R (h_sa)

    double h_sa,
            bd,
        k_f,
        rho,
        rhov,
```

```
                    Pr,
                sigma;

        k_f=liquid_conductivity(T_s);
    rho = liquid_density(T_s);
    rhov=vapour_density(T_s);
        Pr= liquid_Prandtl(T_s);
    sigma=surface_tension(T_s);

    bd = 0.0146*35.0*pow(2.0*sigma/(g*(rho-rhov)),0.5);   // contact angle=35.0

    h_sa=207.0*k_f/bd*pow(q*bd/(k_f*(T_s+273.15)),0.745)*pow(rhov/rho,0.581)
        *pow(Pr,0.533);

    return h_sa;
}

double phys_property_index(double T_s)
{// start Froude_number

        double ppi,
                rhov,
                mu_f,
                mu_g,
                rho;

        rhov = vapour_density(T_s);
        rho = liquid_density(T_s);
        mu_f=liquid_viscosity(T_s);
        mu_g=vapour_viscosity(T_s);

        ppi =pow(rho/rhov,0.5)*pow(mu_g/mu_f,0.125);

        return ppi;
}

double Jung_coeff(double ID,double T_s,double mdot,double x,double q)
{// start Jung_coeff: correlation to determine two phase heat transfer-
//              coefficient

    double h_tp,
            N,
            h_sa,
            F,
            X_tt,
            h_l;
```

```cpp
    N = nb_factor(ID,T_s,mdot,x,q);
    h_sa = nb_coeff(T_s,q);
    F = ht_factor(T_s,x);
    h_l = laminar_coeff(ID,T_s,mdot,x);

    h_tp = N*h_sa + F*h_l;

    return h_tp;
}

double press_drop(double ID,double T_s,double mdot, double x,double l)
{// start press_drop : function to determine two phase pressure drop
//              from Souza's 1995 correlation.

    double dp,
            Re,         // Reynold number
            G,
            mu_f,
            rho,
                f,          // friction factor
            multi,      // pressure drop multiplier
                ppi,        // physical property index
            X_tt,
                C1,
                C2;

    rho=liquid_density(T_s);
    G = mass_velocity(ID,mdot);
    ppi = phys_property_index(T_s);
    mu_f= liquid_viscosity(T_s);
    X_tt = Martinelli(T_s,x);


    Re = (G*ID)/mu_f;
    f = 0.079/pow(Re,0.25);

    multi= 1+((ppi*ppi-1)*pow(x,1.75))*(1+0.9524*ppi*pow(X_tt,0.4126));
        dp = (2.0 * f*G*G*l*multi)/(rho*ID);

    cout<<"TUBESIDE:  multi = " <<multi<<endl;
        cout<<"TUBESIDE:  ppi = " <<ppi<<endl;
    return dp;
}

double press_drop_acc(double ID,double T_s, double mdot, double x)
{// start press_drop_acc: function to determine two phase accerational pressure drop
//              from Martinelli's correlation.
```

```c
        double dp_a,
              rho,
              rhov,
              G;

    rho= liquid_density(T_s);
    rhov=vapour_density(T_s);
        G=mass_velocity(ID,mdot);

    dp_a=0.00689*(pow(G,2.0)/g)*((1-x)+x*(rho/rhov)-1)/rho;

    return dp_a;
}

double compact(double T_air, double V_air, double T_s, double OD)
{// Start compact: calculate heat transfe coefficient airside of compact
// heat exchanger

double Re_air,
       Nu_air,
       Pr_air;

double h_air,
       rho_air,
       mu_air,
       T_a,
       T_w,
       k_air;

        T_w=T_s+2.1;
        T_a=(T_air+T_w)/2;

        rho_air=air_density(T_a);
        Pr_air=air_Prandtl(T_a);
        k_air= air_conductivity(T_a);
        mu_air=air_viscosity(T_a);

// Air_side heat transfer coefficient

        Re_air = (V_air*OD*rho_air)/mu_air;
        Nu_air = 0.683*pow(Re_air,0.466)*pow(Pr_air,2.0);
        h_air = (Nu_air*k_air)/OD;

return h_air;

}
```

```cpp
double HTC_super(double T_s, double mdot, double ID)
{// start HTC_super: calcuate superheated HTC using Dittus and Boelter

        double h_SH,
               Re_g,
               mu_g,
               Pr_g;

    mu_g = vapour_viscosity(T_s);
    Pr_g = vapour_Prandtl(T_s);
    Re_g = (4.0* mdot)/(PI*ID*mu_g);

    h_SH = 0.023*pow(Re_g,0.8)*pow(Pr_g,0.4);

    cout<<mu_g<<endl;
    cout<<Pr_g<<endl;
    cout<<Re_g<<endl;

    return h_SH;
}

double press_drop_super(double ID,double T_s,double mdot,double l)
{     // start press_drop : function to determine pressure drop
      //              in superheated region

    double dp_SH,
           Re_g,            // Reynold number
           rhov,
               mu_g,
               AI,
               U_m,         // mean flow velocity
               f;           // friction factor

    rhov=vapour_density(T_s);
    mu_g= vapour_viscosity(T_s);

    AI = PI*ID*l;
    Re_g = (4.0* mdot)/(PI*ID*mu_g);
    f = 0.316/pow(Re_g,0.25);
    U_m = mdot/(rhov*AI);

    dp_SH =(f*l*rhov*pow(U_m,2.0))/(2.0*ID);

    cout<<"Re_g ="<<Re_g<<endl;
    cout<<"f ="<<f<<endl;
    cout<<"U_m ="<<U_m<<endl;
    return dp_SH;
```

```
}
// end of program
```

APPENDIX II

This appendix contains the equations for liquid and vapour transport properties of R12 which are based on the saturated temperature (°C) of refrigerant.

```cpp
//------------------------------------------
// Transport properties of R12
// Program name: R12.cpp
// Author name : Edwin Au
// Date:      12 January 1994
//------------------------------------------

#include<math.h>

double liquid_conductivity(double T_s)
{    // start liquid_conductivity: function to determine the thermal
     //                conductivity of the liquid from Yata's
     //                equation.

     double k_f,           // liquid thermal conductivity (W/mK)
            T,             // temperature in K
     A = 0.1702,
     B = -0.33941e-3;
     T = T_s + 273.15;
     k_f = (A+B*T);
     return k_f;
}

double liquid_density(double T_s)
{    // start liquid_density: function to determine the density of saturated
     //                liquid

     double rho,       // liquid density (kg/m3)
            T,         // temperature in K
         Trm,
     T_c = 385.0;

     T = T_s + 273.15;
     Trm = pow((1.0-T/T_c),1.0/3.0);

     rho = 1463.6338-1888.1474*Trm +2687.143*Trm*Trm;
     return rho;
}
```

```
double liquid_enthalpy (double T_s)
{    //start liquid_enthalpy: function to determine the liquid enthalpy from
     //              A.C.Cleland's equation.

     double i_f;

     i_f = 200000.0+923.88*T_s+0.83716*pow(T_s,2.0)+5.3772e-3*pow(T_s,3.0);
     return i_f;
}

double liquid_spec_heat(double T_s)
{    //start liquid_spec_heat:function to determine the liquid specific
     //              heat capacity.

     double Cp,
          Trm,
            T,
        Tc=385.0;

     T = T_s+273.15;
     Trm = pow((1.0-T/Tc),1.0/3.0);

     Cp = 904.187+897.68*Trm -1277.77*Trm*Trm;
     return Cp;
}

double liquid_viscosity(double T_s)
{    // start liquid_viscosity: function to determine the dynamic viscosity
     //              of saturated liquid from Phillips' equation.

     double mu_f,          // liquid viscosity (Pa.s)
              T,           // temperature in K
        A = -2.14142,
        B = 309.1170,
        C = 0.29104e-2,
        D = -0.469771e-5;

     T = T_s + 273.15;
     mu_f = (pow(10, A + B/T + C*T + D*T*T))*1e-3;
     return mu_f;
}

double liquid_Prandtl(double T_s)
{    // start liquid_Prandtl: function to determine Prandtl number of liquid

     double Pr_f,
```

```cpp
            mu_f,
            k_f,
         Cp;

    mu_f=liquid_viscosity(T_s);
            k_f = liquid_conductivity(T_s);
            Cp = liquid_spec_heat(T_s);

    Pr_f = Cp * mu_f/k_f;
    return Pr_f;
}

double saturated_pressure(double T_s)
{    // start saturated_pressure: function to determine the saturated pressure
    //              from A.C.Cleland's equation.

    double P_s;

            P_s = exp(20.82963-(2033.5646/(T_s+248.3)));
    return P_s;
}

double surface_tension(double T_s)

{    // start surface_tension: function to determine the surface tension
    //              of R12

    double T_c =385.0,      // critical temperature
        sigma_c=56.52e-3;  // critical surface tension

    double T_r,           // reduced temperature
        sigma;          // surface tension (N/m)
 T_r = (T_s+273.15)/T_c;
 sigma = sigma_c * pow((1.0 -T_r),1.27);
 return sigma;
}

double vapour_density(double T_s)
{    // start vapour_density:function to determine the density of saturated
    //              vapour

    double v_g,          // saturated vapour specific volume
        rhov;

    v_g=exp((-11.58643+2372.495/(T_s+273.15))*(1.00755+4.94025e-4*T_s-
        6.04777e-6*pow(T_s,2.0)-2.29472e-7*pow(T_s,3.0)));
    rhov=1.0/v_g;
```

```
        return rhov;
}

double vapour_enthalpy(double T_s)
{     // start vapour_enthalpy: function to determine the vapour enthalpy
      //              from A.C.Cleland's equation.

      double i_g;

      i_g = 187565.0+428.992*T_s-0.75152*pow(T_s,2.0)-5.6695e-3*pow(T_s,3.0)
          +163994.0;
      return i_g;
}

double vapour_viscosity(double T_s)
{     // start vapour_viscosity: function to determine the dynamic viscosity
      //              of saturated vapour

      double mu_g,          // dynamic viscosity of vapour  (Pa.s)
             zeta,          // compression constant
             T_r;           // reduced temperature

      double T_c = 385.0,     // critical temperature
             P_c = 4.18,      // critical pressure
             Z_c = 0.2834,    // compressibility constant
             M_w = 102.91;    // molecular weight

      T_r = (T_s +273.15)/T_c;
      zeta= pow(T_c,(1.0/6.0))*pow(M_w,-0.5)*pow(P_c,(-2.0/3.0));
      mu_g= ((pow((0.5124*T_r-0.0517),0.82)*pow(Z_c,-0.81))/zeta)*1e-6;
      return mu_g;
}

double wet_enthalpy(double T_s, double x)
{       // start wet-enthalpy

        double i_fg,
               i_f,
               i_g;

        //      function to determine the enthaly of wet vapour of R134a
        //      dryness fraction x

        i_f = liquid_enthalpy(T_s);
        i_g = vapour_enthalpy(T_s);

        i_fg = i_f + x *(i_g - i_f);
```

```c
        return i_fg ;

}       // end wet_enthalpy

double saturated_temperature(double P_s)
{       // start saturated_temperature: function to find saturation temperature for a given
pressure

    double T_s;

    T_s = (-2033.5646/(log(P_s)-20.82963))-248.30;

    return T_s;
}    // end sat_temperature

double vapour_conductivity(double T_s)
{    // start vapour_conductivity

    double k_g,
            T,
    A = -0.012605,
    B = 1.09279e-4,
    C = -1.604876e-7,
    D = 3.036155e-10;

    T = T_s+273.15;

    k_g = A + B*T+C*pow(T,2.0) + D*pow(T,3.0);
    return k_g;
}

double vapour_spec_heat(double T_s)
{    // start vapour_spec_heat

    double cp_g,
            T,
    A = 0.131419,
    B = 0.003006,
    C = -2.23892e-6,
    D = 5.97826e-10,
    E = 430.0077;

    T =T_s +273.15;

    cp_g=(A+B*T+C*pow(T,2.0)+D*pow(T,3.0)+E/pow(T,2.0))*1000.0;
    return cp_g;
}
```

```
double vapour_Prandtl(double T_s)
{     //start vapour_Prandtl

    double Pr_g,
          cp_g,
          mu_g,
          k_g;

    Pr_g=(vapour_spec_heat(T_s)*vapour_viscosity(T_s))/vapour_conductivity(T_s);
    return Pr_g;
}
```

This appendix contains the equations for liquid and vapour transport properties of R134a which are based on the saturated temperature (°C) of refrigerant.

```
// ----------------------------------------
// Program name:   R134a
// Author name:    Edwin Au
// Date:           29 November 1993
// ----------------------------------------

#include <math.h>

// properties of R134a to be called as functions
// This file is to be used with funtions.cpp

double saturated_pressure(double T_s)

{       // start saturated_pressure: a function to find saturation pressure for a given
temperature

        double P_s;    // saturation pressure

        P_s = exp(21.51297 - 2200.9809/(246.61 + T_s));

        return P_s ;

}       // end sat_press

double saturated_temperature(double P_s)
{     // start saturated_temperature: function to find saturation temperature for a given
pressure

        double T_s;

        T_s = (-2200.9809/(log(P_s)-21.51297))-246.61;

        return T_s;

}     // end sat_temperature

double vapour_enthalpy(double T_s)
```

```
{        // start vapour_enthalpy: to determine the enthalpy of saturated vapour

        double i_g,
               x,
               T;
        T = 273.15+T_s;
        double T_c=374.15;
        x = pow((1.0-T/T_c),1.0/3.0);
        i_g = 195801.0+(702668.0*x )-
(1034310.0*pow(x,2.0))+(285478.0*pow(x,3.0));


        return i_g;

}        // end vapour enthalpy

double liquid_enthalpy(double T_s)
{        // start liquid_enthalpy: function to determine the enthalpy of saturated liquid

        double i_f,
               T,
               x ;
        double T_c = 374.15;
        T = T_s +273.15;
        x = pow((1.0-T/T_c),1.0/3.0);

        i_f = 292019.9-(117497.0*x)+(8096.516*pow(x,2.0))-(542859.0*pow(x,3.0))+
            (154988.7*pow(x,4.0));
        return i_f;

}        // end liquid_enthalpy

double vapour_density(double T_s)
{        // start vapour_density: function to determine the specific volume of saturated
vapour

        double rhov,
               v_v;

        v_v = exp(-12.4539+(2669.0/(273.15+T_s)))*
            (1.01357+(1.06736e-3*T_s)-(9.2532e-6*pow(T_s,2.0))
            -(3.2192e-7*pow(T_s,3.0)));
        rhov = 1/v_v;

        return rhov;

}        // end vapour_density
```

```
double liquid_density(double T_s)
{       // start liquid_density: function to determine the specific volume of saturated
liquid

        double rho,
                D1 = 819.6183,
                D2 = 1023.582,
                D3 = -1156.757,
                D4 = 789.7191,
                T_r,            // reduced temperature
                btr;            // local constant

        double T_c = 101.15,    // critical temperature
                rho_c = 508.0;  // critical density

        T_r = (T_s+273.15)/(T_c+273.15);
        btr = 1.0 - T_r;

        rho =rho_c + D1*pow(btr,(1.0/3.0)) + D2*pow(btr,(2.0/3.0)) + D3*btr +
D4*pow(btr,(4.0/3.0));

        return rho;

}       // end liquid_volume

double vapour_viscosity(double T_s)
{       // start vapour_viscosity: function to determine the dynamic viscosity"of
saturated vapour

        double mu_g,    // dynamic viscosity of vapour
                zeta,   // compression constant
                T_r;    // reduced temperature

        double T_c = 101.15,    // critical temperature
                P_c = 4.067e+6, // critical pressure
                Z_c = 0.262;    // compressibility constant

        double M_w = 102.03;            // molecular weight

        T_r = (T_s+273.15)/(T_c+273.15);

        zeta = pow((T_c + 273.15),(1.0/6.0))*pow(M_w,-0.5)*pow(P_c*1e-6,(-
2.0/3.0));
        mu_g = ((pow((0.5124*T_r - 0.0517),0.82)*pow(Z_c,-0.81))/zeta)*1e-6;

        return mu_g;
```

```
}         // end vapour_viscosity

double liquid_viscosity(double T_s)
{         // start liquid_viscosity: function to determine the dynamic viscosity of saturated
liquid

        double mu_f,
            a;

        a = -5.82061+(738.606/(T_s + 273.15)) + (0.013854*(T_s + 273.15)) -
            (0.164426e-4*pow((T_s + 273.15),2.0));

        mu_f = pow(10.0,a)/1000.0;

        return mu_f;

}         // end liquid_viscosity

double surface_tension(double T_s)
{         // start surface_tension: function to determine the surface tension of freon

        double sigma;

        double T_c = 101.15,        // critical temperature
            sigma_c = 60.8e-3;      // critical surface tension

        double T_r;                 // reduced temperature

    T_r = (T_s+273.15)/(T_c+273.15);

    sigma = sigma_c*pow((1.0 - T_r),1.260);

    return sigma;

}         //end surface_tension

double press_slope(double T_s)
{         // start press_slope: function to determine the slope of saturation pressure vs
temperature curve at T_s

        double dpdt;

        dpdt = (2200.9809/pow((246.61+T_s),2.0))*
            exp(21.51297 - (2200.9809/(246.61+T_s)));

        return dpdt;
```

```
}        // end press_slope

double liquid_conductivity(double T_s)
{        // start liquid_conductivity: function to determine the thermal conductivity of the
liquid form ICI data sheet

        double k_f,              // liquid R143a thermal conductivity
        A = 0.0460164,
        B = 0.0533949,
        C = -0.120467,
        D = 0.2424306,
        y;                       // used in polynomial fit

        double T_c = 101.15; // critical temperature

        y = pow(1.0-((T_s+273.15)/(T_c+273.15)),1.0/3.0);

        k_f = A + B*y + C*pow(y,2.0) + D*pow(y,3.0);

        return k_f;

}        // end liquid_conductivity

double liquid_spec_heat(double T_s)
{        // start liquid_spec_heat: function to determine the specific heat capacity of the
liquid

        double Cp,                        // specific heat capacity of liquid
               T,
               T_c,
               x;

    T = T_s + 273.15;
    T_c=374.15;
    x = pow((1.0-T/T_c),1.0/3.0);

    Cp = 5629.0 -16602.0*x + 22121.0 *pow(x,2.0)-10453.0*pow(x,3.0);

    return Cp;

}        // end liquid_spec_heat

double liquid_Prandtl(double T_s)
{        // start liquid_Prandtl: function to determine the Prandtl number of the liquid

        double Pr_f,     // Prandtl number of liquid
```

```cpp
        Cp,         // specific heat capacity of liquid
        k_f;        // thermal conductivity of liquid

    Pr_f = (liquid_spec_heat(T_s)*liquid_viscosity(T_s))/liquid_conductivity(T_s);

    return Pr_f;

}       // end liquid_Prandtl

double wet_enthalpy(double T_s, double x)
{       // start wet-enthalpy

    double i_fg,
                i_f,
                i_g;

    //      function to determine the enthaly of wet vapour of R134a
    //      dryness fraction x

    i_f = liquid_enthalpy(T_s);
    i_g = vapour_enthalpy(T_s);

    i_fg = i_f + x *(i_g - i_f);
    return i_fg ;

}       // end wet_enthalpy

double mixed_volume(double T_s, double x)
{       // start mixed_volume

    double v_fg,    // specific volume of liquid/vapour mix
           rho,
           rhov,
           v_f,     // specific volume of liquid
           v_g;     // specific volume of vapour

    rho = liquid_density(T_s);
    rhov = vapour_density(T_s);

    v_fg = (1/rho)*(1 - x) + (1/rhov) * x;

    return v_fg;

}       // end mixed_volume

double vapour_conductivity(double T_s)
{    // start vapour_conductivity
```

```
        double k_g,
                T,
        A = -0.012605,
        B = 1.09279e-4,
        C = -1.604876e-7,
        D = 3.036155e-10;

        T = T_s+273.15;

        k_g = A + B*T+C*pow(T,2.0) + D*pow(T,3.0);
        return k_g;
}

double vapour_spec_heat(double T_s)
{       // start vapour_spec_heat

        double cp_g,
                T,
        A = 0.131419,
        B = 0.003006,
        C = -2.23892e-6,
        D = 5.97826e-10,
        E = 430.0077;

        T = T_s +273.15;

        cp_g=(A+B*T+C*pow(T,2.0)+D*pow(T,3.0)+E/pow(T,2.0))*1000.0;
        return cp_g;
}

double vapour_Prandtl(double T_s)
{       //start vapour_Prandtl

        double Pr_g,
                cp_g,
                mu_g,
                k_g;

        Pr_g=(vapour_spec_heat(T_s)*vapour_viscosity(T_s))/vapour_conductivity(T_s);
        return Pr_g;
}
```

APPENDIX IV

This appendix contains the equations for thermal properties of air which are based on the temperature (°C).

```cpp
//------------------------------------
// Thermal properties of air
// Program name: air.cpp
// Author name : Edwin Au
// Date:      9 November 1995
//------------------------------------

#include<math.h>

double air_viscosity(double T_a)
{    // start air_viscosity:a function to find dry air viscosity for a given
     //                temperature

    double mu_air,
          T,                // absolute temperature
          A = 0.671692,
          B = 85.22974,
          C = -2111.475,
          D = 106417.0;

   T = T_a + 273.15;

   mu_air = sqrt(T)/(1.0e6*(((D/T+C)/T+B)/T+A));

   return mu_air;

}

double  air_conductivity(double T_a)
{
        double k_air,  // thermal conductivity
             T;      // absolute temperature

     int i;

     double B[3][4];
     // store 12 values in array
     B[0][0]= 385.859;
```

```
    B[0][1]= 9.11440E+04;
    B[0][2]= -2.68667E+06;
    B[0][3]= 5.52604E+7;
    B[1][0]= 328.052;
    B[1][1]= 1.67320E+05;
    B[1][2]= -3.02953E+07;
    B[1][3]= 3.05682E+09;
    B[2][0]= 539.544;
    B[2][1]= -3.32903E+05;
    B[2][2]= 3.59756E+08;
    B[2][3]= -9.67202E+10;

    T = T_a+273.15;

    if (T<300.0)
        i=0;
    else if (T<600.0)
        i=1;
    else
        i= 2;

    k_air = sqrt(T)/((((B[i][3]/T + B[i][2])/ T+B[i][1])/T + B[i][0]);

    return k_air;
}

double air_specific_heat(double T_a)
{    //start air_spec_heat:function to determine the air specific
    //                    heat capacity.

    double Cp_air,    // specific heat capacity
            T;

    int i;

    double B[3][4];

    // STORE 12 VALUES IN ARRAY

    B[0][0]= 1.04336E+00;
    B[0][1]= -3.15976E-4;
    B[0][2]= 7.07909E-7;
    B[0][3]= -2.70340E-10;

    B[1][0]= 1.00205E+00;
    B[1][1]= -1.62983E-04;
    B[1][2]= 5.69525E-07;
```

```
        B[1][3]= -2.68081E-10;

        B[2][0]= 8.73749E-01;
        B[2][1]= 3.22598E-04;
        B[2][2]= -3.58454E-8;
        B[2][3]= -1.99063E-11;

        T = T_a +273.15;

        if (T<610.0)
            i=0;
        else if (T<900.0)
            i=1;
        else
            i=2;

        Cp_air = 1000.0*( B[i][0] + T*B[i][1] + pow(T,2.0) * B[i][2] +pow(T,3.0)*B[i][3]);

        return Cp_air;
}

double air_Prandtl(double T_a)
{    // start air_Prandtl: function to determine dry air Prandtl number for a given
     //                   a given temperature

        double  Pr_air;    // Prandtl number

        Pr_air = air_specific_heat(T_a)*air_viscosity(T_a)/air_conductivity(T_a);

        return Pr_air;

}

double air_enthalpy(double T_a)

{       // start air_enthaply: function to determine dry air enthaply for a
        //                   given temperature

        double  T,
                i_air;

        T = 273.15+T_a;

        i_air = -285598.68+1066.84*T - pow(T,2.0)*0.0845;

        return i_air;
}
```

```
double air_density(double T_a)
{        // start air_density: function to determine dry air density for a given
         //                            temperature

         double T,
                rho_air;

      double P_a=1.0e5;

      T = 273.15 + T_a;
      rho_air=P_a/(287.0552*T);

      return rho_air;
}

// program end
```